Tracer Technologies for Hydrological Systems (Proceedings of a Boulder Symposium, July 1995). IAHS Publ. no. 229, 1995.

Use of caesium-137 and lead-210 as tracers in soil erosion investigations

D. E. WALLING, Q. HE & T. A. QUINE
Department of Geography, University of Exeter, Exeter EX4 4RJ, UK

Abstract Recent years have seen increasing interest in the potential for using caesium-137 as a tracer in soil erosion investigations and caesium-137 measurements are now accepted as an effective and valuable means of producing retrospective information on medium-term rates and patterns of soil redistribution. There are, however, two important limitations to the general application of the approach. These involve the complications introduced by inputs of Chernobyl-derived radiocaesium in many areas of Europe and the relatively low caesium-137 inventories encountered in some parts of the globe where fallout rates were low. Unsupported lead-210, a natural fallout radionuclide, can offer a viable alternative to caesium-137 as a sediment tracer in many environments. In addition, when used in combination with caesium-137, it offers potential as a complementary tracer, which can provide additional information on the erosional history of a site. The results of a study of soil redistribution within a small cultivated field at Butsford Barton, Colebrooke, Devon, UK, aimed at comparing the estimates provided by caesium-137 and unsupported lead-210 measurements, are presented. These results confirm the potential for using unsupported lead-210, both as an alternative to, and in combination with, caesium-137 in soil erosion investigations.

THE CONTEXT

Recent years have seen increasing interest in the potential for using caesium-137 as a tracer in soil erosion investigations (cf. Walling & Quine, 1992). This manmade fallout radionuclide was released into the global environment as a result of the atmospheric testing of thermonuclear weapons, which took place primarily from the mid-1950s to the mid 1970s. In most environments, radiocaesium reaching the soil surface as fallout was rapidly and strongly adsorbed by the surface soil horizons and its subsequent redistribution occurred in association with soil particles. It therefore affords an effective and valuable means of assessing medium-term (ca. 30 year) rates and patterns of soil redistribution (cf. Campbell *et al.*, 1988; Walling & Quine, 1991). The caesium-137 approach to documenting soil erosion has now been used in a wide range of environments in different regions of the world (cf. Walling & Quine, 1992) and its greatest value arguably lies in its capacity to provide *retrospective* information on rates and patterns of soil loss, based on a single site visit. There are, however, a number of limitations to the general application of the approach. More particularly, these limitations relate to, firstly, the additional inputs of caesium-137 which occurred in many areas of Europe in 1986 as a result of the Chernobyl accident and which have

Table 1 Latitudinal variation of mean bomb-derived strontium-90 inventories at the end of 1983, based on data presented by Larsen (1985).

Latitude band	Mean strontium-90 inventory (Bq m^{-2})	
	Northern Hemisphere	Southern Hemisphere
0-10	953	526
10-20	1370	491
20-30	2075	841
30-40	2862	967
40-50	3867	1124
50-60	3585	672
60-70	2084	455
70-80	897	276
80-90	409	154

Inventory values have been estimated from the cumulative strontium-90 deposition on the land and ocean surface of individual latitudinal belts.

necessarily complicated the relationship between contemporary radiocaesium inventories and medium-term rates of erosion and deposition, and, secondly, the global pattern of caesium-137 fallout inputs. Although a detailed assessment of the global pattern of caesium-137 inventories in undisturbed soils which would be representative of fallout inputs has yet to be undertaken, it is known that such inventories are much lower in the southern hemisphere than in the northern hemisphere and that inputs to equatorial areas were probably considerably lower than those to the mid-latitude areas of Europe and North America, where most work on exploiting the potential of the caesium-137 approach has been undertaken. Table 1 presents generalised information on the global distribution of the fallout of strontium-90, another fission product of atmospheric weapons testing, based on data reported by Larsen (1985). In view of the common origin of both strontium-90 and caesium-137, the global pattern of caesium-137 fallout will be similar to that for strontium-90, and Table 1 indicates that in equatorial areas and over large regions of the southern hemisphere, caesium-137 inventories are likely to be <30% of those recorded in the mid-latitudes of the northern hemisphere. The low caesium-137 inventories associated with these areas of reduced fallout receipt introduce important measurement problems in terms of both detection limits and the long count times required to obtain results with an acceptable degree of precision.

In attempting to address some of the limitations of caesium-137 outlined above, the authors have explored the potential for using unsupported lead-210 as an alternative and complementary fallout radionuclide tracer in soil erosion investigations.

LEAD-210 AS A SEDIMENT TRACER

Lead-210 is a natural product of the uranium-238 decay series derived from the decay of gaseous radon-222, the daughter of radium-226. Radium-226 occurs naturally in soils and rocks and will generate lead-210 which will be in equilibrium with its parent. Diffusion of a small quantity of the radon-222 from the soil introduces lead-210 into the atmosphere, and its subsequent fallout provides an input of this radionuclide to surface soils and sediments which is not in equilibrium with its parent radium-226. This fallout component is termed "unsupported" or "excess" lead-210, since it cannot be accounted for (or supported by) decay of the in-situ parent. The amount of unsupported or atmospherically-derived lead-210 in a sediment sample can be calculated by measuring both lead-210 and radium-226 (via lead-214) and subtracting the supported or in-situ component. Recent developments in the use of low background, low energy, gamma spectrometry (cf. Appleby *et al.*, 1986; Joshi, 1987; Murray *et al.*, 1987) make such measurements relatively easy to undertake.

Although lead-210 has been widely used for dating lake sediment cores, its potential for estimating soil erosion rates has been largely ignored to date. As a fallout radionuclide that is rapidly and strongly adsorbed by the surface soil, unsupported lead-210 will behave in a similar manner to caesium-137, except that its fallout input has been essentially constant through time and the supply to the soil surface is therefore continuously replenished. The lead-210 half-life of 22.26 years is also similar to that of caesium-137 (30.17 years). However, because lead-210 was not present in Chernobyl fallout, it does not face the problems associated with interpreting caesium-137 measurements in those areas that received inputs of both bomb- and Chernobyl-derived radiocaesium. Furthermore, existing evidence of the global pattern of lead-210 fallout and associated soil inventories, although somewhat limited, indicates that the variability involved is considerably less than that indicated for caesium-137 in Table 1. The annual

Table 2 Global variation in the total annual deposition of lead-210.

Location	Mean Pb-210 deposition rate (dpm cm^{-2} $year^{-1}$)
Suva, Fiji	0.48
Auckland, New Zealand	0.30
Delhi, India	0.80
Calcutta, India	0.61
Bombay, India	1.50
Sydney, Australia	0.32
Alice Springs, Australia	0.34
Darwin, Australia	0.57
Hokkaido, Japan	2.20
Milford Haven, UK	0.51
Moscow, Russia	0.69
New Haven, USA	0.92

Based on Turekian *et al.* (1977).

deposition rate of lead-210 on the earth's surface is of the order of 1 dpm cm^{-2} $year^{-1}$ (cf. Krishnaswami & Lal, 1978), and the selection of annual deposition rates for specific sites throughout the world listed in Table 2 suggests that it should be possible to use it as a sediment tracer in a wide range of locations and environments.

In addition, by virtue of its continuous replenishment, lead-210 will not face the problems of progressively declining levels of activity associated with caesium-137. At present, only about 50% of the total input of bomb-derived caesium-137 fallout remains and in 30 years time this value will have reduced to ca. 25%.

As well as providing an alternative to caesium-137 as a sediment tracer in areas that received significant inputs of Chernobyl-derived radiocaesium or where the caesium-137 inventories are low, lead-210 also offers potential as a complementary tracer. By comparing the behaviour of caesium-137, the input of which was effectively limited to a period of ca 15 years extending from the late 1950s to the early 1970s, with that of lead-210 for which the input has been essentially constant, it may prove possible to obtain additional information on the erosional history of a study site. In order to examine further the potential of lead-210 as both an alternative and complementary sediment tracer to caesium-137 in soil erosion investigations, the findings of an investigation aimed at using both tracers and comparing the results obtained will be presented.

A COMPARISON OF CAESIUM-137 AND LEAD-210 MEASUREMENTS

In order to compare the effectiveness of caesium-137 and unsupported lead-210 measurements for estimating rates and patterns of soil erosion on agricultural land, a study of the erosional redistribution of the two radionuclides was undertaken within a small (7.5 ha) cultivated field at Butsford Barton near Colebrooke, Devon, UK. Several soil cores collected from neighbouring areas of undisturbed permanent grassland were used to establish the current reference inventories for the site and these were estimated to be ca. 275 mBq cm^{-2} and 600 mBq cm^{-2} for caesium-137 and unsupported lead-210 respectively.

Field sampling and sample analysis

More than 200 bulk soil cores were collected from the study field at the intersections of a 20 m grid, using a motorised percussion corer equipped with a 6.9 cm diameter core tube. These cores were ca. 70 cm in length and the basal 2 cm portion of each core was retained for separate analysis, in order to confirm that the core had penetrated the full depth of soil containing caesium-137 and unsupported lead-210. In all cases, penetration was confirmed. In addition, a number of larger 12 cm diameter cores were collected from representative locations, both within the field and in neighbouring areas of undisturbed permanent pasture which served as reference sites. These were sectioned into 2 cm increments, in order to provide information on the vertical distribution of radiocaesium and unsupported lead-210 within the profile. After collection, all core samples were air dried, disaggregated, and sieved to <2 mm prior to loading into Marinelli beakers for gamma assay. Gamma spectrometry was undertaken using an ORTEC low-background, n-type, 30 mm deep, coaxial detector which was capable of spanning the range of energy levels required for measurements of both caesium-137 and lead-210/lead-214. Count times were ca. 50 000 s and these typically provided a precision (95% level of confidence) of ca. 6% and 8% for caesium-137 and unsupported lead-210 determinations respectively.

Comparing profile distributions

Figure 1 provides examples of the vertical distribution of caesium-137 and unsupported lead-210 in soil cores collected from undisturbed reference locations adjacent to the study site (A) and areas of the study field experiencing soil loss (B) and deposition (C). In each case, the profile distributions associated with the two fallout radionuclides are very similar, indicating that they both respond in a similar manner to soil redistribution. There are, however, some minor differences between the profile distributions for the two radionuclides which reflect their different fallout patterns. In the case of the undisturbed reference sites (A), there is some evidence of greater downward migration of the unsupported lead-210, which undoubtedly reflects the longer period available for such movement to occur. Whereas caesium-137 inputs did not commence until the mid 1950s, those of unsupported lead-210 have been continuous. Equally, because significant caesium-137 fallout effectively ceased in the 1970s, there has been an opportunity for bioturbation and related processes to produce near-constant caesium-137 concentrations in the upper 10 cm of the profile. In contrast, however, the continuous inputs of unsupported lead-210 fallout to the soil surface have maintained a layer of maximum activity at the surface and an exponential reduction in activity below this level. The depth distributions of the two radionuclides in the cores collected from the cultivated field (B and C) exhibit many similarities. In the case of the core collected from the area of the field experiencing soil loss (B), the frequent mixing associated with tillage causes the activities of both radionuclides to be near-constant in the zone extending from the surface to the plough depth (ca. 20 cm). For both radionuclides, the reduction in inventory associated with this eroding site is of a similar magnitude, but the somewhat greater reduction evidenced by unsupported lead-210 (44%) compared to caesium-137 (32%) can be tentatively interpreted as indicating that most of the erosion in the study field has occurred relatively recently (eg. during the past 20 years). If this period postdated the main period of caesium-137 fallout, the radiocaesium would have been mixed within the plough layer, whereas, because of its continuous input, some of the unsupported lead-210 would be concentrated at the surface prior to its incorporation into the profile by cultivation. Erosion of a given depth of soil would therefore result in removal of a greater proportion of the unsupported lead-210 inventory. In the depositional area (C), both caesium-137 and unsupported lead-210 are found to much greater depths, because of the accumulation of sediment carrying both radionuclides. There is therefore evidence of ca. 20 cm of recent deposition at this site. The lack of any significant difference in the depth to which the two radionuclides are found suggests that this deposition has occurred almost exclusively since the period of caesium-137 fallout (i.e. ca. 1960). Furthermore, the lack of any appreciable decline in the activity of unsupported lead-210 in the lower portion of the profile suggests that the deposition at this site may have been even more recent, since burial of the original plough layer will cause its lower portions to be isolated from further inputs associated with the mixing of recent lead-210 fallout into the

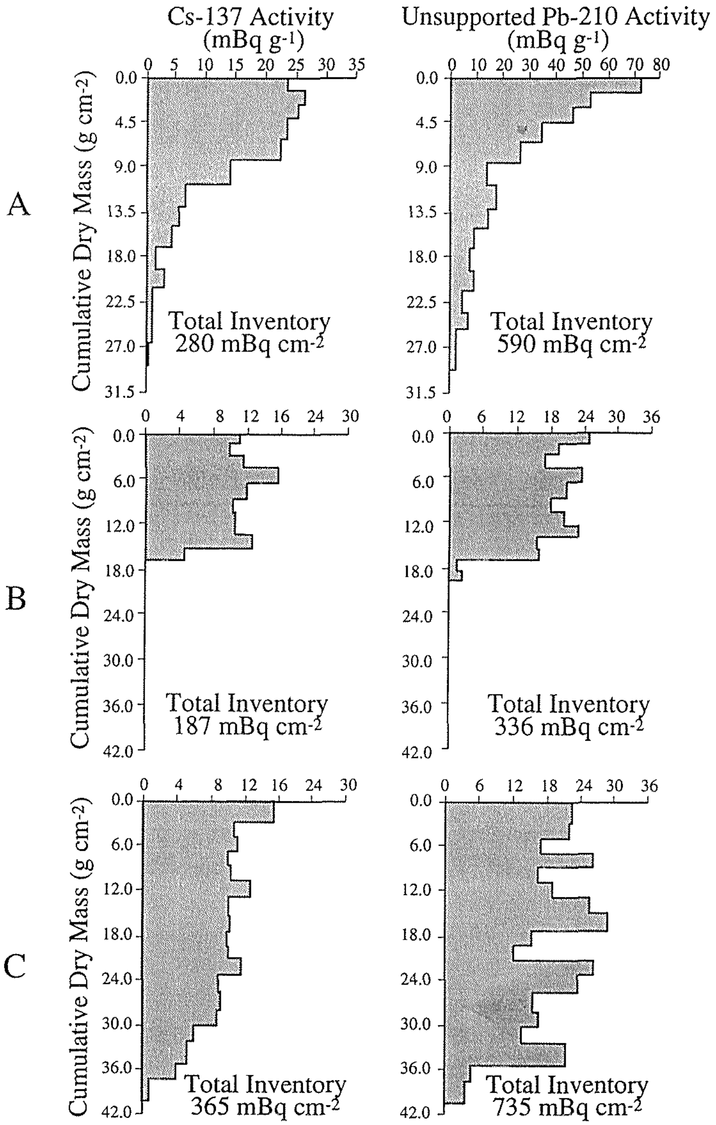

Fig. 1 Representative examples of the vertical distribution of caesium-137 and unsupported lead-210 at undisturbed locations adjacent to the study field (A), and at locations in the study field evidencing erosion (B) and deposition (C).

plough layer by tillage, and unsupported lead-210 activities in the isolated zone would therefore subsequently decline due to radioactive decay.

Comparing the spatial pattern of inventories

Figure 2 presents maps of the caesium-137 and unsupported lead-210 inventories within the study field, interpolated from the grid of core samples using the UNIRAS computer

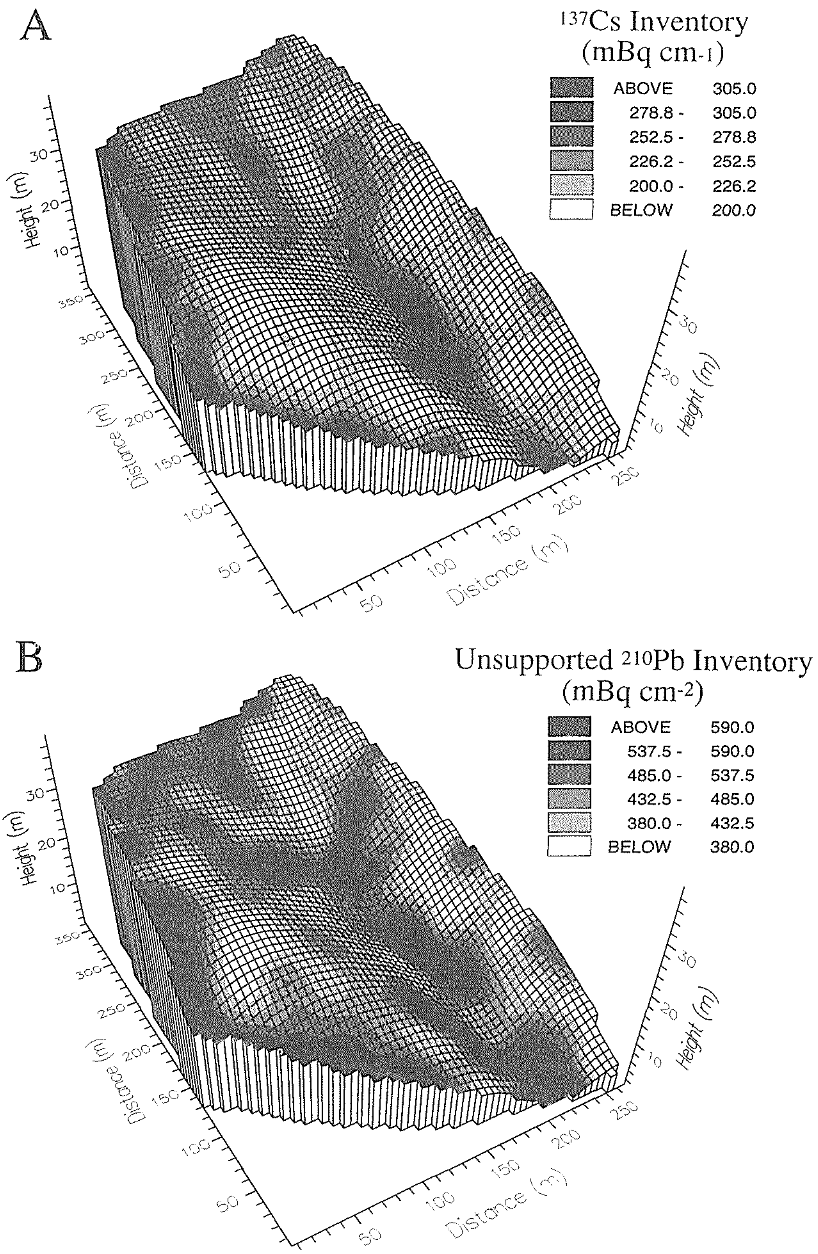

Fig. 2 The distribution of caesium-137 (A) and unsupported lead-210 (B) inventories in the study field.

package. Both maps show very similar patterns, with reduced inventories on the slope convexities and increased inventories within the depression or small valley which traverses the centre of the field, along the hedge boundary at the bottom of the field, and along the fenceline which forms the left-hand boundary. This pattern of reduced and enhanced inventories reflects the impact of both water erosion and soil redistribution by tillage. In particular, the accumulation of both radiocaesium and unsupported lead-210 around the lower end of the depression can be seen as reflecting deposition by surface wash, whereas the low inventories encountered on the upper slopes of the spur which lies to the left of the depression and along the hedge which forms the boundary of the

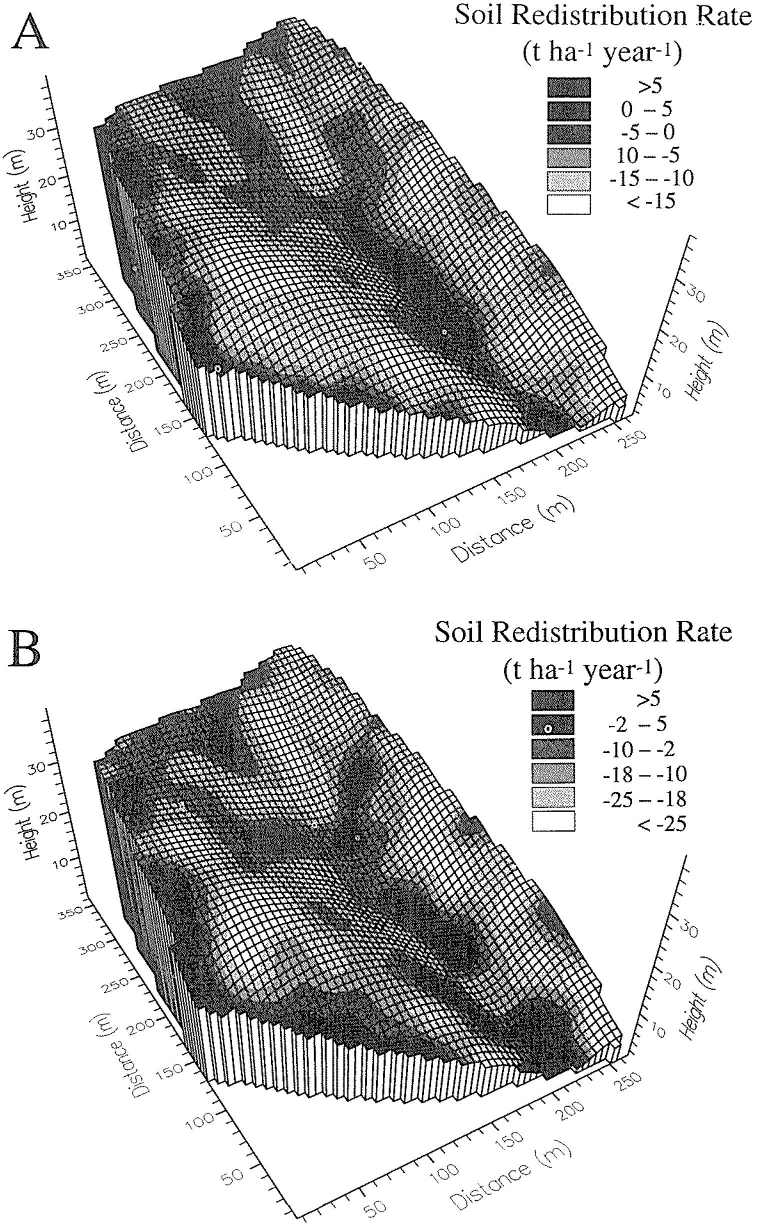

Fig. 3 The distribution of soil redistribution rates within the study field estimated using the caesium-137 (A) and unsupported lead-210 (B) measurements.

field on its right side reflect the role of tillage in the downslope displacement of soil from the slope convexities. Overall, there are few differences between the patterns shown by the two fallout radionuclides, suggesting that they can both be used as a basis for establishing rates and patterns of soil loss within the study field. Considering the field as a whole, the loss of caesium-137 and unsupported lead-210 relative to their respective reference inventories, amounts to 12.7% and 16.7% respectively. The increased loss and slightly greater range of inventory values associated with the unsupported lead-210 measurements could again be seen as indicating that most of the erosion in the study field has occurred relatively recently.

A comparison of the estimates of soil redistribution rates based on the caesium-137 and unsupported lead-210 measurements

By comparing the values of the caesium-137 and unsupported lead-210 inventories obtained for individual sampling points with the equivalent reference inventories for the study site and calculating the degree of increase or reduction involved, it is possible to derive estimates of the rates of soil loss and deposition associated with each sampling point. Walling & Quine (1990) provide a review of the various approaches that have been used to establish relationships between the magnitude of the gain or loss in the caesium-137 inventory and the rate of soil loss or deposition. The authors favour the use of a site-specific mass balance or theoretical accounting procedure (cf. Walling & Quine, 1992) and this approach has been used to convert the caesium-137 inventory data presented in Fig. 2A to an equivalent map of medium-term erosion and deposition rates (Fig. 3A). A similar theoretically-derived calibration relationship has been used to derive the map of long-term average soil redistribution rates presented in Fig. 3B from the unsupported lead-210 inventory data contained in Fig. 2B. In this case the accounting procedure incorporated values for the annual lead-210 deposition flux derived from the reference inventory, the plough depth, and the initial depth distribution of fresh fallout prior to incorporation into the soil profile by tillage, and assumed that cultivation had been continuous for ca. 50 years.

The maps of soil redistribution rates based on the caesium-137 and unsupported lead-210 data presented in Figs 3A and 3B again evidence a high degree of similarity, although the maximum rates of erosion estimated from the unsupported lead-210 data

Table 3 A comparison of soil redistribution rate estimates for the study field based on the caesium-137 and unsupported lead-210 measurements.

Parameter	Caesium-137	Unsupported lead-210
Percentage area eroding (%)	79	76
Percentage area depositing (%)	20	23
Mean erosion rate for the eroding area (t ha^{-1} year^{-1})	10	15
Mean deposition rate for the deposition zones (t ha^{-1} year^{-1})	7.5	9.5
Net erosion rate for the field (t ha^{-1} year^{-1})	6.5	9
Sediment delivery ratio (%)	81	81

are slightly greater than those generated using the caesium-137 data. Table 3 also provides a comparison of the estimates of various general measures of the rates of soil redistribution operating in the field derived using both the caesium-137 and unsupported lead-210 measurements. These values also demonstrate close similarities. Further refinement of the relationships used to estimate erosion and deposition rates could involve incorporation of an estimate of the precise period during which significant erosion has occurred.

PERSPECTIVE

The results presented above suggest that unsupported lead-210 can provide a viable alternative to caesium-137 as a tracer for use in soil erosion investigations. In the case of the field at Butsford Barton investigated in this study, the information on rates and patterns of soil redistribution provided by the unsupported lead-210 measurements were essentially identical to those produced using caesium-137 measurements. Although further studies are required to confirm the potential for using unsupported lead-210 measurements in other environments, it would seem likely that they can be used effectively in areas where either low inventories or complications due to Chernobyl-derived radiocaesium preclude or hamper the use of caesium-137 measurements. Moreover, although further work is clearly required to explore such potential, detailed comparisons of both the depth distributions and the spatial patterns of the inventories of the two fallout radionuclides may provide additional information on the erosional history of a study site. Since measurements of both caesium-137 and unsupported lead-210 can be made simultaneously, if suitable low energy detectors are available, there may be advantages in using both fallout radionuclides in combination in future studies.

Acknowledgement The authors gratefully acknowledge the assistance of Jim Grapes with gamma spectrometry and of Zhang Yusheng and Tom Walling with field sampling.

REFERENCES

Appleby, P. G., Nolan, P., Gifford, D. W., Godfrey, M. J., Oldfield, F., Anderson, N. J. & Battarbee, R. W. (1986) ^{210}Pb dating by low background gamma counting. *Hydrobiol.* **142**, 21-27.

Campbell, B. L., Loughran, R. J. & Elliott, G. L. (1988) A method for determining sediment budgets using caesium-137. In: *Sediment Budgets* (ed. by M. P. Bordas & D. E. Walling) (Proc. Porto Alegre Symp., December 1988), 171-180. IAHS Publ. no. 174.

Joshi, S. R. (1987) Nondestructive determination of lead-210 and radium-226 in sediments by direct photon analysis. *J. Radioanal. Nucl. Chem.* **116**, 169-182.

Krishnaswami, S. & Lal, D. (1978) Radionuclide Limnochronology. In: *Lakes, Chemistry, Geology and Physics* (ed. by A. Lerman), 153-177. Springer-Verlag, New York.

Larsen, R. J. (1985) *Worldwide Deposition of ^{90}Sr through 1983.* Dept. of Energy, New York.

Murray, A. S., Marten, R., Johnston, A. & Martin, P. (1987) Analysis for naturally occurring radionuclides at environmental concentrations by gamma spectrometry. *J. Radioanal. Nucl. Chem.* **115**, 263-288.

Turekian, K. K., Nozaki, Y. & Benninger, L. K. (1977) Geochemistry of atmospheric radon and radon products. *Ann. Rev. Earth Planet. Sci.* **5**, 227-255.

Walling, D. E. & Quine, T. A. (1990) Calibration of caesium-137 measurements to provide quantitative erosion rate data. *Land Degradation and Rehabilitation* **2**, 161-175.

Walling, D. E. & Quine, T. A. (1991) The use of caesium-137 measurements to investigate soil erosion on arable fields in the UK: potential applications and limitations. *J. Soil Sci.* **42**, 147-165.

Walling, D. E. & Quine, T. A. (1992) The use of caesium-137 measurements in soil erosion surveys. In: *Erosion and Sediment Transport Monitoring Programmes in River Basins* (ed. by J. Bogen, D. E. Walling & T. Day) (Proc. Oslo Symp., August, 1992), 143-152. IAHS Publ. no. 210.

Tracer Technologies for Hydrological Systems (Proceedings of a Boulder Symposium, July 1995). IAHS Publ. no. 229, 1995.

Collecting tracers in the vadose zone

FLORIAN M. BRANDI-DOHRN & CHRISTIAN LEIBUNDGUT
Institut für Hydrologie, Albert-Ludwigs-Universität Freiburg, Werderring 4, D-79098 Freiburg, Germany

RICHARD P. DICK
Department of Crop and Soil Science, Agricultural Life Sciences, Oregon State University, Corvallis, Oregon 97331, USA

JOHN S. SELKER
Department of Bioresource Engineering, Gilmore Hall, Oregon State University, Corvallis, Oregon 97331, USA

Abstract Vadose zone soil-pore water sampling techniques have certain inadequacies that limit their range of possible applications. Passive Capillary Samplers (PCAPS), which apply suction to the soil pore-water via a fibreglass wick, have shown promising results in preliminary experiments, in terms of their collection efficiency for water and for bromide tracers. We evaluated 32 PCAPS and 32 ceramic suction cup samplers in the field without disturbing the soil profile, to determine their ability to estimate the mean concentration of three different tracers. The mean concentration of the two sorbing tracers, Rhodamine WT and blue dye, were lower in the suction cup samplers as compared to the PCAPS, which indicates that for sorbing compounds a lower mean concentration can be expected in the suction cup samplers due to preferential flow phenomena. For a bromide tracer, the leachate concentration, as calculated using the arithmetic mean of suction cup sampler measurements, produces a bias of up to −97%, as compared to the flow-weighted means of PCAPS measurements. This was explained by the concept that PCAPS collect bromide concentrations that are strongly influenced by large volumes of preferential flow, whereas suction cup samplers collect bromide concentrations that are influenced mainly by diffusion processes. The initially positive and subsequently decreasing correlation between water flux collected by the PCAPS and bromide content confirmed this concept.

INTRODUCTION

Currently used methods of vadose zone pore liquid monitoring, such as soil coring, porous ceramic suction cup samplers, or zero tension lysimeters, have certain inadequacies that limit their application in vadose zone tracer experiments.

The usefulness of soil coring is limited when measuring changes over time, since it is destructive and does not permit repetitive measurements at the same point. Due to the small size of soil cores, a large number of samples must be taken to characterize spatial variability adequately. Suction cup samplers are widely used due to the ease of installation and their low cost. Some of the difficulties associated with this device are that the soil volume sampled by a suction cup is not known (England, 1974) and that the water flux is not measured. In addition, preferential flow, which constitutes a major part of recharge to groundwater (e.g. Flury *et al.*, 1994), may not be represented correctly in either time (non-continuous vacuum) or space (cross-sectional area too small) (Shaffer *et al.*, 1979; Barbee & Brown, 1986). Sorption, desorption, and cation exchange by porous ceramic cups have also been reported for a variety of solutes (ASTM, 1992). Zero tension pan samplers collect, by definition, only gravitational water. Therefore the soil matrix above the sampler must become saturated prior to sample collection, resulting in a matric potential greater than zero. This can lead to a diversion of flow away from the sampler due to the matrix potential gradient (Jemison & Fox, 1992). Collection efficiency, defined as the ratio of observed to expected percolation, is low, ranging from 45% to 58% (Jemison & Fox, 1992).

Combining the ideas of applying tension to the soil-water and intercepting a large area of flow by a pan, Brown *et al.* (1986) developed the wick pan lysimeter, which has been called the Passive Capillary Sampler (PCAPS). The wetted wick acts as a hanging water column and develops *in situ* a suction of 0-50 cm H_2O, depending on the flux. The matric potential at the top of the wick can be matched to the expected matric potential in the soil as a function of the flux by applying the design equation of Knutson & Selker (1993b). Consequently, the disturbance introduced to the natural flow regime will be minimal. No external application of suction is necessary.

There is currently little information available on the performance of PCAPS under field conditions. Field experiments with a limited number of replicates and under controlled conditions were undertaken by Holder *et al.* (1991) and by Steenhuis *et al.* (1991). The latter found that the two PCAPS tested were a great improvement over the zero-tension lysimeters. The collection efficiency, as estimated using a water balance, was 103% in a silt loam. This compares to 27% for the two zero-tension pan samplers. Recovery of a bromide tracer amounted to 63% in the PCAPS and to 6.5% in the zero-tension pan samplers (Steenhuis *et al.*, 1991). The error in flux measurement of the 32 PCAPS installed in the present study amounted to −20%, as determined using a water balance (Brandi-Dohrn *et al.*, 1994). The objective of this study was to evaluate 32 Passive Capillary Samplers and 32 ceramic suction cup samplers under field conditions, in order to determine their ability to estimate the mean concentration of three different tracers.

MATERIALS AND METHODS

The experiment was carried out on a 0.9 ha field site at the North Willamette Research and Extension Center, Aurora, Oregon, USA. The soil, which is of glaciolacustrine origin, is classified as a Willamette Variant loam, wet (fine-loamy mixed mesic Pachic Ultic Argixeroll). Some basic properties of the soil are listed in Table 1. The climate is classified as temperate oceanic. During the rainy season (November-April), 74% of the 1036 mm total annual precipitation is expected.

PCAPS were constructed from a fibreglass box (32 × 85.5 × 62 cm) and a stainless steel panel, which fitted exactly into the top opening of the fibreglass box (Fig. 1). The panel is subdivided into three 31 × 28 cm sections, each containing one wick and one

Table 1 Organic carbon content, pH, bulk density, particle size distribution, and saturated hydraulic conductivity (K_{sat}) of Willamette Variant loam, wet. The numbers in parenthesis are the coefficients of variation.

Depth	Organic carbon	pH[‡]	Bulk density	Particle size distribution (%)[¶]			K_{sat}
	(g kg^{-1})[†]		(Mg m^{-3})[§]	Clay	Silt	Sand	($\times$ 10^{-6} m s^{-1})[#]
13	12 (13)	6.2 (7)	1.24 (4)	16.8	50.0	33.2	60 (72)
64	1.9 (49)	5.7 (3)	1.35 (1)	27.3	46.8	25.9	7 (115)
114	0.8 (38)	5.8 (2)	1.29 (2)	17.4	38.7	43.9	0.7 (83)

[†] Organic carbon content was measured with a Dohrmann Carbon Analyzer.
[‡] 1:2 solution of soil and distilled water.
[§] Determined from soil cores.
[¶] Determined according to Gee & Bander (1986).
[#] Determined from soil cores using constant head in a tempe cell following Klute & Dirkensen (1986).

collection vessel, thus establishing three sampling units within each sampler. The wick employed was a 2.93 cm Amatex fibreglass wick (braided medium density 1 inch fibreglass wick, #10-863KR-08, Amatex Co., Norristown, Pennsylvania, USA). The wick was cleaned in the manner recommended by Knutson *et al.* (1993a) by combusting it at 400°C in a kiln for 12 h. At installation, the filaments of the wick were spread out radially on the top panel and fixed at the edge of the stainless steel pan with one drop of silicone sealant per strand. Since only non-adsorbing materials (fibreglass, stainless steel, glass, HDPE) (Topp & Smith, 1992) were used, the sampler is also well suited for pesticide monitoring.

High flow porous ceramic cups (5 cm OD, 6 cm length, 1 bar air entry pressure) obtained from Soilmoisture Equipment, Santa Barbara, California, USA (no. 653X01.B1M3) were used to construct the 32 suction cup samplers.

PCAPS were installed from trenches dug with a back hoe. At a depth of 120 cm, 1.2 m long tunnels for the PCAPS were excavated. Upon installation, a good contact with the roof of the tunnel was ensured by filling the top panel of the sampler with sieved native soil and by using two wedges. The samplers were hydraulically isolated from the trench by packing a 4 cm thick dry bentonite seal between sampler and trench. The trenches were refilled by a back hoe. Suction cup samplers were installed 30 cm from each side of every other PCAPS, at the same depth as the PCAPS (1.20 m). A vacuum of 53 kPa was applied to each suction cup sampler on the sample date prior to sample collection.

Three tracers were applied on 4 November 1992: (a) Bromide as a conservative tracer; (b) FD&C Blue No. 1 as a non-conservative tracer to model the movement of compounds; and (c) Rhodamine WT as a backup to the blue dye. Blue dye with a reported retardation factor of 5.6 has been cited to be a surrogate for atrazine (Andreini & Steenhuis, 1990). The tracer solution was applied to neighbouring pairs of PCAPS across a rectangular area of 3 × 7.5 m, using a 3 m wide pesticide sprayer in eight passes. On average, samples were taken every 10.4 days from 4 November 1992 to 10 June 1993.

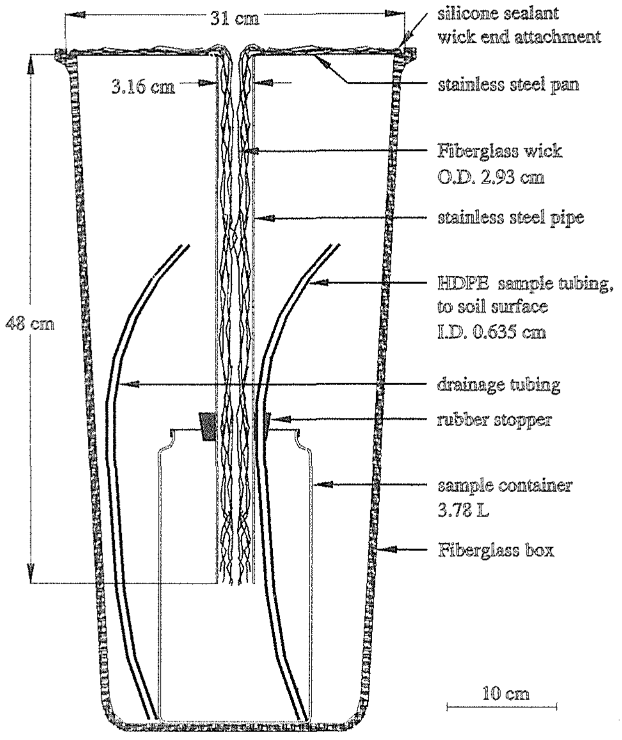

Fig. 1 Cross-sectional view of PCAPS (drawn to scale).

RESULTS

Blue dye and Rhodamine WT breakthrough

Chemical compounds with strong sorptive behaviour, such as pesticides or the dyes used in this experiment, are most susceptible to leaching via macropores shortly after application at times of high infiltration, such as during irrigation or heavy precipitation events (Andreini & Steenhuis, 1990). Macropores, such as cracks or burrows, are most pronounced in heavy soils under dry conditions, but essentially all soils contain some macropores (Beven & German, 1982).

Upon installation, macropores were observed just above the samplers with an average incidence of 0.8 macropores per sampler, with a diameter ranging from 0.5 cm to 1 cm. Since these macropores are too small for mice and too big for earth worms, they probably originate from root activity. Old roots and one old tree trunk found in the profile support this hypothesis. Soil moisture content at the time of tracer application (4 November) was not measured. However, it can be assumed to be close to saturation in the upper part of the profile, since some large precipitation events 5 days before tracer application added a total of 82 mm. According to extrapolated matric potential measurements beginning two weeks later, the soil moisture content at the depth of the samplers was still fairly low.

Observed dye concentrations were very low, with a maximum observation of 0.15% of the initial concentration, C_o, of Rhodamine WT and 0.08% of C_0 for blue dye, 21 and 37 days after application, respectively. This implies that preferential flow-paths were not active immediately after application. Several reasons might explain this fact. Backfilling and twice compacting the trench with a back hoe, might have damaged the inherent soil structure through vibration. This is, however, unlikely given the firm to very firm consistency of the soil. A more likely explanation is that the Ap horizon, where the development of a macropore system is hindered by tillage, and which was close to saturation at the time of application, served as a mixing zone for the tracers. Thus the tracers were transported via matrix flow through the Ap horizon before reaching a macropore system. Therefore, they were exposed to a much greater surface area and to longer residence times. Greater surface area and longer residence times would both greatly enhance sorption, thus explaining the very low early breakthrough due to macroporosity.

Comparison of concentration measurements as obtained by suction cup samplers and PCAPS

At this site, the bromide application increased the mean seasonal bromide concentration to 5.2 mg l^{-1}, which is 370 times the background level. Soil heterogeneities cause transport of this solute to be highly variable. The percentage of the 32 suction cup samplers, which collected bromide concentrations three times greater than the background concentration, was 4%, 8 and 15 days after tracer application, and 32%, 21 days after application. In comparison, the percentage of the 32 PCAPS, which collected bromide concentrations three times higher than the background concentration, was 12%, 8 days after tracer application, 14%, 15 days after application, and 77%, 21 days after application. This indicates that the smaller size of the suction cup sampler results in a lower likelihood of this device being placed within preferential flow paths.

If one combines all samples obtained, in the way that an aquifer integrates all recharge, the concentration will be the flow-weighted concentration. Hence, taking a flow-weighted mean of concentration measurements is usually preferred to taking a simple arithmetic mean. When using suction cup samplers, the mean solute concentration is estimated by the arithmetic mean of sample concentrations, since the device gives no data on flux.

The arithmetic mean of the 32 suction cup samplers was compared to the flow-weighted mean of the corresponding 16 PCAPS for bromide, Rhodamine WT, and blue dye. The significance of the difference was evaluated using a two-tailed paired difference t-test, pairing the arithmetic mean of the two suction cup samplers adjacent to each PCAPS with the flow-weighted mean of this PCAPS. The mean bromide concentration in the suction cup samplers deviated by up to −97% in the early part of the tracer breakthrough curve, and by 32% by the end of the season (Fig. 2). The mean seasonal concentration in the suction cup samplers was on average 2.2 mg l^{-1}, or 34%, lower than in the PCAPS. This deviation was significant ($P < 0.05$) for 41% of the season (Table 2).

The arithmetic mean will be a biased estimator of the true, flow-weighted mean, if the volume collected and solute content are not independent. This is the case when (a)

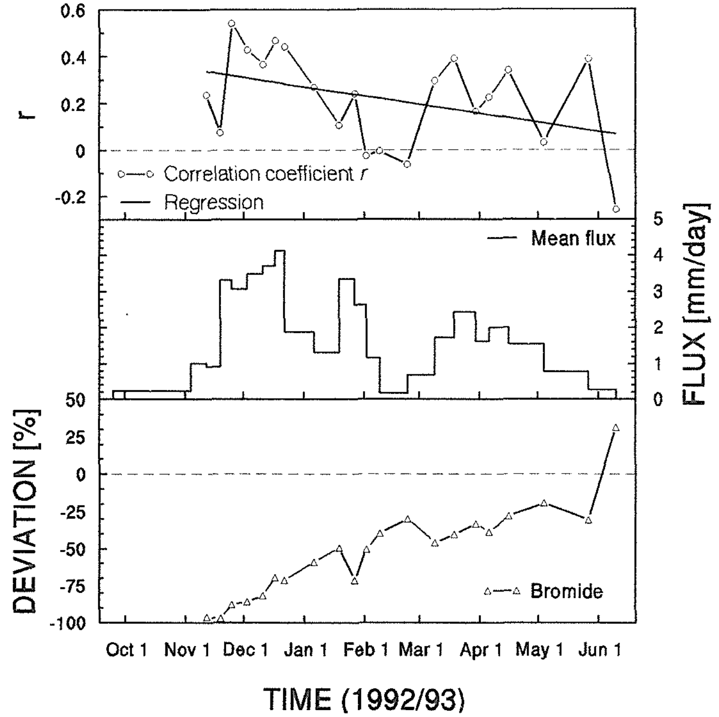

Fig. 2 Correlation coefficient r between flux and bromide concentrations for the PCAPS, mean flux between sampling dates, and deviation of the arithmetic mean concentration in suction cup samplers from the flow-weighted mean concentration in PCAPS for bromide. The data presented correspond to the rising portion of the bromide breakthrough curve.

water percolates through the vadose zone faster than its solute content can equilibrate with the solute content of the matrix pore-water; and (b) if the fast percolating leachate moving at lower tensions is associated with a larger flux than the slow matrix flow. The faster percolating water is usually termed preferential flow. If, for example, the concentration of the preferential flow is lower than that of the matrix flow, then flux and solute content will correlate negatively. Consequently, an arithmetic mean will be an

Table 2 Deviation of suction cup sampler mean from flow-weighted PCAPS mean.

	Deviation (%)		
Solute	Observed range	Seasonal mean	Percent time significant[†]
Bromide	−97 to 32	−34	41
Blue Dye[‡]	−100 to −58	−78	50
Rhodamine WT[‡]	−81 to 34	−41	25

[†] Percent of sampling dates when $P < 0.05$.

[‡] Values for the four sampling dates after tracer application.

upward biased estimator of the true, flow-weighted mean, since it does not take into account the large amounts of water associated with lower concentrations.

Here, in the case of the one-off bromide application, the concept is that the tracer will be distributed by diffusion and dispersion more or less evenly throughout the Ap horizon, the mixing zone. Beginning in the B horizon, the concentration of any preferential flow will be higher than the overall matrix concentration. Over time, as the bromide peak moves downwards through the profile, the Ap horizon will be depleted of its bromide content. This will result in a gradual change to a lower concentration in the preferential flow and to a higher concentration in the matrix flow. In other words, the arithmetic mean will be a downward biased estimator of the flow-weighted mean for the rising portion, and an upward biased estimator for the decreasing portion of the tracer curve.

When comparing the arithmetic mean of the suction cup samplers with the flow-weighted mean of the PCAPS, the basic assumption is that both devices collect the same proportions of preferential and matrix flow. However, as was pointed out earlier, the suction cup samplers collect a smaller proportion of preferential flow. This will result in an even stronger bias of the arithmetic mean of the suction cups as compared to the flow-weighted mean of the PCAPS. As can be seen from Fig. 2, the deviation of the arithmetic mean of the suction cup samplers reflects the above trend: On the rising portion of the tracer breakthrough curve, it is lower compared to the flow-weighted mean of the PCAPS. As the tracer moves downward, it becomes more and more associated with the concentration of the matrix flow. The suction cup sampler mean converges on, and surpasses, the PCAPS mean as the tracer breakthrough peak comes closer to the PCAPS.

Similarly, the correlation between bromide content and volume collected in the PCAPS is positive during the initial stage of the tracer experiment (Fig. 2). Because the bromide peak is moving closer to the samplers, the bromide concentration of the preferential flow will decrease compared to the concentration of the matrix flow, which results in a decreasing correlation coefficient between flux and bromide concentration with time. The *P*-value of the decreasing trend with time is 0.07.

The mean Rhodamine WT concentration was lower by 0.02 g l^{-1} (50%) in the suction cup samplers, as compared to the PCAPS for 12 November to 3 December (four sample dates after tracer application), when significant amounts of Rhodamine WT were observed. On 25 November, the deviation was −95%, which was significant. On 12 and 19 November, however, the deviation was positive (46% and 37%). In the case of these first two sampling dates for the suction cup samplers, the apparent fluorescence might have been influenced by elutes from the ceramic cups.

Similarly, blue dye concentrations were lower by 0.03 mg l^{-1} (78%) in the suction cup samplers as compared to the PCAPS, for 12 November to 3 December. The deviation was significant only on 25 November and consistently negative by at least 58%. These numbers indicate that for sorbing compounds a lower mean concentration in the suction cup samplers is to be expected due to preferential flow phenomena. Further research at different sites is necessary to provide more widespread evidence of this behaviour.

CONCLUSIONS

The selection of a sampler depends on the research goal, the site characteristics, and the length of the experiment. The criteria listed below will assist in the selection of an appropriate sampler.

A suction cup sampler will give a close estimate of the mean concentration of the recharge to the groundwater, if the transport processes are fairly uniform. Since field soils and infiltration patterns are rarely uniform, we follow Biggar & Nielsen (1976) and recommend that suction cup samplers should be used for monitoring relative changes in concentration. An estimate of the mean concentration of the leachate obtained using suction cup samplers is likely to be biased, since large quantities of preferential flow characterized by solute concentration different from that of the matrix flow are not correctly represented by suction cup sampler measurements. This is due to the small size of the suction cup sampler and the absence of measurements of water flux. Therefore estimates of the mass transport of a solute obtained using suction cup samplers are questionable. Although the percolation rate may be estimated from a water balance, the lognormal distribution of the magnitude of the flux (Biggar & Nielsen, 1976) and the correlation between flux and solute concentration prohibit multiplying the simple arithmetic means of these two parameters. Particularly for pulse-applied tracers, a strong correlation is expected due to the highly variable transport. If sampling for sorbing compounds, the suction cup sampler will always underestimate the mean concentration, because concentration and flux will be positively correlated.

Since the PCAPS collect both matrix flow and preferential flow, they will give an accurate estimate of the soil-water flux for most soils, as long as the significant water movement takes place at tensions from 0 to 50 cm. Knowing the soil-water flux permits the calculation of a flow-weighted mean concentration and a mass balance for the pollutant concerned. To our knowledge, sorbing compounds can be sampled without introducing any error to the measurement. Therefore the PCAPS are well suited for monitoring tracers or pesticide leaching.

Acknowledgement We thank the Oregon Water Resources Research Institute, Corvallis, Oregon, USA, and the USDA CSRS Special Water Quality Program Grant #91-34214-6140 for funding this study. We also thank Bob Christ and Joan Sandeno for their invaluable assistance, and Christoph Kuells for his comments on the paper.

REFERENCES

Andreini, M. S. & Steenhuis, S. T. (1990) Preferential paths of flow under conservation and conventional tillage. *Geoderma* **46**, 85-102.

ASTM (1992) Standard guide for pore-liquid sampling from the vadose zone. ASTM Subcommittee D18.21 on Ground Water Vadose Zone Investigations, Designation D 4696-92. ASTM, Philadelphia, Pennsylvania.

Barbee, G. C. & Brown, K. W. (1986) Comparison between suction and free drainage soil solution sampler. *Soil Sci.* **141** (2), 149-154.

Beven, K. & German, P. (1982) Macropores and water flow in soils. *Wat. Resour. Res.* **18**(5), 1311-1325.

Biggar, J. W. & Nielsen, D. R. (1976) Spatial variability of the leaching characteristics of a field soil. *Wat. Resour. Res.* **12**(1), 78-84.

Brandi-Dohrn, F., Dick, R. P., Wang, M.-C. & Selker, J. S. (1994) Field evaluation of passive capillary samplers. Submitted to *Soil Sci. Soc. Am. J.*

Brown, K. W., Thomas, J. C. & Holder, M. W. (1986) Development of a capillary wick unsaturated zone water sampler. Cooperative Agreement CR812316-01-0. US Environmental Protection Agency, Environmental Monitoring Systems Laboratory, Las Vegas, Nevada.

England, C. B. (1974) Comments on "A technique using porous cups for water sampling at any depth in the unsaturated zone" by Warren W. Wood. *Wat. Resour. Res.* **10**(5), 1049.

Flury, M., Flühler, H., Jury, W. A. & Leuenberger, J. (1994) Susceptibility of soils to preferential flow of water: A field study. *Wat. Resour. Res.* **30**(7), 1945-1954.

Gee, G. W. & Bander, J. W. (1986) Particle Size Analysis. In: *Methods of Soil Analysis* (ed. by A. Klute), 383-411. Part 1. 2nd edn. Agron. Monographs 9, ASA, Madison, Wisconsin.

Holder, M., Brown, K. W., Thomas, J. C., Zabcik, D. & Murray, H. E. (1991) Capillary-wick unsaturated zone soil pore water sampler. *Soil Sci. Soc. Am. J.* **55**, 1195-1202.

Jemison, J. M. & Fox, R. H. (1992) Estimation of zero-tension pan lysimeters collection efficiency. *Soil Sci.* **154**(2), 85-94.

Klute, A. & Dirkensen, C. (1986) Hydraulic conductivity and diffusivity: Laboratory methods. In: *Methods of Soil Analysis* (ed. by A. Klute), 687-734. Part 1. 2nd edn. Agron. Monogr. 9. ASA, Madison, Wisconsin.

Knutson, J. H., Lee, S. B., Zhang, W. Q. & Selker, J. S. (1993a) Fiberglass wick preparation for use in Passive Capillary Wick Soil Pore-Water Samplers. *Soil Sci. Soc. Am. J.*

Knutson, J. & Selker J. S. (1993b) Unsaturated hydraulic conductivities of fiber glass wicks and designing Capillary Wick Pore-Water samplers. *Soil Sci. Soc. Am. J.*

Shaffer, K. A., Fritton, D. D. & Baker, D. E. (1979) Drainage water sampling in a wet, dual-pore system. *J. Environ. Qual.* **8**(2), 241-246.

Steenhuis, T. S. *et al.* (1991) *In situ* vadose zone water quality sampling: Methods for preferential flow conditions. In: *Through the 1980's and into the 1990's.* (Proc. ASTM Conference on Groundwater and Vadose Zone Investigations, San Diego, California, January 1991).

Topp, E. & Smith, W. (1992)Sorption of the herbicides atrazine and metachlor to selected plastics and silicone rubber. *J. Environ. Qual.* **21**, 316-317.

Tracer Technologies for Hydrological Systems (Proceedings of a Boulder Symposium, July 1995). IAHS Publ. no. 229, 1995.

Determination of the flow and transport parameters of the unsaturated zone using dye tracers

J. MEHLHORN, Ch. LEIBUNDGUT
Department of Hydrology, University of Freiburg, Werderring 4, 79098 Freiburg, Germany

HANS ROGG
FEW (Energy and Water Supply of Freiburg), Tullastraße 61, 79108 Freiburg, Germany

Abstract Usually the determination of the flow and transport parameters of the unsaturated zone of groundwater aquifers is limited by monitoring conditions in field tracer experiments since the sampling has to be done within the saturated zone. Using a double tracer experiment and its evaluation by a convolution integral introduces a method to determine the flow and transport parameters of the unsaturated zone without the influence of the saturated zone. The method developed was tested successfully in a case study and the parameters determined were considered reliable.

INTRODUCTION

Field tracer experiments in the vadose zone are limited by monitoring conditions. In the literature three different methods are described. The first technique carries out the experiment in a lysimeter. In the second case the tracer is applied to the top of a slope and the samples are taken in a spring at the foot of the slope. The third technique monitors the tracer by suction cups or passive capillary samplers (Brandi-Dohrn *et al.*, 1995) placed into the unsaturated zone.

Conducting the experiment in field conditions each of the above described methods has its disadvantages. Normally there is no lysimeter available in the study area. Very often the location is situated in a plain or there are no springs in the test area. Using suction cups causes problems if the thickness of the unsaturated zone exceeds some metres and the layer contains greater rocks. The objective of this study is to develop a practicable method to determine the flow and transport parameters of the unsaturated zone by a field tracer experiment.

METHOD

The requirement for the method described below is the existence of two corresponding wells in the study area, one for tracer injection and the other for tracer sampling. The double tracer experiment is split into two phases (Fig. 1). First the tracer is applied directly into the groundwater via the injection well and the tracer breakthrough is measured in the second well. In the second phase the tracer is applied to the surface over

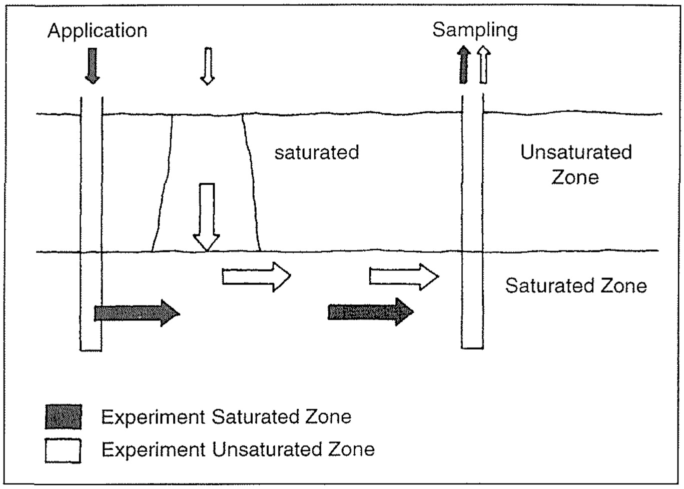

Fig. 1 Arrangement of field tracer experiment.

the flow pathway of the first experiment. To get steady state conditions the unsaturated zone is saturated by water at the point of application. After application the steady state conditions are maintained by water rinsing. The tagged water percolates through the unsaturated zone under saturated conditions and is transported later by the groundwater flow to the sampling point.

Dye tracer experiments are black box experiments. The input is the known mass or concentration of tracer which is injected into the system at time $t = 0$. The output is the measured concentration as function of time $C(t)$ (Fig. 2(a)). Fitting theoretical curves to the measured concentration curve yields the wanted system parameters. For porous media the time dependent concentration $C(t)$ at the sampling point can be calculated with the dispersion model (Maloszewski, 1992):

$$C(t) = \frac{M}{Qt_{mean}} \frac{1}{\sqrt{4\pi P_D (t/t_{mean})^3}} \exp\left[-\frac{(1-t/t_{mean})^2}{4P_D t/t_{mean}}\right] \tag{1}$$

where M and Q are the injected mass of tracer and groundwater recharge respectively, $t_{mean} = x/v_{mean}$ is the mean residence time, x the distance between the injection and sampling points, v_{mean} the mean water velocity and $P_D = \alpha_L/x$ is the dispersion parameter with longitudinal dispersivity α_L.

Both phases of the tracer experiment are black box experiments. The black box of the first experiment considers the saturated zone as a single system. The flow and transport parameters of the aquifer are determined in the above described way. In the second phase the tracer passes the unsaturated and the saturated zone. Now the black box contains two systems (Fig. 2(b)). System 1 represents the unsaturated and system 2 represents the saturated zone. The input into the black box is known and the output is measured. Wanted is the output of system 1, which serves as input into system 2. The reaction of system 2 to a given input is known from the first phase. If the reaction function $h(t - u)$ of a time invariant and linear system is known, than the output

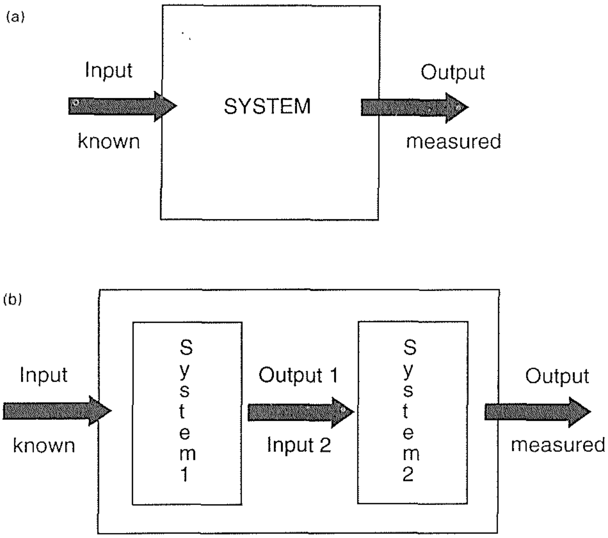

Fig. 2 Conceptual black-box models for experiment (a) saturated zone and (b) unsaturated zone.

function a(t) to any input function e(u) can be calculated by the convolution integral (Dyck & Peschke, 1983):

$$a(t) = \int_0^t e(u)\, h(t-u)\, du \tag{2}$$

Under saturation the tracer transport condition in the unsaturated zone is equal to that of the saturated zone (Matthess, 1984). Therefore, the input $e(u)$ to system 2 is a function given by equation (1) and can be taken, however, with the parameters $P_{D,sys1}$ and $t_{mean,sys1}$ unknown. Theoretical curves $a(t)$, calculated via the convolution integral according to equation (2), are then fitted with the method of least squares to the measured output of system 2. The result of the least square method are the values $P_{D,sys1}$ and $t_{mean,sys1}$ which describe the flow and transport behaviour of the unsaturated zone in saturated conditions.

CASE STUDY

The study area with the two groundwater collecting drains North and South and the main drain SII is depicted in Fig. 3. Quaternary glacio-fluvial sands and gravels with a thickness of approximately 10 m form the groundwater layer. The rivers Dreisam and Brugga bound the investigation area. The groundwater yield is 2500 m^3 day^{-1}. The "collecting drain North" can be reached over the shafts Z, M and E. In front of the drains a groundwater monitoring system with the wells PE18-PE21 and PE24 is installed. The groundwater table gradient is directed to the collecting drains. Due to the high concentration of bicarbonate the groundwater is slightly acid (pH = 6.3).

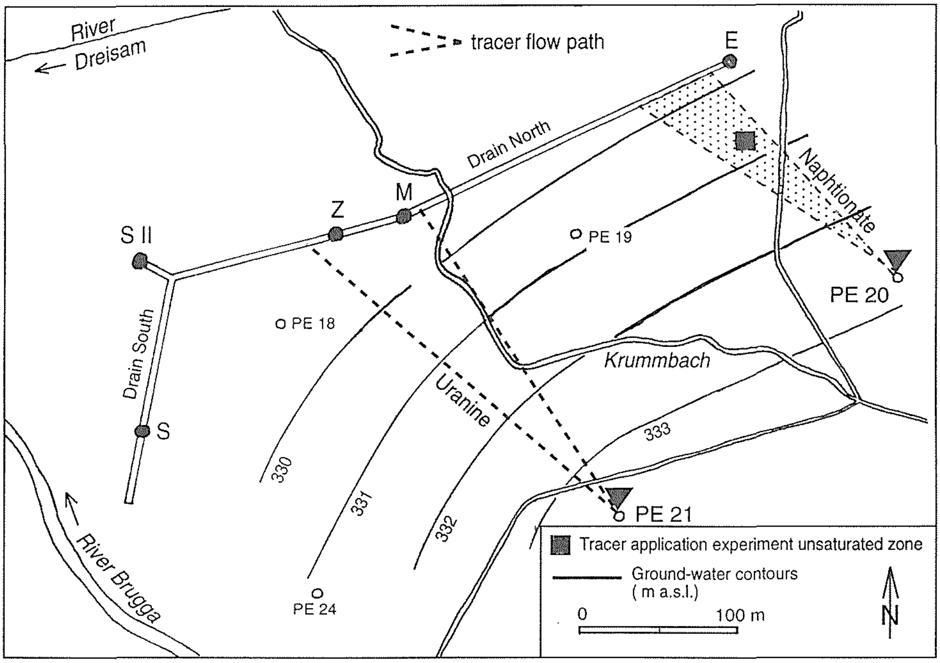

Fig. 3 Study area.

Tracer experiment: saturated zone

To determine flow pathways and transport parameters in the saturated zone two tracer experiments were carried out. Uranine was injected to PE21 and naphthionate was injected to PE20. Automatic sampling devices were installed in SII and the shafts Z, M and E. In addition daily samples were taken in PE18, PE19, PE24 and S. At the sampling points E, PE18, PE19, PE24 and S no tracer was found. The highest concentrations of naphthionate and uranine were detected in M and Z, respectively. Due to these facts and the known groundwater table gradient the flow pathways could be determined (Fig. 3). The tracer breakthrough curves of uranine in SII and of naphthionate in M show clearly a strong difference between the uranine and naphthionate breakthroughs (Fig. 4). The naphthionate curve shows a peaked shape with little tailing whereas the uranine breakthrough curve ascends only slowly, without a clear peak but a strong tailing. This shape of the uranine breakthrough curve is explained by unexpected strong reversible sorption processes because of the slight acid environment. Due to sorption uranine was not used further for determination of the flow and transport parameters. The parameters v_{mean} and P_D were determined by fitting the theoretical curve $C(t)$ of equation (1) to the measured naphthionate breakthrough curve. The resulting best fit curve is shown in Fig. 4. The values of P_D and v_{mean} obtained from the naphthionate breakthrough curve are listed in Table 1.

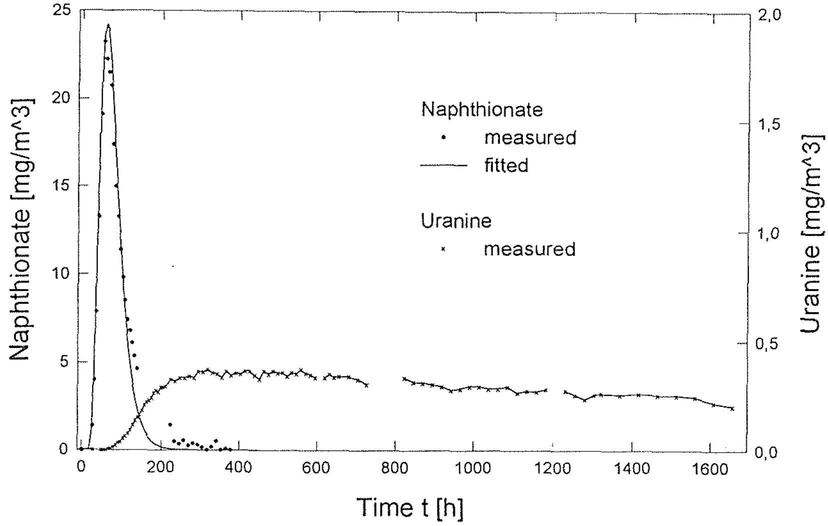

Fig. 4 Measured uranine and measured and fitted naphthionate tracer breakthrough curves experiment saturated zone.

Tracer experiment: unsaturated zone

The point of tracer application was chosen to be above the flow pathway of naphthionate in the experiment "Saturated Zone" (Fig. 3). In order to obtain a tracer breakthrough curve including both the saturated and the unsaturated zone with emphasis on the unsaturated part the distance of the flow pathway in the saturated zone was reduced to 50 m. The groundwater table was situated approximately 10 m below the ground surface. The sampling points of the experiment "Saturated Zone" could be maintained for this experiment.

In order to get steady state conditions and to avoid a high tracer loss in the unsaturated zone a special application equipment was used. The so-called double-square system, designed on the basis of the double-ring infiltrometer, is composed of two different sized steel frames with square cross sections. The smaller (1 m^2 area) is situated in the lager (2 m^2 area) square. So there are two equal areas of 1 m^2. Tracer application was carried out in the following way:

- saturation of the unsaturated zone on both squares by 16 m^3 water beginning one day before application,
- application of the tracer only in the inner square, and
- rinsing the application site by 30 m^3 water on both squares for two days.

Table 1 Parameter values experiment saturated zone.

t_{mean} [h]	x [m]	v_{mean} [m h^{-1}]	P_D	α_L [m]
75.7	190	2.51	0.077	14.6

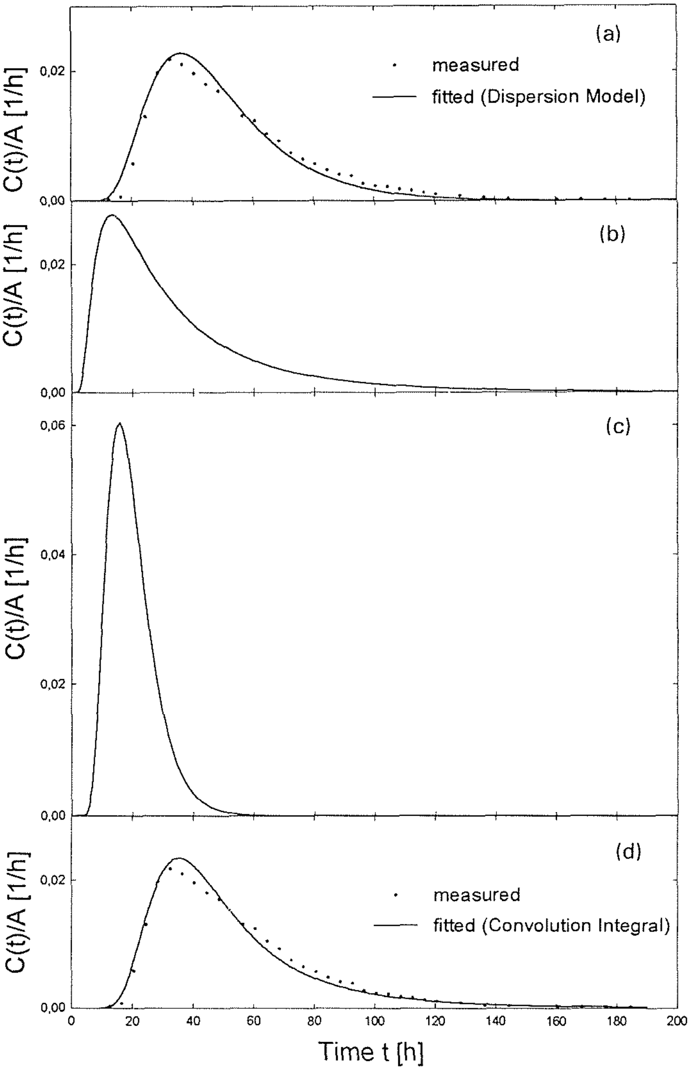

Fig. 5 Measured and with dispersion model fitted (a) naphthionate tracer breakthrough curves, experiment unsaturated zone (b) with convolution integral calculated input function, (c) reaction function and (d) measured and with convolution integral fitted output function.

Using the double square system for tracer injection the tagged water was protected by a shield of water from the outer square during percolation through the unsaturated zone. In this way the tracer loss in the unsaturated zone due to capillary suction was minimized and steady state conditions were achieved.

The tracer breakthrough measured at the sampling point M represents the combination of the unsaturated and the saturated zone (Fig. 5(a)). In a first evaluation the combination of the unsaturated and the saturated zone is considered as a single system. This simplification is possible due to the saturation of the vadose zone. Fitting the measured breakthrough curve with equation (1) leads to the flow and transport parameters representing the combination of the unsaturated and the saturated zone (Table 2, line 3). The best fit to the measured breakthrough curve is shown in Fig. 5(a).

Using the convolution integral of equation (2) it is possible to determine the flow and transport parameters of the unsaturated zone without the influence of the saturated zone. The input function e(u) in equation (2) is the wanted reaction function of the unsaturated zone. The reaction function h(t-u) of the saturated zone is known from the experiment "Saturated Zone". The input function e(u) and reaction function h(t-u) are functions of the type given by equation (1). The output function a(t) is measured in experiment "Unsaturated Zone". Because of the reduced flow distance in the saturated zone from 190 m to 50 m the residence time was linearly reduced to the value t_{mean} = 20 h with the assumption of constant flow velocity v_{mean} = 2.5 m h^{-1}. The dimensionless parameter P_D = 0.077 was maintained. With these parameters the reaction function h(t-u) of the saturated zone was fixed (Table 2, line 2 and Fig. 5(c)). By varying the parameters P_D and t_{mean} in the input function e(u) the convolution integral of equation (2) was fitted to the measured breakthrough curve. The parameters P_D and t_{mean} of the unsaturated zone determined by the best fit method are listed in Table 2, line 1. The corresponding input function is plotted in Fig. 5(b). The best fit curve a(t) is shown in Fig. 5(d) together with the measured breakthrough curve. For purpose of comparison the curves in Fig. 5 are normalized to have equal areas:

Table 2 Parameter values experiment unsaturated zone.

	t_{mean} [h]	x [m]	v_{mean} [m h^{-1}]	P_D	α_L [m]
Input	31.9	10	0.31	0.34	3.40
Reaction	20.0	50	2.5	0.077	3.85
Output	50.4	60	1.19	0.098	5.87

$$\int_0^\infty \frac{C(t)}{A}\mathrm{d}t = 1 \tag{3}$$

DISCUSSION AND CONCLUSIONS

With the combination of the double tracer experiment and the evaluation of the tracer breakthrough curve by using the convolution integral it is possible to determine the flow and transport parameters of the unsaturated zone. The determined flow velocity in the described field experiment was 0.31 m h^{-1} with longitudinal dispersivity of 3.4 m. In an independent investigation using natural tracers ^{18}O and nitrate the seepage velocity in the unsaturated zone of the study area after intensive precipitation was 0.12 m h^{-1} (Ehrminger *et al.*, 1993). Nemeth (1983) observed seepage velocities of about several decimetres per hour in glacio-fluvial gravels after saturation because of intensive rainfall. Compared to the result of the natural tracer investigation the result of the dye tracer experiment seems to be reliable. Certainly the observed flow velocity v_{mean} in the dye tracer experiment is three times higher than the flow velocity found for the natural tracers, but this can be explained by the saturated conditions of the unsaturated zone in the dye tracer experiment. The value of the dye tracer experiment represents the unsaturated zone at the application site, whereas the values obtained by natural tracers describe more the areal behaviour. The high dispersivity expresses high variability of the flow velocity in the unsaturated zone. This represents the different flow velocities in the soil because of the composition of macro and micro pores and the difference between the soil and the unsaturated part of the groundwater layer. The soil is sandy with a great portion of fluvial loam whereas the groundwater layer is composed of sands and gravels streaked with fluvial loam layers. This horizontal stratification and – in addition – imbrication, which can often be observed in gravel deposits (Bouwer, 1978) explain the high anisotropy of the groundwater layer. Horizontal flow velocity exceeds the vertical flow velocity by a factor of eight.

Compared with other methods the method described leads to flow and transport parameters of the unsaturated zone under saturated conditions. Due to saturation steady state conditions in the unsaturated zone are established and the parameters determined represent the upper boundary of the flow and transport behaviour of the unsaturated zone. These extreme values are useful for the outlining of protection zones of intake areas because with these values the maximum risk can be assessed.

The high dispersivity determined shows clearly that macro and micro pores control the water flow through the unsaturated zone and that both systems are recorded by the method presented. Using suction cups in the unsaturated zone implies a relatively low chance of monitoring a preferential flow (Bronswijk *et al.*, 1995), so that the effect of the macro pore system on the flow and transport behaviour of the unsaturated zone is neglected. This implies a false parameter estimation and can lead to an incorrect outlining of protection areas.

As a recommendation for further investigations different techniques such as suction cups or PCAPS for tracer sampling should be used in combination with the method described to compare theoretically derived and measured tracer breakthrough curves and to improve the estimation of flow and transport parameters in the unsaturated layer of an aquifer.

REFERENCES

Bouwer, H. (1978) *Groundwater Hydrology*. McGraw-Hill Kogakusha, Tokyo.

Brandi-Dohrn, F. M., Leibundgut, C., Dick, R. P. & Selker, J. S. (1995) Collecting tracers in the vadose zone. In: *Tracer Technologies for Hydrological Systems* (ed. by Ch. Leibundgut). IAHS Publ. no. 229 (this volume).

Bronswijk, J. J. B., Hamminga, W. & Oostindie, K. (1995) Field-scale solute transport in a heavy clay soil. *Wat. Resour. Res.* **27**, 517-526.

Dyck, S. & Peschke, G (1983) *Grundlagen der Hydrologie*. Ernst & Sohn, Berlin.

Ehrminger, B., Herdeg, U., Graf, W. & Trimborn, P. (1993) *Isotopenhydrologische Untersuchungen im Einzugsbereich des Wasserwerks Ebnet*, 136-150. GSF-HY 1/94.

Maloszewski, P. (1992) *Bemerkungen über die Interpretation von Makierversuchen im Grundwasser*, 2-19. GSF HY 1/92.

Matthess, G. (1984) Geochemical and transport processes in the unsaturated zone during groundwater recharge. In: *Proc. Int. Symposium RIZA*, vol. 1, 7-17.

Nemeth, G. (1983) Das Verhalten von Sickerfronten in ungesättigten Kiesen der Münchner Schotterebene. *Z. Dt. Geol. Ges.* **134**, 657-668.

6 Surface Water and Runoff Separation

Tracer Technologies for Hydrological Systems (Proceedings of a Boulder Symposium, July 1995). IAHS Publ. no. 229, 1995.

Stream hydrograph separation on two small Guianese catchments

T. BARIAC, A. MILLET, B. LADOUCHE & R. MATHIEU
Laboratoire de Biogéochimie Isotopique, Université Pierre et Marie Curie,
Case 20, 4, place Jussieu, F-75252, Paris, France

C. GRIMALDI & M. GRIMALDI
Present address: Station de Science du Sol, INRA, 65, rue de St-Brieuc, Rennes,
Cedex, France

P. HUBERT & H. MOLICOVA
Centre d'Informatique Géologique, École des Mines de Paris, 35, rue Saint-
Honoré, F-77305 Fontainebleau, France

L. BRUCKLER & P. BERTUZZI
Station de Science du Sol, INRA, Domaine de Saint-Paul, BP 91, 84143,
Montfavet, France

J. BOULÈGUE
Laboratoire de Géochimie et de Métallogénie, Université Pierre et Marie Curie,
Case 124, 4, place Jussieu, F-75252 Paris, France

Y. BRUNET
Station de Bioclimatologie, Domaine de la Grande Ferrade, 71, Avenue Édouard
Bourleaux, BP 81, F-33883 Villenave-d'Ornon, France

R. TOURNEBIZE
Station d'AgroPédologie de la Zone Caraïbe, INRA, Domaine Duclos Petit-Bourg,
BP 1232, F-97185 Pointe-à-Pitre, France

A. GRANIER
Station de Recherches Forestières, INRA, Champenoux, F-54280 Seichamps,
France

Abstract Intensive sampling of runoff was carried out in a tropical forest on two small but highly responsive catchments (Saint Elie's track, French Guiana). After deforestation, one of them is now a meadow, while the other is still a primary forest. A hydrograph separation, based on ^{2}H, ^{18}O, and hydrochemical tracers, has been performed to separate streamflow into subsurface quick flow, mixing zone and groundwater slow flow contributions. Nevertheless, soil water (surface and deep layers) plays a significant role in the generation of stream water chemistry. Applying some reasonable assumptions at different steps of storm flow generation, a two, then a three, and finally, a two-component model recognizing contributions from different compartments can explain the temporal variation of the geochemical tracers observed in the streamflow response in the study area.

INTRODUCTION

The hydrograph separation in different components (direct runoff on ground surface, subsurface interflow and groundwater outflow) is classically undertaken from a graphical decomposition method (Barnes, 1939). The excessive use of this method has largely fed the debate around the status and the future of hydrology (Beven, 1987). Especially, the graphical separation method can largely overestimate the contribution of direct runoff to the stream. This problem remains relatively secondary when the aim is the reconstitution or the prediction of the streamflow rate. It becomes an important problem when the aim is the reconstitution or the prediction of the stream water quality (Hubert, 1989).

In order to allow more specific and realistic separation of stream hydrograph sources, different hypotheses have suggested that precipitation moving rapidly overland or through soils dominates storm flow (DeWalle *et al.*, 1988):

(a) overland flow (Horton, 1933),
(b) partial-area overland flow (Betson, 1964; Ragan, 1968),
(c) saturation overland flow (Beven, 1978; Dunne & Black, 1970a,b),
(d) macropore flow (Jones, 1971; Beasley, 1976; Pilgrim *et al.*, 1978; Mosley, 1982).

The application of isotopic methods as a tool for tracing water movement is able to provide an interpretation for the origin of water within and/or at the inflows/outflows of the catchment under study. In association with hydrochemical studies, it is therefore usable at the catchment scale within the framework of hydrograph separation (Sklash & Farvolden, 1979; Kennedy *et al.*, 1986; Rodhe, 1987; Wels *et al.*, 1990; Wels *et al.*, 1991; McDonnell & Kendall, 1992). However, the use of these two tracers families allows identification of the origin of water in simple cases (Hubert, 1989). When the reality is complex (for example, a molecule of water from precipitation that has first been intercepted by vegetation, then has become overland flow, then has percolated into the soil to participate in the subsurface outflow before rejoining the groundwater outflow to finally discharge into the stream), one can reasonably doubt the quality of information on the different parts of the molecule history discovered by the geochemical method.

EXPERIMENTAL SITE DESCRIPTION

This study was conducted on two catchments in the North of French Guiana (Saint Elie's track, near Sinnamary, Fig. 1). The ECEREX experimental catchments have been monitored since 1977 (Sarrailh, 1990; Fritsch, 1990). After deforestation, one ("A") of the basins is now a meadow (1.3 ha), the other ("B") is still a primary forest (1.6 ha). These two catchments, without permanent flow, have been retained because they present similar characteristics for soils, slope steepness and rainfall input. They differ only by their canopy: grass on catchment "A", dense primary forest on catchment "B". Mean annual precipitations range from 3500 to 3900 mm (Roche, 1982).

The soil characteristics (Grimaldi *et al.*, 1990) show essentially the existence of a clayey horizon situated at varying depths (from −0.30 m to −1.00 m). During events, this horizon limits the rainwater infiltration and can constitute the floor of a temporary groundwater. This saturation, associated with a slope effect (15 to 20%), provokes lateral flow through the macroporosity along the slope from the upper part of the

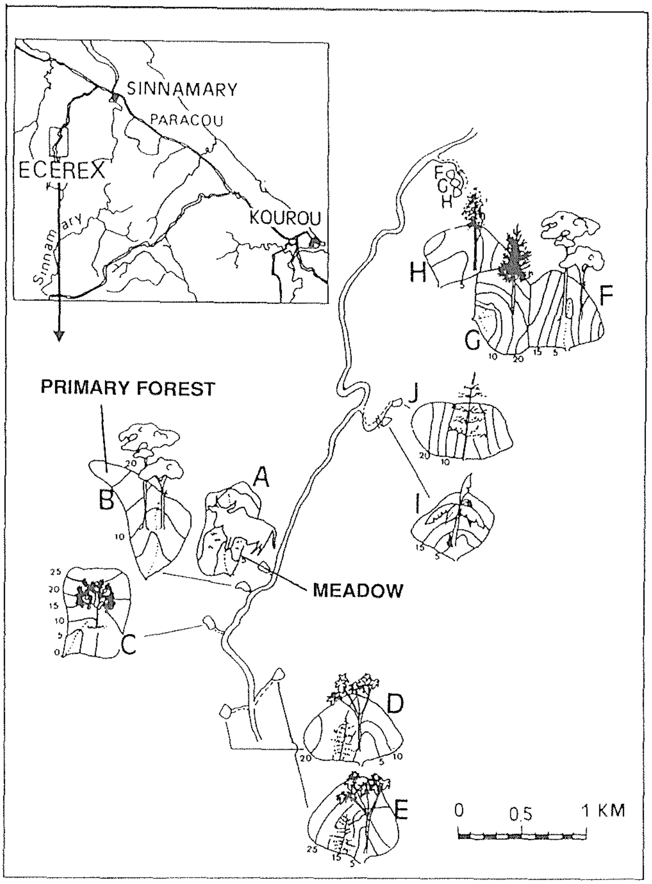

Fig. 1 Location of the two experimental catchments (basins "A" and "B") in the vicinity of Sinnamary (ECEREX operation, Saint Elie's track, French Guiana).

catchment to the stream (Grimaldi & Boulet, 1989). According to the depth of this layer, two families of soils can be characterized by the nature of their drainage (Boulet, 1990):

- soil with deep and free vertical drainage (10% of the soil area, in the upper part of the catchment covered in a primary forest),
- soil with deep but delayed vertical drainage (100% of the grass area, and 90% of the primary forest area).

HYDROGRAPH SEPARATION METHOD: GENERALITIES

At the outlet of the catchment, the isotopic compositions (^{18}O, ^{2}H, ^{3}H) and the chemical concentrations of an element are imposed by a mixing of waters with different origins and different histories. Chemical and isotopic characteristics of water sampled at the outlet will depend therefore on the proportions of the mixing between "ancient" waters (anterior to the event) and "new" waters (brought by the event). This allows one to write a two-component mass balance equation: one for water flow and one for isotope or chemical tracer:

$$Q_{discharge} = Q_{event} + Q_{preevent} \qquad (1)$$

$$C_{discharge}Q_{discharge} = C_{event}Q_{event} + C_{preevent}Q_{preevent} \qquad (2)$$

where Q and C are flow and isotopic compositions and/or chemical concentrations of the natural tracers (discharge, new and old water).

The stream water level has been measured and converted into a flow rate. One can therefore determine $Q_{preevent}$ and Q_{event}. But this approach requires different assumptions (Sklash & Farvolden, 1982):

(1) the content in heavy isotopes of the considered event has to be significantly different from that of ancient water (Crouzet *et al.*, 1970);
(2) the content in heavy isotopes of the intrastorm rainfall does not present spatial and temporal variations;
(3) the content in heavy isotopes of the ancient water remains constant during the flood; and
(4) the ancient water has the isotopic composition of the baseflow.

Assumption (1) is often verified but has to be nevertheless controlled by an adapted sampling (Kennedy *et al.*, 1986). Assumption (2) has to be imperatively rejected: the isotopic composition of the rainwater evolves over very short time periods (Dansgaard, 1964; Jouzel, 1986; McDonnell *et al.*, 1990; Kendall & McDonnell, 1993). Assumption (3) is not always verified. The isotopic composition of the fraction of groundwater that discharges into flood can be modified by the infiltration of precipitated water with a different isotopic signature. However, this case has been only rarely observed in the literature (Kennedy *et al.*, 1986). On the other hand, the isotopic composition of the soil water (temporarily and/or non saturated layers) is strongly modified by the infiltration of precipitations with an isotopic time-space evolution. Assumption (4) is generally justified: baseflow coming from groundwater does not generally offer geochemical discontinuity.

The geochemical analysis of the hydrograph separation, taking into account the age of the water ("ancient" and "new"), reveals generally a strong "old" water contribution to a flood. In this case, the runoff contribution does not exceed some percentage of the total volume measured at the outlet (Crouzet *et al.*, 1970).

SAMPLING, METHODS AND TECHNIQUES

On 24 May 1992, water sampling was undertaken between 06.00 h and 23.00 h as described below:

(a) stream water samples were collected continuously (5 to 15 minute intervals) at the gauging station (catchment outlets). Stream discharge were recorded at a V-notch weir at the catchment outlet;
(b) 15 minute rainfall intensities and precipitation samples were collected in nonrecording gauges (eight on basin "A", 31 on basin "B");
(c) water from infiltration ditch at different depths on basin "B".

Tensiometer measurements were realized throughout the experiment on basin "A" (3 stations) and basin "B" (3 stations). The day before the experiment, soil waters were taken at different depths near the six tensiometer stations in order to characterize an initial isotopic state of the water in the soil.

RESULTS AND DISCUSSIONS

The isotopic composition of precipitation

During rainfall, the liquid fraction is enriched in heavy isotopes as compared to the residual vapour phase. Evolution of isotopic compositions of water vapour in the clouds and of the resulting precipitation is most often interpreted through the model of Rayleigh distillation (Dansgaard, 1964). On 24 May 1992, from 04.00 h to 14.30 h, four (basin "B") or five (basin "A") distinct rainy events composed the rainfall (Figs 2 and 3). Rainfall amounts were respectively 53.8 mm (throughfall, basin "B") and 56.7 mm (open area, basin "A"). The difference between these two values represents a 5.6% loss due to rain interception by the canopy.

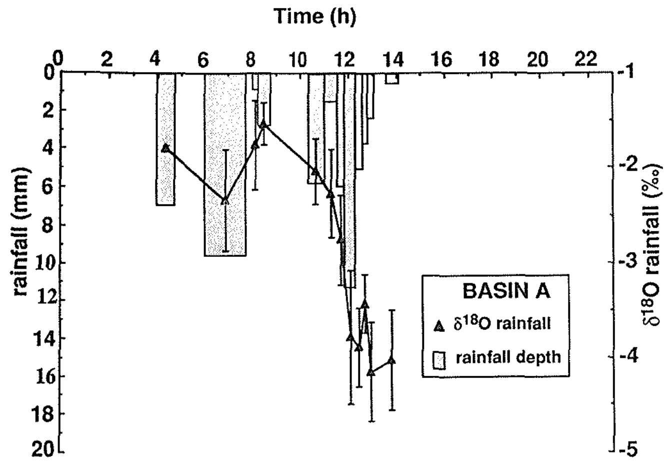

Fig. 2 Rainfall depth and isotopic composition of precipitation ("A" catchment, 24 May 1992).

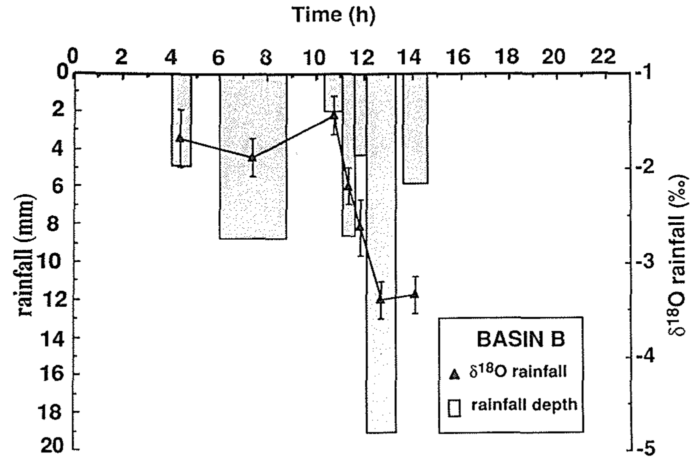

Fig. 3 Rainfall depth and isotopic composition of precipitation ("B" catchment, 24 May 1992).

Small differences appeared between the isotopic composition of the intercepted and rain fractions because evaporation occurs in an atmosphere with a high relative humidity (Gat & Tzur, 1967).

The isotopic composition of the rainwater varied very slightly in the space (Figs 2 and 3) on the two catchments and appears to be independent of rain amount.

Under primary forest, 31 raingauges were randomly distributed along a line parallel (100 m) to the stream channel in order to study the organization (decametrical scale) of the throughfall samples. The variograms thus determined were of a pure random type with an important nugget effect. The throughfall process has therefore to be considered as a discontinuous phenomenon, without spatial organization. The variograms relative to the isotopic composition of the rainwater under the canopy did not demonstrate the existence of a spatial structure and confirmed therefore the independence of the raingauge device. So, the isotopic composition of rainwater appeared to be independent of raingauge location.

The isotopic composition of stream water

A complex shower caused two successive floods. During the first flood (07.58 h-10.08 h), the stream rate was not substantially affected by the shower intensity. The second flood began during the third rainy event (11.35 h). The three peaks (especially, the main peak recorded at 12.35 h) correspond to the higher intensity values of the rainfall (Figs 4 and 5).

The isotopic composition of the water sampled at the outlet of the catchments tended toward that of the rainwater without ever reaching it (Figs 4 and 5). This could be attributed to:

(1) A spatial variability of the isotopic composition of the rain at the scale of the catchment which would question the representativity of the raingauge and of the

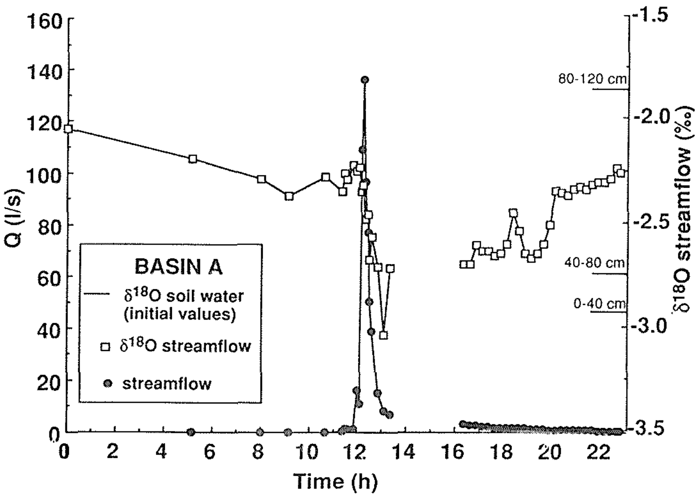

Fig. 4 Total stream discharge ("A" catchment, 24 May 1992). Stream $\delta^{18}O$ and initial $\delta^{18}O$ soil water are presented elsewhere.

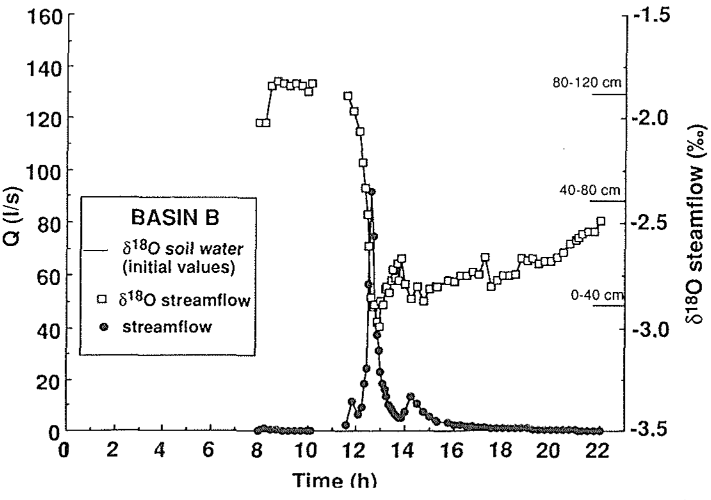

Fig. 5 Total stream discharge ("B" catchment, 24 May 1992). Stream δ^{18}O and initial δ^{18}O soil water are presented elsewhere.

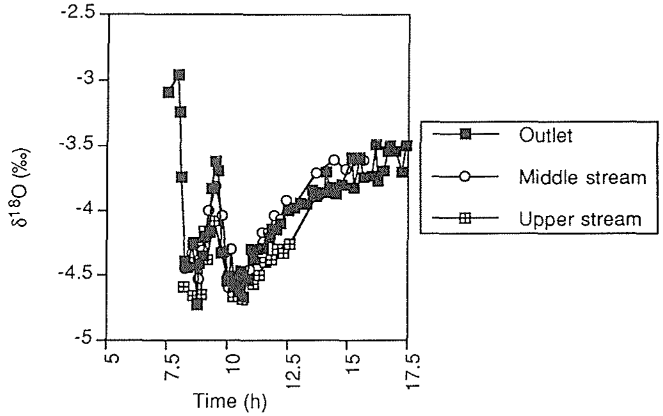

Fig. 6 δ^{18}O spatial evolution along the stream water ("B" catchment, 15 May 1993).

isotopic signature of the rain thus determined. But another experiment (15 May 1993) revealed an absence of δ^{18}O spatial evolution along the stream (Fig. 6) which demonstrates that only the temporal evolution of isotopic signatures of rainwater and temporarily saturated soil layers cause that of the stream water.

(2) Mixing between rainwater and pre-event old water in the soil with a different isotopic composition. It is to be noted that the temporal variability of the isotopic signature of the rainwater covers the spatial variability (vertical profile) of the initial isotopic signature of the soil water (Figs 4 and 5).

Meteoric water line and evaporation line

The meteoric water line characterizes the isotopic composition of precipitations that have escaped to evaporation during their fall in the atmosphere. So the δ^{18}O of rainfall is

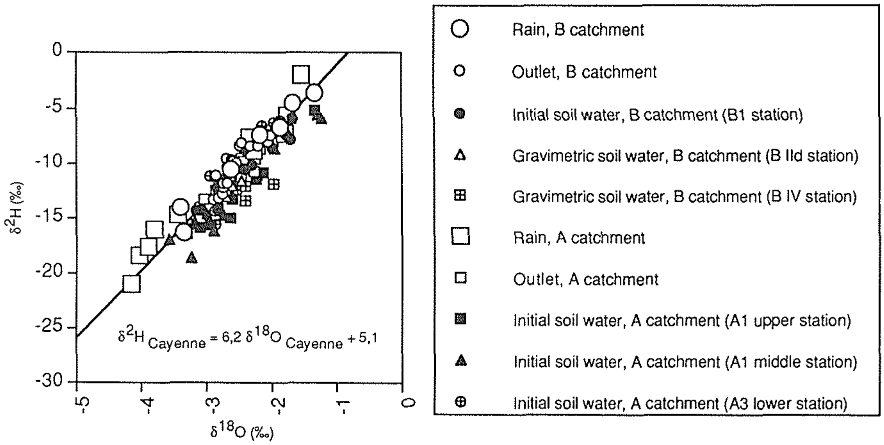

Fig. 7 Isotopic compositions of precipitation, stream and soil water in a δ^2H-δ^{18}O diagram ("A" and "B" catchments, 24 May 1992).

linked to that of δ^2H by the following empirical relationship (Yurtsever & Gat, 1981):

$$\delta^2H = (8.17 \pm 0.08)\delta^{18}O + (10.6 \pm 0.6) \qquad (3)$$

Values of the meteoric water line parameters only depend on the atmospheric humidity deficit value that governs the ocean evaporation (Merlivat & Jouzel, 1979). Laws that govern the fractionation process during evaporation produce an identical effect on the two stable isotopes of water. This effect tends to concentrate in ^{18}O and in ^{2}H the residual water of a reservoir (surface water body, soil, leaf...). Different studies (Craig, 1961; Craig & Gordon, 1965; Gat, 1971) showed that points that represent the evolution of the isotopic composition of a water submitted to evaporation are all situated under the meteoric water line in a diagram δ^2H-δ^{18}O.

During this experimentation, the representation of the isotopic composition of water (rain, soil and stream water samples) in a diagram δ^2H-δ^{18}O (Fig. 7) revealed the absence of:

- an evaporation line in the case of the soil water; and
- a mixing line between the different components of the stream discharge.

All these points were linearly related following a meteoric water line [$\delta^2H = 6.3$ ($\pm$ 0.3) $\delta^{18}O$ + 5.7 ($\pm$ 0.7)]: the isotopic compositions of waters sampled at the catchment outlet were governed only by the condensation process in the clouds. During infiltration, rainfall (new water) only displaced stored soil water (from ancient events without loss by evaporation). New addition of rain in the soil displaced an approximately equivalent amount of old water (Hewlett & Hibbert, 1967). The non-evaporation of the soil water under these canopies was equally confirmed by micro-meteorological and physiological measurements realized during the dry season (Fig. 8).

The initial isotopic composition of the soil water

The different isotopic profiles realized in the soil (upper, middle and lower parts of the catchment "A") presented a similar trend (Fig. 9). The absorption root and capillary rise

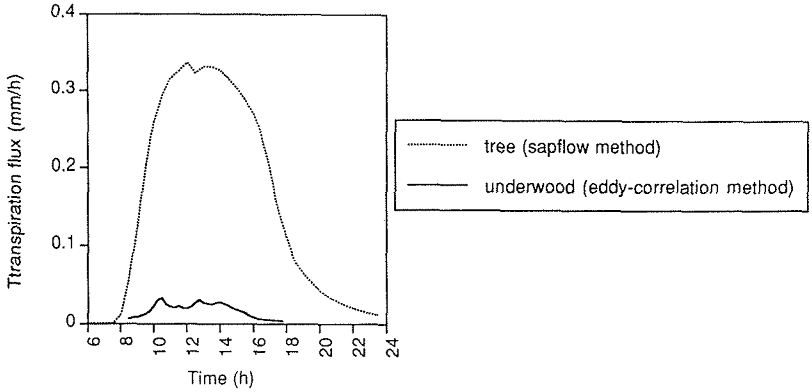

Fig. 8 Evapotranspiration flux (trees and underwood, "B" catchment).

did not provoke isotopic fractionation (Zimmermann *et al.*, 1967). In the absence of evaporation, these results allow one to characterize a succession of precipitations infiltrated in the soil. Isotopic compositions of these ancient precipitations were different and more or less homogenized by the transfer process in the soil (rapid infiltration in

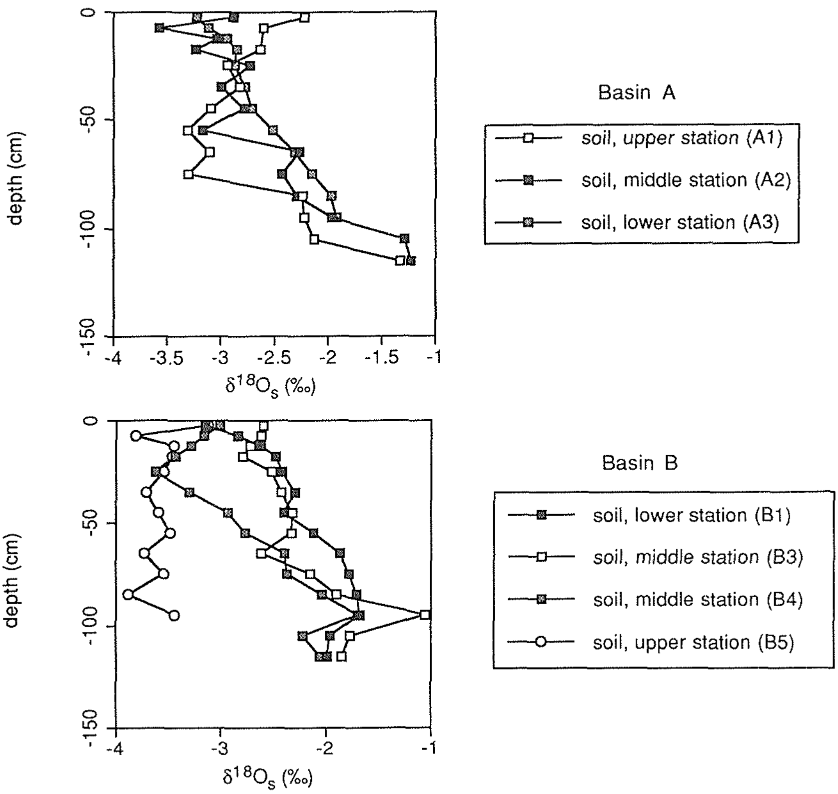

Fig. 9 Initial values of the isotopic composition of the soil water (3 stations) measured before the event ("A" catchment, 24 May 1992). The initial values of the isotopic composition of the soil water (4 stations on "B" catchment) are presented elsewhere.

upper horizons, slower infiltration in deeper horizons). On catchment "B" (Fig. 9), isotopic profiles of the soil water presented a comparable evolution to that of profiles measured on catchment "A". These profiles can therefore be interpreted in an analogous manner: infiltration more or less rapid at the surface accompanied by a mixing more or less complete along the profile. On the other hand, the profile realized in the upper part of this catchment presented a good $\delta^{18}O$ homogenization probably linked to its situation in a free vertical drainage area.

Analysis of the evolution of water potentials in the soil (catchment "B")

The three stations retained on this catchment presented a different hydrodynamical behaviour during the shower. The soil reacted very superficially to the shower (Fig. 10) in the case of the station closest to the stream channel (B1). Only the upper horizons (from 0 to −0.4 m) reached or had a tendency to reach the saturation state when the

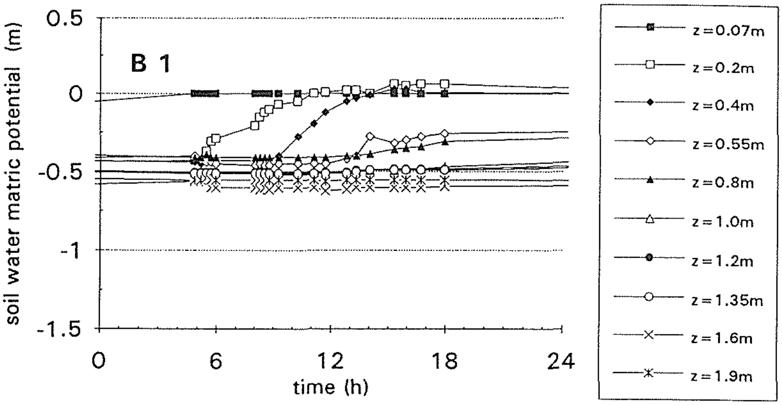

Fig. 10 Time evolution of soil matrix potentials measured at different depths (24 May 1992, "B" catchment, B1 station: lower part of the catchment).

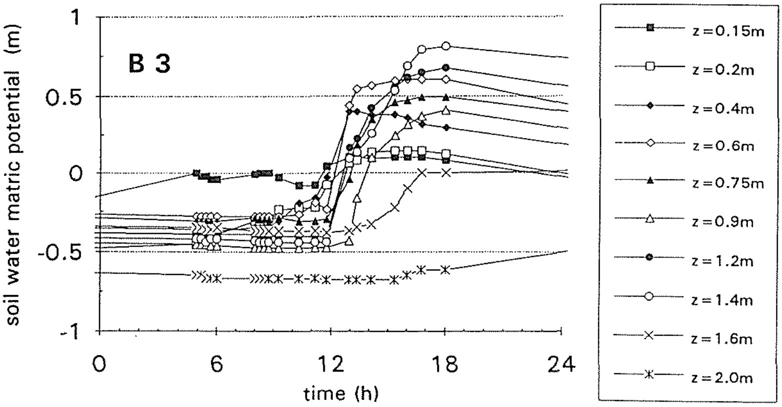

Fig. 11 Time evolution of soil matrix potentials measured at different depths (24 May 1992, "B" catchment, B3 station: middle part of the catchment).

main stream peak was recorded (12.35 h). Then, water potentials of these horizons remained constant. Between −0.50 m and −0.80 m, the potential variations remained weak. Beyond −1.00 m, variations of potential were non-existent.

With a soil profile nevertheless similar, the station B3 reacted very differently (Fig. 11). At first (06.00 h-11.00 h), the water potential presented small variations whatever the horizons. Only the horizon at −0.15 m was then saturated. Between 11.00 h (superficial layers) and 13.00 h (deeper layers), water potentials increased strongly, except for the deepest horizons (−2.00 m). These potentials stabilized between 13.00 h and 16.00 h, then decreased slowly beyond 18.00 h. At the peak of stream (12.35 h), the saturation in the soil was reached to −1.40 m: the infiltration therefore rapidly reached the deepest layers.

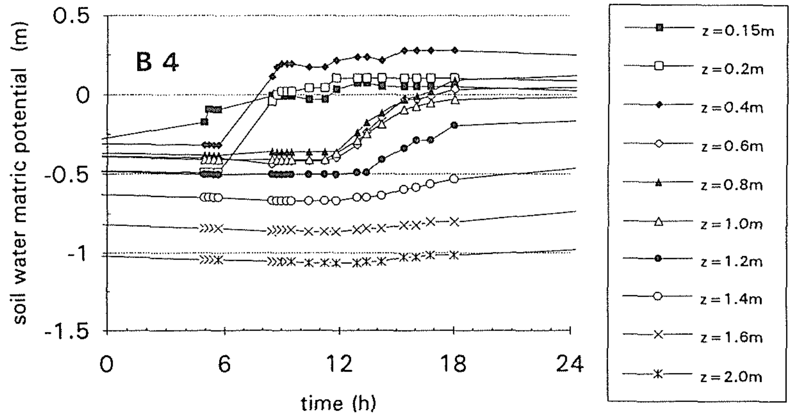

Fig. 12 Time evolution of soil matrix potentials measured at different depths (24 May 1992, "B" catchment, B4 station: upper part of the catchment).

From 08.00 h, the soil of the station B4 was saturated up to −0.40 m (Fig. 12). Then subsequently, the water potential of superficial horizons increased very feebly. On the other hand, the intermediate horizon potential (from −0.60 m to −1.00 m) increased only from 12.00 h. These horizons saturated at 17.00 h. Between −1.00 and -2.00 m, variations of potential were gradually lessened and saturation was never reached. In a quantitative manner, and despite a great variability of hydrodynamical properties of the soil layers, some results may be noted:

- There was a reduction of one to two orders of magnitude in hydraulic conductivity between superficial horizons and deeper ones. The existence of a "less permeable barrier " seems therefore confirmed.
- The drainage at the profile base was negligible (inferior to 1 mm).
- The water recharge of the soil profile was only 10 to 20 mm at the different sites: an important amount of the rain was deflected laterally and was available for lateral flow in the soil profile.

In conclusion, the soil layers of the B catchment could be described as being the superposition of 3 horizons:

- upper soil horizon with a high infiltration rate flow (from 0 to −0.40 m);
- intermediate horizon less permeable (above the red clayey horizon); and
- deep soil horizon (under the red clayey horizon).

Relationship between isotopic composition of stream water and stream discharge

The compartmentalization of water which reaches the stream channel influences the isotopic evolution of stream water (Herrmann & Stichler, 1981). This compartmentalization can be approached through the relationship established between the content in heavy isotopes of the stream water and the outflow. This relationship can present an hysteresis loop, attributed by Sklash & Farvolden (1979) to a mixing among three components, with different isotopic compositions (rainwater, soil water, groundwater), and temporal contributions evolving to the stream discharge. The experimentation realized on these two catchments confirmed the existence of this hysteresis loop relationship (Fig. 13). However, this relationship can equally be explained by the isotopic evolution of the rain water during time in the case of a simple two-component mixing model.

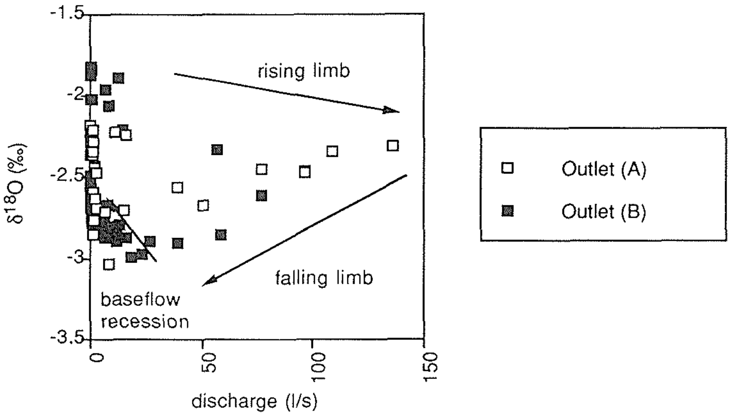

Fig. 13 $\delta^{18}O$ stream water versus stream discharge ("A" and "B" catchments, 24 May 1992).

Relationships between isotopic and hydrochemical tracers

The use of the relationships between chemical and isotopic tracers allows one to clarify the analysis of the different components that contribute to stream discharge (Maule & Stein, 1990). The isotopic method allows one to distinguish new waters from old waters when their contents in heavy isotopes are significantly different. It allows one equally to characterize waters in the soil affected by mixing (old waters "contaminated" by new waters during the infiltration of the rain) and whose isotopic composition is therefore intermediate between those of old and new waters.

The hydrochemistry method allows one to distinguish waters that have preserved the character of new waters (without chemical exchange with the soil layers) from those that have lost it (chemical exchanges with an organic or mineral horizon). Naturally, this last hypothesis has to be adapted according to the nature of the mineral horizon and the canopy (leaching process).

From a geochemical diagram (Maulé & Stein, 1990), different components can be thus distinguished:

(1) Recent waters *s. s.*, situated above the soil-atmosphere interface (direct rain, direct runoff), whose isotopic composition is imposed by the rain and that are not marked by a chemical tracer. However, no direct runoff is observed on studied catchments.

(2) Recent waters *s. l.* (subsurface flow), situated under the interface ground-atmosphere, that present the isotopic composition of the precipitation and that are marked by a chemical tracer (chemical exchanges with the litter and the first mineral horizons). By reason of a limited mixing between the infiltrated rain and the ancient water present in superficial layers of the soil one can consider that these waters circulate rapidly in zones temporarily saturated.

(3) Mixing water ("intermediate waters") which present an isotopic composition intermediate between that of the rain and that of deep waters are marked by a chemical tracer. Due to the fact of important mixing of waters between the rain and the old water in the soil, one can suppose that these waters circulate more slowly.

(4) Ancient waters *s. s.*, which present the isotopic composition of the saturated zone ("ancient waters ") and that are marked by a chemical tracer.

It is of interest, therefore, to find the chemical tracers allowing one to characterize the different reservoirs. In general, geochemical elements in the soil can be divided into two groups (Hirata & Muraoka, 1993): those (silica, sodium, chloride...) that are not essential to the development of vegetation and whose concentration increases with depth, and those (nitrate, potassium, calcium...) that are essential to vegetation, and have a tendency to concentrate at the soil surface.

These general observations are clearly to be adapted to the mineralogical nature of studied soils and to the influence of the local climate on the alteration of the soil. In the case of these catchments, one can observe that (Grimaldi, 1988):

- Contamination in chloride or in sodium of the soil solution does not exist during the alteration of minerals; these elements are not present in the minerals. These elements are necessarily brought by rain. The ions are very little absorbed by the vegetation (notably Cl^-) and are going therefore to concentrate in deep old waters.
- Potassium and the calcium are weakly created by the soil (very slow dissolution of muscovite). They are equally liberated during the decomposition of the litter or by canopy leaching, but are very rapidly absorbed by the vegetation (especially K^+). K^+ and Ca^{++} are going therefore to be found essentially in superficial new waters.

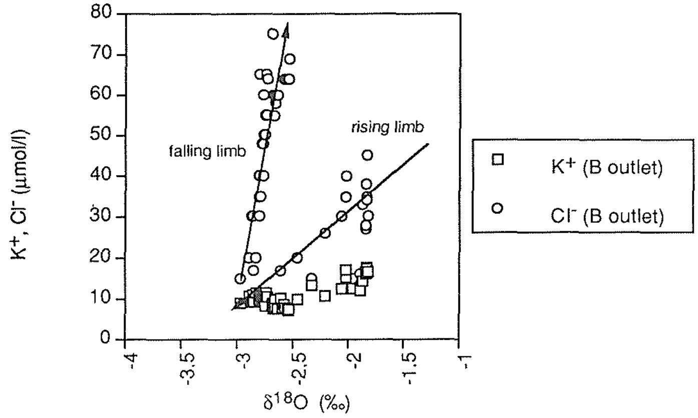

Fig. 14 Chloride and potassium concentrations versus $\delta^{18}O$ (stream water, 24 May 1992, "B" catchment).

Thus, on these catchments, superficial waters will be characterized by high concentrations in potassium and very low in chloride. An opposite phenomenon will characterize deep waters.

The diagram "deep water chemical tracer (Cl^-)-isotopic tracer (^{18}O)" demonstrates the existence of a hysteresis loop relationship between these two tracer families (Fig. 14):

- the downward part of the hysteresis loop (rising limb of the hydrograph) is imposed by an isotopic depletion linked to the fall of this signal in precipitations and to the arrival of water from superficial soil layers weakly marked in Cl^-; and
- the climbing part of the hysteresis loop (falling limb and baseflow recession) is created by the rain stopping and the arrival of deeper water at the outlet which is concentrated in Cl^- and more isotopically enriched.

This hysteresis loop relationship disappears in the case of the diagram "superficial water chemical tracer (K^+)-isotopic tracer (^{18}O)" (Fig. 14): the observed relationship is essentially imposed by isotopic depletion in precipitation mentioned above. At the outlet, the arrival of deep water weakly concentrated in potassium no longer modifies this relationship.

Mass balance equations (water, chemical and isotopic tracers) may be used for separating the stream hydrograph in different components. This allows therefore to determine qualitatively the water origin and quantitatively the different component contributions.

So as to be able to determine the respective contribution (Figs 15 and 16) from the soil (subsurface waters, intermediate waters above the red clayey horizon, deep waters) susceptible to reach the stream, the parameters used were:

- average $\delta^{18}O$ in precipitations, after having regrouped successive weak events;
- initial average $\delta^{18}O$ in the soil water, after having regrouped successive horizons with similar isotopic compositions;
- average $\delta^{18}O$ in the infiltration ditch water; and
- associated chemical concentrations (K, Cl).

This decomposition obtained revealed an important contribution from intermediate zones of the soil, above the red clayey level.

On catchment "B", the subsurface flow contribution to the hydrograph peak was important (70%). During the falling limb and baseflow recession, the contribution from the deep water increased gradually to reach 93% to 22.00 h.

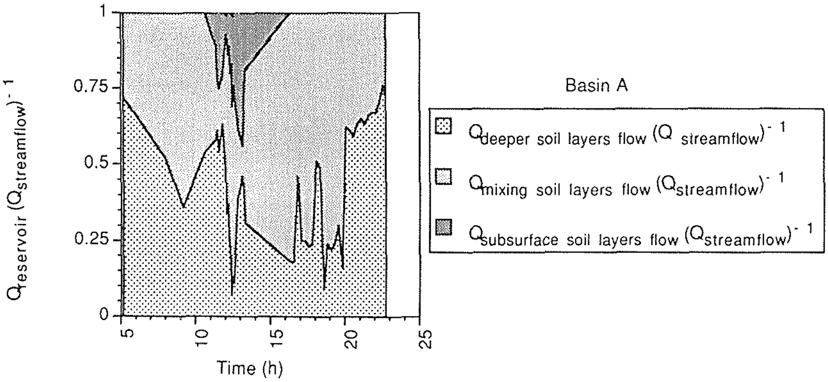

Fig. 15 Geochemical stream hydrograph separation (24 May 1992, "A" catchment).

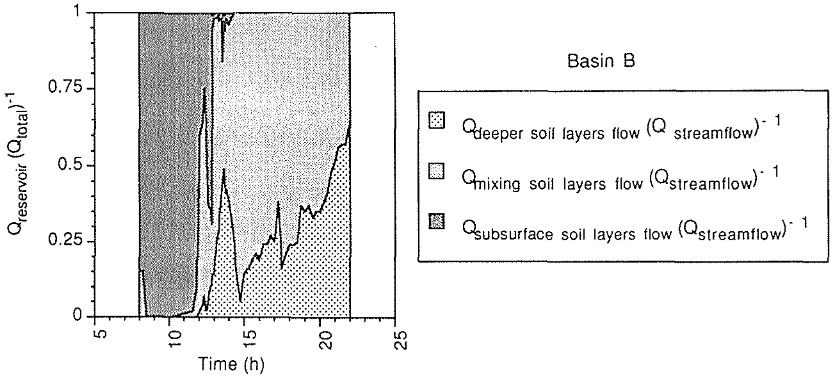

Fig. 16 Geochemical stream hydrograph separation (24 May 1992, "B" catchment).

On catchment "A", the stream discharge was mainly insured by the superficial soil layers (70%). During the baseflow recession period, the contribution from the temporary groundwater did not cease to increase and finished by reaching similar values to those calculated during the beginning of the flood.

The percentage of the volume of water flowing to the outlet compared with precipitation is 41% on catchment "A" against 28% in the case of catchment "B". This difference cannot be entirely attributable to losses due to interception since according to calculations, that was only 5%. These differences of hydrological behaviours are probably attributable to the nature of the canopy and to the action of the vegetation on the soil porosity. Indeed, the deforestation process causes an increase in the volume of rain arriving at the ground and an increase in the volume of water contained in the soil (Sklash *et al.*, 1986).

CONCLUSION

This study showed clearly the interest of the simultaneous use of chemical and isotopic information for the hydrograph separation.

The analysis of stream water by the isotopic method showed that a flood is a mixture of water from different soil layers. However, the isotopic tool alone is insufficient to appreciate the depth of the water mobilized in the soil. Indeed, on the catchments studied, the temporal variability of the isotopic signal of the rainwater was very similar to the spatial variability of the isotopic signal of the soil water. Soil water in catchments is not submitted to evaporation: the isotopic composition of the soil water is governed by successions of infiltrated anterior rainwater.

The use of chemical tracers provided valuable information for the characterization of the soil layers. Thus, the use of combined chemical and isotopic information provided the identification and the quantification of the different component contributions (subsurface flow, intermediate and deep waters).

Contents in ^{18}O and ^{2}H of rain water have a strong temporal evolution, but a weak variation in space, by reason of the small catchment areas. This temporal variability indicates not to use an average isotopic signal during the calculation of the contribution of the component "new water".

Further fieldwork is now necessary to study the spatial and the temporal evolution of geochemical tracers in soil water.

REFERENCES

Barnes, B. S. (1939) The structure of discharge recession curves. *Trans. Am. Geophys. Un.* **20**, 721-725.

Beasley, R. S. (1976) Contribution of subsurface flow from the upper slopes of forest watersheds to channel flow. *Soil Sci. Soc. Am. J.* **40**, 955-957.

Betson, R. P. (1964) What is watershed runoff? *J. Geophys. Res.* **69**, 1541-1551.

Beven, K. (1978) The hydrological response of headwater and sideslope areas. *Hydrol. Sci. Bull.* **23**, 419-437.

Beven, K. (1987) Toward a new paradigm in hydrology. In: *Water for the Future: Hydrology in Perspective* (Proc. Rome Symp., avril 1987), 393-403. IAHS Publ. no. 164.

Boulet, R. (1990) Organisation des couvertures pédologiques des bassins versants ECEREX. Hypothèses sur leur dynamique. In: *Mise en Valeur de l'Ecosystème Guyanais: Opération ECEREX*, 15-45. INRA-CTFT.

Crouzet, E., Hubert, P., Olive, Ph., Siewertz, E. & Marcé, A. (1970) Le tritium dans les mesures d'hydrologie de surface. Détermination expérimentale du coefficient de ruissellement. *J. Hydrol.* **11**, 217-229.

Craig, H. (1961) Isotopic variations in meteoric waters. *Science* **133**, 1702-1703.

Craig, H. & Gordon, L. (1965) Deuterium and oxygen-18 variations in the ocean and the marine atmosphere. In: *Stable Isotopes in Oceanographic Studies and Paleotemperatures* (ed. par E. Tongiorgi), 9-130. CNR, Laboratorio di Geologia Nucleare, Pisa.

Dansgaard, W. (1964) Stable isotopes in precipitation. *Tellus* **16**, 436-468.

DeWalle, D. R., Swistock, B. R. & Sharpe, W. E. (1988) Three-component tracer model for stormflow on a small Appalachian forested catchment. *J. Hydrol.* **104**, 301-310.

Dunne, T. & Black, R. D. (1970a) An experimental investigation of runoff prediction in permeable soils. *Wat. Resour. Res.* **6**, 478-490.

Dunne, T. & Black, R. D. (1970b) Partial area contribution to runoff in a small New England watershed. *Wat. Resour. Res.* **6**, 1296-1311.

Fritsch, J. M. (1990) Les effets du défrichement de la forêt amazonienne et de la mise en culture sur l'hydrologie de petits bassins versants. Opération ECEREX en Guyane française. Thèse de Doct. Univ. Montpellier II, Sciences et Techniques du Languedoc.

Gat, J. R. & Tzur, Y. (1967) Modification of the isotopic composition of rainwater by processes which occur before groundwater recharge. In: *Proc. 2nd IAEA Symposium on Isotopes in Hydrology*, 49-59. IAEA, Vienna.

Gat, J. R. (1971) Comments on the stable isotope method in regional groundwater investigation. *Wat. Resour. Res.* **7**, 980-993.

Grimaldi, C. (1988) Origine de la composition chimique des eaux superficielles en milieu tropical humide: exemple de deux petits bassins versants sous forêt en Guyane française. *Sci. Géol. Bull.* **41**(3-4), 247-262.

Grimaldi, M. & Boulet, R. (1989) Relation entre l'espace poral et le fonctionnement hydrodynamique d'une couverture pédologique sur socle en Guyane française. *Cah. ORSTOM Sér. Pédol.* **XXV**(3), 263-275.

Grimaldi, C., Grimaldi, M. & Boulet, R. (1990) Etude d'un système de transformation sur schiste en Guyane française. Approches morphologique, géochimique et hydrodynamique. In: *Organisation et Fonctionnement des Altérites et des Sols* (ed. par J. C. Wackermann) (Séminaire ORSTOM 90), 81-98. ORSTOM.

Herrmann, A. & Stichler, W. (1981) Groundwater-runoff relationships. *Catena* **7**, 251-263.

Hewlett, J. D. & Hibbert, A. R. (1967) Factors affecting the response of small watersheds to precipitation in humid areas. In: *International Symposium on Forest Hydrology* (ed. par W. E. Sopper & H. W. Lull), 275-290. Pergamon, Oxford.

Hirata, T. & Muraoka, K. (1993) The relation between water migration and chemical processes in a forest ecosystem. In: *Tracers in Hydrology* (Proc. Yokohama Symp., July 1993), 31-40. IAHS Publ. no. 215.

Horton, R. E. (1933) The role of infiltration in the hydrological cycle. *Trans. Am. Geophys. Un.* **14**, 446-460.

Hubert, P. (1989) La séparation de l'hydrogramme. Apports des méthodes isotopiques. *Hydrogéol.* **3**, 143-150.

Jones, J. A. A. (1971) Soil piping and stream channel initiation. *Wat. Resour. Res.* **7**, 602-610.

Jouzel, J. (1986) Isotopes in cloud physics: multiphase and multistage condensation process. In: *Handbook of Environmental Isotope Geochemistry*, vol. II: *The Terrestrial Environment* (ed. par P. Fritz & J. Ch. Fontes), 61-112. Elsevier.

Kendall, C. & McDonnell, J. J. (1993) Effect of intrastorm isotopic heterogeneities of rainfall, soil Water and groundwater on runoff modeling. In: *Tracers in Hydrology* (Proc. Yokohama Symp., July 1993), 41-48. IAHS Publ. no. 215.

Kennedy, V. C., Kendall, C., Zellweger, G. W., Wyerman, T. A. & Avanzino, R. J. (1986) Determination of the components of stormflow using water chemistry and environmental isotopes, Mattole River basin, California. *J. Hydrol.* **84**, 107-140.

Maule, P. S. & Stein, J. (1990) Hydrologic flow path definition and partitioning of spring meltwater. *Wat. Resour. Res.* **26**, 2959-2970.

McDonnell, J. J., Bonnell, M., Stewart, M. K. & Pearce, A. J. (1990) Deuterium variations in storm rainfall: implications for stream hydrograph separation. *Wat. Resour. Res.* **26**, 455-458.

McDonnell, J. J. & Kendall, C. (1992) Stable isotopes in catchment hydrology. *EOS, Trans. Am. Geophys. Un.* **73**, 260-261.

Merlivat, L. & Jouzel, J. (1979) Global climatic interpretation of the deuterium-oxygen 18 relationship for precipitation. *J. Geophys. Res.* **84**, 5029-5033.

Mosley, M. P. (1982) Subsurface flow velocities through selected water soils, South Island, New Zealand. *J. Hydrol.* **55**, 65-92.

Pilgrim, D. H., Huff, D. D. & Steele, T. D. (1978) A field evaluation of surface and subsurface runoff, 2. Runoff processes. *J. Hydrol.* **38**, 319-341.

Pinder, G. F. & Jones, J. F. (1969) Determination of the groundwater component of peak discharge from the chemistry of total runoff. *Wat. Resour. Res.* **5**, 438-445.

Rodhe, A. (1987) The origin of stream water traced by oxygen 18. PhD Thesis, Uppsala University, Dept Phys. Geogr., Div. Hydrol. Report Ser. A., Sweden.

Ragan, R. M. (1968) An experimental investigation of partial area contributions. In: *General Assembly of Bern, September-October 1967: Hydrological Aspects of the Utilization of Water*, 241-249. IAHS Publ. no. 76.

Roche, M. A. (1982) Comportements hydrologiques comparés et érosion de l'écosystème forestier amazonien à ECEREX en Guyane. *Cah. ORSTOM, Sér. Hydrol.* **29**(2), 81-114.

Sarrailh, J. M. (1990) *Mise en Valeur de l'Ecosystème Guyanais: Opération ECEREX.* INRA-CTFT.

Sklash, M. G. & Farvolden, R. N. (1979) The role of groundwater in storm runoff. *J. Hydrol.* **43**, 45-65.

Sklash, M. G. & Farvolden, R. N. (1982) The use of environmental isotopes in the study of high-runoff episodes in streams. In: *Isotope Studies of Hydrologic Processes* (ed. par E. C. Perry Jr & C. W. Montgomery), 65-73. Northern Illinois University Press, DeKalb, Illinois.

Sklash, M. G., Stewart, M. K. & Pearce, A. J. (1986) Storm runoff generation in humid headwater catchments. (2) A case study of hillslope and low-order stream responses. *Wat. Resour. Res.* **22**, 1273-1282.

Wels, C., Cornett, R. J. & Lazerte, B. D. (1990) Groundwater and wetland contribution to stream acidification: an isotopic analysis. *Wat. Resour. Res.* **26**, 2993-3003.

Wels, C., Cornett, R. J. & Lazerte, B. D. (1991) Hydrograph separation: a comparison of geochemical and isotopic tracers. *J. Hydrol.* **122**, 253-274.

Yurtsever, Y. & Gat, J. R. (1981) Atmospheric waters. In: *Stable Isotope Hydrology: Deuterium and Oxygen-18 in the Water Cycle*, 103-142. Tech. Reports Series no. 210, IAEA.

Zimmermann, U., Ehhalt, D. & Münnich, K. O. (1967) Soil water movement and evapotranspiration: changes in the isotopic composition of the water. In: *Isotopes in Hydrology* (Proc. Symp., IAEA, Vienna), 567-585. IAEA, Vienna.

Tracer Technologies for Hydrological Systems (Proceedings of a Boulder Symposium, July 1995). IAHS Publ. no. 229, 1995.

Modélisation par une loi gamma de la distribution des temps de séjour de l'eau dans des systèmes hydrogéologiques en régime permanent

PIERRE HUBERT
URA CNRS 1367, CIG, Ecole des Mines de Paris, Fontainebleau, 35, rue Saint-Honoré, F-77305 Fontainebleau, France

PHILIPPE OLIVE
Centre de Recherches Géodynamiques, Université Paris VI, Thonon, France

Résumé En hydrologie isotopique, on désigne généralement comme le modèle d'un système hydrogéologique en régime permanent la fonction $\phi(\tau)$ décrivant la densité de probabilité des temps de séjour des molécules d'eau dans le système considéré. Cette fonction peut également être interprétée comme la réponse impulsionnelle du système à une injection de traceur affectant la forme du signal de Dirac. La fonction $\phi(\tau)$ décrivant la distribution des temps de séjour doit être soigneusement distinguée de la fonction $\psi(\tau)$ décrivant la distribution des âges des molécules d'eau présentes dans le système. Le temps de séjour moyen τ_s, moyenne de la distribution décrite par $\phi(\tau)$, peut être, selon le système considéré, inférieur, égal ou supérieur à l'âge moyen τ_a, moyenne de la distribution décrite par $\psi(\tau)$. Nous proposons l'utilisation d'un modèle protéiforme, fondé sur une loi gamma à deux paramètres, dont la plupart des modèles classiques, en particulier les modèles piston et exponentiel, sont des cas particuliers. Ce modèle a été appliqué aux systèmes des sources minérales de la Versoie et d'Evian (Haute-Savoie, France) pour lesquels nous disposons de longues séries de mesures chimiques et isotopiques. Ce modèle, applicable sans hypothèse particulière, permet d'estimer le temps de séjour moyen et d'obtenir quelques informations concernant la structure des systèmes étudiés, et il devrait se révéler utile dans la reconnaissance et la caractérisation globales des systèmes aquifères.

Les différentes phases du cycle de l'eau peuvent être modélisées comme des réservoirs recevant de l'eau de l'amont et fournissant de l'eau à l'aval, et possédant un double caractère de stock et de flux. Très souvent, il sera possible de supposer, au moins en première approximation, que ces réservoirs sont en régime hydrologique permanent. Dans ce cas, un réservoir contiendra un volume d'eau V, recevra et restituera un débit Q, ces quantités restant constantes au cours du temps. Nous distinguerons deux notions relatives au passage d'une molécule d'eau à travers un réservoir, l'âge d'une molécule défini à chaque instant durant le séjour de cette molécule dans le réservoir et le temps de séjour d'une molécule dans le réservoir, notions très clairement définies par Bolin & Rodhe (1973), dont nous reprendrons ici les notations.

A un instant donné, nous définirons l'âge d'une molécule d'eau particulière présente dans le réservoir comme le temps écoulé depuis le moment où elle est entrée dans le réservoir. Soit t_a cet âge. La distribution des âges des molécules d'eau présentes dans le réservoir à un instant donné peut être décrite par une fonction densité de probabilité ψ, ou de façon équivalente par une fonction de répartition Ψ.

$$\mathrm{prob}[\tau \leq t_a \leq \tau + \mathrm{d}\tau] = \psi(\tau)\mathrm{d}\tau \tag{1}$$

$$\mathrm{prob}[t_a \leq \tau] = \Psi(\tau) \tag{2}$$

$$\text{avec } \psi'(\tau) = \Psi(\tau) \tag{3}$$

Puisque nous sommes en régime permanent, cette distribution ne variera pas au cours du temps. La moyenne de cette distribution:

$$\tau_a = \int_0^\infty \tau\psi(\tau)\mathrm{d}\tau \tag{4}$$

est l'âge moyen des molécules d'eau du réservoir et, par extension, l'âge moyen de l'eau du réservoir.

Nous définirons d'autre part le temps de séjour d'une molécule d'eau dans le réservoir comme le temps écoulé depuis le moment où elle est entrée dans le réservoir jusqu'au moment où elle quitte le réservoir. Soit t_s ce temps de séjour. La distribution des temps de séjour des molécule d'eau dans le réservoir, identique à la distribution des âges des molécules d'eau quittant le réservoir à chaque instant, peut être décrite par une fonction densité de probabilité ϕ ou par une fonction de répartition Ψ. Comme la distribution des âges, la distribution des temps de séjour ne variera pas au cours du temps puisque nous sommes en régime permanent. La moyenne de cette distribution est le temps de séjour moyen des molécules d'eau dans le réservoir et, par extension, le temps de séjour moyen de l'eau dans le réservoir.

$$\tau_s = \int_0^\infty \tau\varphi(\tau)\mathrm{d}\tau \tag{5}$$

Les fonctions décrivant la distribution des âges et la distribution des temps de séjour ne sont pas indépendantes. Considérons en effet ce qui se passe pendant un intervalle de temps dt. Dans le volume $Q\mathrm{d}t$ quittant le réservoir pendant cet intervalle de temps, il se trouve un volume

$$Q[1 - \Phi(\tau)]\mathrm{d}t \tag{6}$$

de molécules d'âge supérieur à τ. Or, en régime permanent, la proportion de molécules d'âge supérieur à τ doit rester constante. Le volume de molécules d'âge supérieur à τ quittant le réservoir doit donc être exactement compensé par le volume des molécules ayant franchi l'âge τ pendant l'intervalle de temps dt, c'est à dire celles dont l'âge était compris entre $\tau - \mathrm{d}t$ et τ au début de l'intervalle de temps dt. Ce dernier volume s'exprime d'après (2) comme:

$$V\psi(\tau)\mathrm{d}t \tag{7}$$

et on peut donc écrire en égalant (6) et (7) $Q[1 - \Phi(\tau)]\mathrm{d}t = V\psi(\tau)]\mathrm{d}t$ c'est à dire:

$$1 - \Phi(\tau) = \frac{V}{Q}\psi(\tau) \tag{8}$$

relation qui est valable quel que soit τ. En particulier, pour $\tau = 0$, comme $\Phi(0) = 0$,

$$\psi(0) = \frac{Q}{V} \tag{9}$$

ce qui constitue une condition initiale pour l'équation différentielle obtenue en dérivant l'équation (8)

$$\varphi(\tau) = -\frac{V}{Q}\frac{\mathrm{d}\psi(\tau)}{\mathrm{d}\tau} \tag{10}$$

La fonction Φ, qui est une fonction de répartition, est par nature non décroissante. D'après l'équation (8) on peut déduire que la fonction ψ est non croissante, mais l'équation (10) nous montre que le comportement de la fonction ϕ peut être plus capricieux.

L'équation (9) permet d'atteindre le temps de séjour moyen τ_s défini par l'équation (5):

$$\tau_s = \int_0^\infty \tau\varphi(\tau)\mathrm{d}\tau = -\frac{V}{Q}\int_0^\infty \tau\frac{\mathrm{d}\psi(\tau)}{\mathrm{d}\tau}\mathrm{d}\tau \tag{11}$$

ce qui en intégrant par parties conduit à $\tau_s = V/Q$ expression identique à celle du temps de renouvellement défini comme le rapport du stock au flux.

Selon le cas, l'âge moyen τ_a sera inférieur, supérieur ou égal au temps de séjour moyen τ_s. Dans cette étude nous proposons l'utilisation d'une fonction densité de probabilité protéiforme, susceptible de rendre compte de ces trois cas.

$$\varphi(t) = \frac{\mathrm{e}^{-t/\tau_s}t^{(\tau_s/\tau_e)-1}}{\tau_e^{\tau_s/\tau_e}\Gamma(\tau_s/\tau_e)} \tag{12}$$

$$\text{où } \Gamma(x) = \int_0^\infty u^{x-1}\mathrm{e}^{-u}\mathrm{d}u$$

La moyenne de cette distribution est égale à τ_s, temps de séjour moyen, et sa variance est égale à $\tau_s\,\tau_e$. Le paramètre τ_e, toujours positif, qui a la dimension d'un temps, caractérise l'étalement de la réponse impulsionnelle du système. L'âge moyen correspondant à cette distribution est $\tau_a = (\tau_s + \tau_e)/2$ qui, suivant la valeur de τ_e, peut être inférieur, égal ou supérieur à τ_s. On retrouve le modèle piston si $\tau_e = 0$ et le modèle exponentiel si $\tau_e = \tau_s$.

Si la concentration d'un traceur radioactif à l'entrée du système varie en fonction du temps selon une fonction $C_e(t)$, la concentration à la sortie du système s'obtient par convolution:

$$C_s(t) = \int_0^\infty \varphi(u)C_e(t-u)\mathrm{e}^{-\lambda u}\mathrm{d}u \tag{13}$$

où λ est la constante de décroissance radioactive du traceur.

Dans le cas où l'entrée est un échelon

$$C_e(t) = 0 \text{ pour } t < 0 \text{ et } C_e(t) = C_0 \text{ pour } t \geq 0$$

$$C_s(t) = \frac{C_0}{(1+\lambda\tau_e)^{\tau_s/\tau_e}} P\left[\frac{\tau_s}{\tau_e}, \left(\frac{1+\lambda\tau_e}{\tau_e}\right) t\right] \tag{14}$$

où P est la fonction gamma incomplète (Abramowitz & Stegun, 1965).

$$P(a,x) = \frac{1}{\Gamma(a)} \int_0^x \mathrm{e}^{-t} t^{a-1} \mathrm{d}t \tag{15}$$

Dans le cas où l'entrée est une impulsion d'amplitude C_0 appliquée depuis le temps $t = 0$ jusqu'au temps $t = \Delta t$.

$$\begin{aligned} &C_e(t) = 0 \text{ pour } t < 0, \quad C_e(t) = C_0 \text{ pour } 0 \leq t \leq \Delta t \text{ et} \\ &C_e(t) = 0 \text{ pour } t > \Delta t \end{aligned} \tag{16}$$

la sortie s'exprime, pour $t > \Delta t$, en superposant un échelon d'amplitude C_0 appliqué au temps $t = 0$ et un échelon d'amplitude $-C_0$ appliqué au temps $t = \Delta t$ maintenus indéfiniment comme

$$C_s(t) = \frac{C_0}{(1+\lambda\tau_e)^{\tau_s/\tau_e}} \left\{ P\left[\frac{\tau_s}{\tau_e}, \left(\frac{1+\lambda\tau_e}{\tau_e}\right) t\right] - P\left[\frac{\tau_s}{\tau_e}, \left(\frac{1+\lambda\tau_e}{\tau_e}\right)(t-\Delta t)\right] \right\} \tag{17}$$

Il est donc aisé, en sommant de telles réponses élémentaires, de calculer la fonction de sortie correspondant à une fonction d'entrée constituée d'une suite d'impulsions de durées et d'amplitudes quelconques.

Nous avons appliqué ce modèle aux sources minérales de la Versoie et d'Evian en utilisant le tritium comme traceur, dans le but de déterminer les paramètres, en particulier le temps de séjour moyen, des systèmes hydrologiques correspondants. Les meilleures estimations des paramètres seront celles qui permettent de calculer des sorties s'approchant au mieux, selon un critère à définir, des sorties réellement observées.

Nous avons choisi un pas de temps annuel, se confondant avec l'année civile. Nous avons admis, en nous basant sur nos mesures (Hubert *et al.*, 1970) et les calculs effectués par Blavoux (1978), que la concentration en tritium de la recharge d'une année donnée était égale à la concentration en tritium des précipitations de cette année. La concentration des précipitations est celle de Thonon, directement mesurée ou calculée par régression linéaire à partir des mesures d'Ottawa pour la période antérieure à 1963.

Les teneurs en tritium de la source de la Versoie ont atteint des valeurs relativement importantes et ont connu de larges fluctuations, laissant présager un temps de séjour relativement court. Nous avons choisi dans ce cas la somme des carrés des différences relatives entre concentrations moyennes annuelles calculées et mesurées, lorsque ces dernières étaient disponibles comme critère caractérisant la proximité des réponses calculées et mesurées,.

Le comportement de ce critère en fonction des paramètres τ_s et τ_e est régulier; il ne présente qu'un seul minimum atteint pour τ_s = 4 ans et τ_e = 9 ans. On a représenté sur la Fig. 1 l'évolution correspondantes des teneurs calculées et mesurées qui apparaît très satisfaisante.

Il nous a semblé inadéquat d'utiliser la même fonction objectif pour la source d'Evian. Les teneurs y sont toujours resté modestes et finalement très comparables. Nous avons donc adopté comme critère d'optimisation la somme des carrés des différences entre concentrations moyennes annuelles calculées et mesurées, lorsque ces dernières étaient disponibles. Ici encore le comportement de la fonction critère est régulier et il ne présente qu'un seul minimum atteint pour τ_s = 51 ans et τ_e = 16 ans. L'évolution comparée des concentrations calculées et mesurées représentée sur la Fig. 2 est moins satisfaisante que dans le cas de la source de la Versoie, mais il faut faire la part des erreurs de mesure qui, compte tenu des faibles teneurs enregistrées, prennent ici une grande importance.

Classiquement, les hydrologues isotopistes considèrent trois types de modèles de réservoirs (Nir, 1964; Prezewlocki & Yurtsever, 1974; Maloszewski & Zuber, 1982; Zuber, 1986). Le **modèle piston**, où la pluie efficace traverse le réservoir à vitesse constante et où toutes les molécules d'eau ont le même temps de séjour. Dans ce cas l'âge moyen τ_a est égal à la moitié du temps de séjour moyen τ_s. **Le modèle exponentiel** ou de mélange parfait, dans lequel la pluie efficace se mélange à l'eau de l'aquifère si bien que chaque section de l'aquifère contient dans les mêmes proportions des molécules

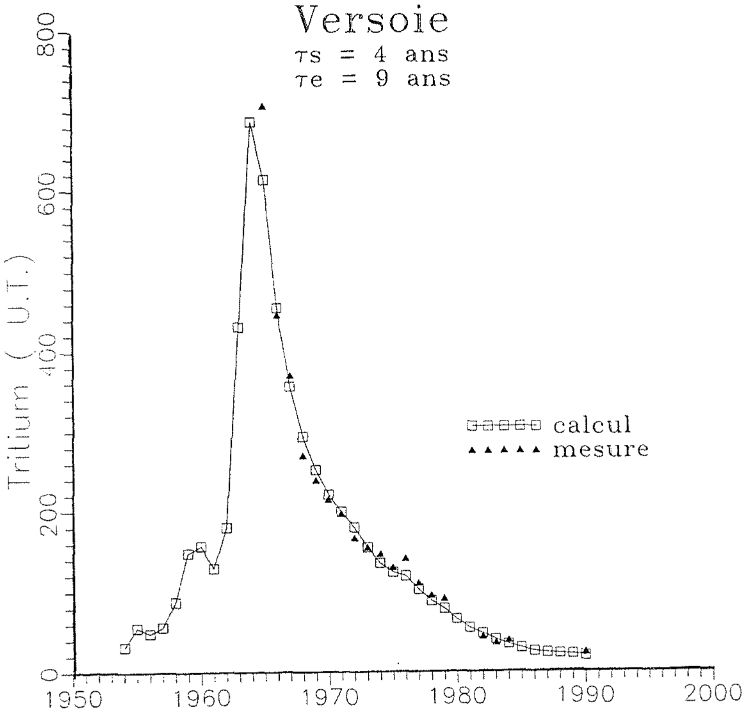

Fig. 1 Ajustement optimal à un loi gamma des données de la source de la Versoie.

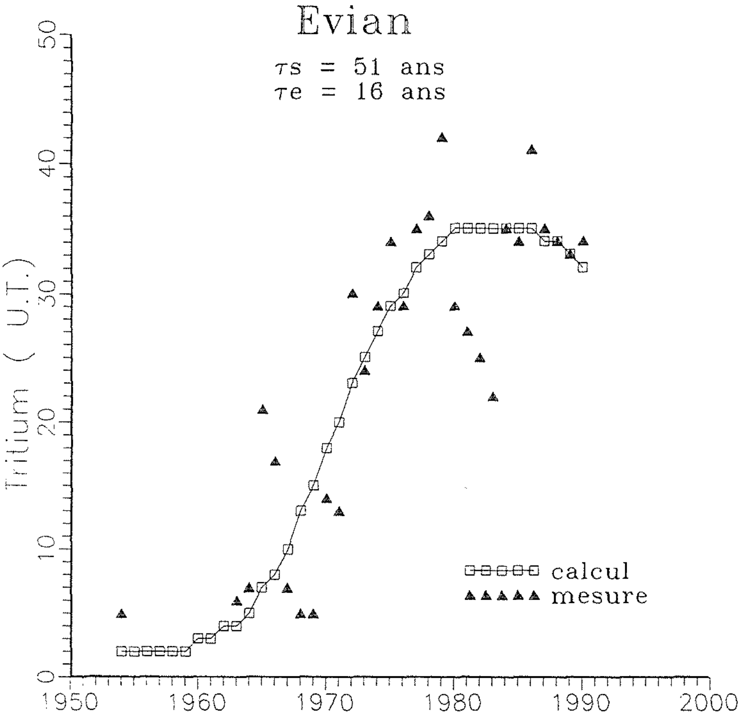

Fig. 2 Ajustement optimal à un loi gamma des données de la source d'Evian.

d'eau de tous les âges. Dans ce cas, l'âge moyen de l'eau τ_a est égal au temps de séjour τ_s. Enfin **le modèle dispersif**, dont le schéma de base est analogue à celui du modèle piston, mais où l'hétérogénéité du milieu entraîne une dispersion du signal isotopique véhiculé par la pluie efficace. Dans ce cas l'âge moyen τ_a est inférieur au temps de séjour τ_s. Le modèle piston et le modèle exponentiel constituent des cas limites du modèle dispersif. Les eaux minérales d'Evian, dont l'âge moyen $\tau_a = 33.5$ ans est inférieur au temps de séjour $\tau_s = 51$ ans illustrent bien le comportement qualifié de dispersif.

La loi gamma permet de plus, en accord avec les travaux de Bolin et Rodhe (1973), de mettre en évidence un nouveau type de modèle que nous qualifierons de **court-circuit**. Dans ce cas l'âge moyen τ_a est supérieur au temps de séjour τ_s. Les eaux minérales de la Versoie où $\tau_a = 6.5$ *ans* et $\tau_s = 4$ ans en sont un exemple. On peut dans ce cas particulier voir une conséquence du rôle joué par le pompage qui écrème les eaux les plus récentes et les plus superficielles de l'aquifère au détriment des eaux plus profondes et plus anciennes. Des systèmes naturels, en particulier des karsts moyés pourraient présenter un comportement analogue.

Cette première application du modèle gamma, bien que gourmande en données expérimentales rarement disponibles sur d'aussi longues durées, nous semble cependant particulièrement intéressante et prometteuse car elle permet de mettre en évidence l'ensemble des modèles isotopiques possibles, depuis le modèle piston jusqu'au modèle court-circuit en passant par le modèle dispersif et le modèle exponentiel, et de les caractériser par deux paramètres.

REFERENCES

Abramowitz, M. & Stegun, I. A. (1965) *Handbook of Mathematical Functions*. Dover Publications, New York.

Blavoux, B. (1978) Etude du cycle de l'eau au moyen de l'oxygène 18 et du tritium. Thèse de doctorat d'état, Université P. et M. Curie, Paris.

Bolin, B. & Rodhe, H. (1973) A note on the concepts of age distribution and transit time in natural reservoirs. *Tellus* **XXV**, 58-62.

Hubert, P., Marcé, A., Olive, P. & Siwertz, E. (1970) Etude par le tritium de la dynamique des eaux souterraines. *C.R. Acad. Sci., Paris* **270**, 908-911.

Maloszewski, P. & Zuber, A. (1982) Determining the turnover time of groundwater systems with the aid of environmental tracers. *J. Hydrol.* **57**, 207-231.

Nir, A. (1964) On the interpretation of tritium "age" measurements of groundwater. *J. Geophys. Res.* **69**, 2589-2595.

Prezewlocki, K. & Yurtsever, Y. (1974) Some conceptual mathematical models and digital simulation approach in the use of tracers in hydrological systems. In: *Isotopes Techniques in Groundwater Hydrology*, 425-450. IAEA, Wien.

Zuber, A. (1986) Mathematical models for the interpretation of environmental radioisotopes in groundwater systems. In: *Handbook of Environmental Isotope Geochemistry* (ed. par P. Frytz & J. C. Fontes), vol. 2, 1-59. Elsevier.

Tracer Technologies for Hydrological Systems (Proceedings of a Boulder Symposium, July 1995). IAHS Publ. no. 229, 1995.

Etude du fonctionnement hydrologique de bassins versants méditerranéens par le traçage naturel chimique et isotopique

VINCENT MARC & YVES TRAVI
Laboratoire d'hydrogéologie, Université d'Avignon, Faculté des Sciences, 33, rue Louis Pasteur, F-84000 Avignon, France

JACQUES LAVABRE
CEMAGREF, Groupement d'Aix-en-Provence, BP 31, Le Tholonet, F-13612 Aix-en-Provence, France

Résumé Sur le bassin versant de recherche du Réal Collobrier (SE de la France), un suivi chimique et isotopique sur plusieurs cycles a été entrepris en 1990 afin de préciser l'organisation des écoulements sur bassin métamorphique en climat méditerranéen. La variété des comportements est présentée ici à partir de l'exemple d'une crue d'automne sur deux sous-bassins (Maurets et Rimbaud) fondamentalement différents par leur géologie, leur pédologie et leur morphologie. D'autre part, la végétation sur le bassin du Rimbaud a été détruite presque totalement par un incendie en août 1990 tandis que le bassin des Maurets n'a pas été affecté. En accord avec les caractéristiques physiques, la décomposition des hydrogrammes réalisée à l'aide des traceurs chimiques et isotopiques montre que le bassin du Rimbaud présente un très fort écoulement superficiel (60% d'eau de pluie) sans contribution significative d'eau du sol tandis que le bassin des Maurets, dont la réaction à la pluie est plus lente, montre une participation de 70-80% d'eau "ancienne" dont environ 60% d'eau préexistante dans les sols. D'un point de vue méthodologique, cette étude nous montre aussi, comme d'autres auteurs l'ont déjà signalé, l'importance de considérer la variabilité temporelle du signal pluie (pour les isotopes) et les effets du pluvio-lessivage (pour les espèces chimiques et Cl^-; particulièrement) pour comprendre l'évolution des traceurs au cours d'une crue en région forestière.

INTRODUCTION

Situé dans le massif cristallin des Maures (à 30 km de Toulon), le bassin de recherche du Réal Collobrier est caractérisé par un climat de type méditerranéen humide et reçoit une pluviosité annuelle de 1000 mm environ. Géré depuis plus de vingt ans par le CEMAGREF, ce bassin a fait l'objet ces dernières années, de recherches multidisciplinaires dans le cadre d'un Groupement d'Intérêt Scientifique (GIS) visant à appréhender les processus d'apparition de l'écoulement en zone forestière méditerranéenne. Dans cette optique, les méthodes chimiques et isotopiques de traçage naturel des eaux, utilisées à l'heure actuelle dans de nombreuses conditions de par le monde (Eshleman *et al.*, 1993; Hinton *et al.*, 1994; Ferguson *et al.*, 1994), offrent d'intéressantes perspectives. Ainsi, un grand nombre de prélèvements de tous les types d'eau (pluie, eau du sol, aquifères et ruisseaux) a été effectué pendant deux ans en se focalisant principalement sur deux sous-bassins différents à plus d'un titre. Hors des contextes géologiques, pédologiques et morphologiques radicalement opposés, l'un des bassins a aussi subi les effets d'un incendie de forêt en août 1990 (Rimbaud) alors que le second est resté très boisé.

Dans cet article, nous examinons et comparons les spécificités hydrologiques de chacun des deux bassins en prenant l'exemple d'une crue représentative de la saison automne-hiver. Cet événement, ayant eu lieu le 9 décembre 1990, permet de proposer, pour chaque bassin, un mode de fonctionnement hydrologique dans des conditions de forte saturation du milieu et de le relier aux caractéristiques physiques des bassins, qu'elles soient naturelles ou d'origine accidentelle (feu). L'investigation chimique et isotopique comparée des deux secteurs d'étude met aussi en lumière certains problèmes méthodologiques liés à l'utilisation des traceurs.

LES SITES D'ETUDE

Le bassin des Maurets (8.4 km^2) est situé sur la face nord du bassin de recherche et présente une forme triangulaire avec une direction d'allongement nord-sud (Fig. 1). Le

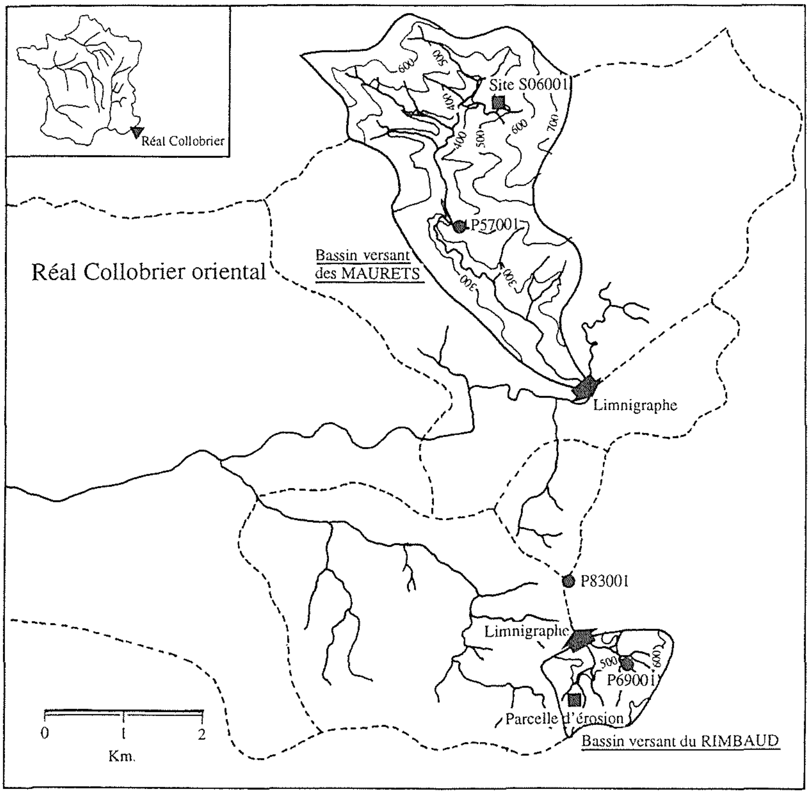

Fig. 1 Situation géographique des bassins versants étudiés.

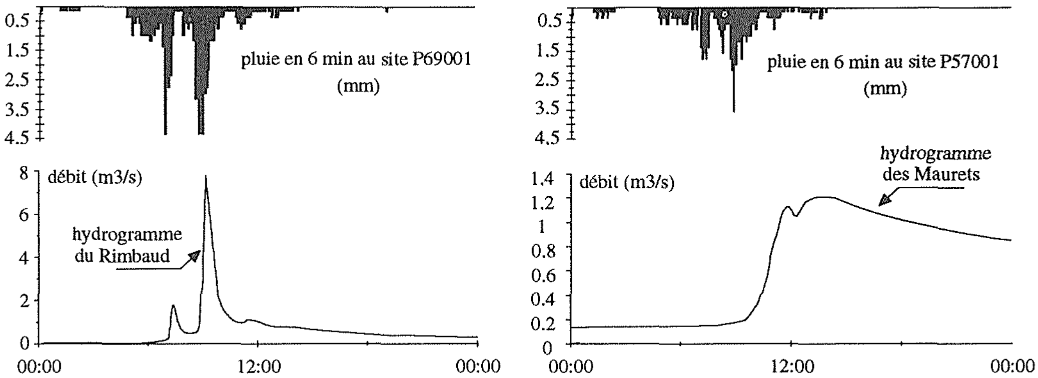

Fig. 2 Hydrogrammes comparés du 9 décembre 1990 sur les bassins des Maurets et du Rimbaud.

relief y est assez accusé puisque 90% du bassin possède une pente supérieure à 10° (Weesakul, 1992). On distingue principalement de larges affleurements de phyllades (partie amont) et d'amphibolites (partie aval). La nature des sols qui surmontent ces formations est très variable, allant du ranker squelettique au sol brun et au sol alluvial (plusieurs mètres d'épaisseur). Le bassin est densément boisé avec une représentation de la majorité des essences méditerranéennes calcifuges (chênes lièges, chênes verts, bruyères, arbousiers, cistes) et des plantations de châtaigniers.

Situé sur la façade sud-est du bassin (Fig. 1), le bassin du Rimbaud, plus petit (1.4 km^2), est aussi plus compact et moins pentu (65% de la superficie totale présente une pente inférieure à 10° (Martin, 1986; Weesakul, 1992) que le bassin des Maurets. Il est constitué uniquement de gneiss surmonté principalement par des sols, peu épais, de type ranker. Parcouru à plus de 84% par un incendie en août 1990, son couvert végétal initial a presque totalement disparu.

METHODES

Au cours de la crue du 9 décembre 1990, un échantillonnage serré des eaux d'écoulement a été réalisé dans le ruisseau du Rimbaud et dans celui des Maurets (pas de temps: 30 mn). Parallèlement, la pluie a été recueillie sur trois pluviographes (P57001, P83001 et P69001) relatifs aux deux secteurs étudiés (Fig. 1). Sur le bassin du Rimbaud, l'eau d'écoulement superficiel de versant a été récoltée sur une parcelle de 75 m^2 destinée à la mesure de l'érosion des sols (Martin, 1986) tandis qu'une tranchée naturelle de sol où l'on observe des écoulements de subsurface (S06001) a été mise à profit sur le bassin des Maurets (Fig. 1).

Les échantillons recueillis ont fait l'objet d'une analyse géochimique complète. Les anions ont été déterminés par chromatographie ionique en phase liquide (chromatographe DIONEX) et les cations par absorption atomique flamme (spectrophotomètre IL 257). La silice a été dosée par analyse d'un complexe silico-molybdique bleu avec un spectrocolorimètre CECIL CE 292. Enfin, le $\delta^{18}O$ a été obtenu par spectrométrie de masse, après équilibration de l'échantillon avec du CO_2. La température atmosphérique est mesurée en continu à la station climatologique Lambert

(Fig. 1) et celle de l'eau au pas de temps de la minute avec la même centrale de mesure que pour les débits (mesures seulement disponibles sur le bassin du Rimbaud à l'occasion de la crue du 9 décembre 1990).

RESULTATS

Hydrologie

La crue du 9 décembre 1990 survient dans un contexte général de forte saturation en eau. En effet, l'événement se produit alors que le bassin du Réal Collobrier a déjà reçu, depuis la fin de l'été, un volume total de pluie de 445 mm. Les dernières précipitations antérieures à la crue, ont été observées entre le 25 et le 29 novembre et représentent, à elles seules, un volume de 120 mm environ.

Sur les deux bassins considérés, la structure de la pluie du 9 décembre est sensiblement la même avec, en particulier, deux pics d'intensité très marqués. Le volume total précipité est de l'ordre de 60 mm sur le bassin des Maurets et de 80 mm sur le bassin du Rimbaud. La Fig. 2 souligne la différence de comportement des deux bassins versants.

L'hydrogramme du bassin du Rimbaud présente deux pics d'importances inégales (1.77 $m^3 s^{-1}$ et 7.75 $m^3 s^{-1}$) qui suivent le centre de gravité des deux averses avec un retard maximum de 20 minutes. Après la seconde pointe de crue, le débit décroît rapidement pour atteindre une valeur de 0.325 $m^3 s^{-1}$ en fin de journée.

Bien que l'on observe aussi deux pics de crue, la situation est bien différente sur le bassin des Maurets. En effet, les débits de pointe sont très comparables et n'excèdent pas 1.2 $m^3 s^{-1}$ (1.125 $m^3 s^{-1}$ pour le premier pic). D'autre part, le temps séparant le corps des averses et les maxima de débit dépasse 4 h. Enfin, le débit relevé le 10 décembre vers 11 h prend encore une valeur de 0.46 $m^3 s^{-1}$.

Investigation chimique et isotopique et décomposition des hydrogrammes

Le bassin versant des Maurets Le comportement chimique et isotopique du ruisseau est montré sur la Fig. 3. On y distingue les phases suivantes:

- au cours de la première pointe de crue, on observe une remarquable dilution de la silice totale concomitamment à un pic de concentration en K^+, NO_3^- et même Cl^-. La silice, absente (ou en très faibles quantités) dans les eaux météoriques et peu influencée par le pluvio-lessivage (Loye-Pilot & Jusserand, 1990), révèle, à cet instant, le rôle majeur de la pluie. Les autres éléments chimiques subissent fortement l'effet du pluvio-lessivage en accord avec les résultats obtenus par ailleurs sur le bassin du Réal Collobrier (Pichon & Travi, 1993; Martin *et al.*, 1993) ou sur d'autres bassins versants (Domingo *et al.*, 1994; Robson *et al.*, 1994). Ces comportements traduisent donc une prédominance de l'eau "nouvelle". Cette interprétation est confirmée par la chute de température observée dans le ruisseau. Notons que le $\delta^{18}O$ est à ce moment très loin de la valeur moyenne de la pluie ($-11.64‰$), ce qui souligne l'importance de la variabilité temporelle du signal isotopique d'entrée.

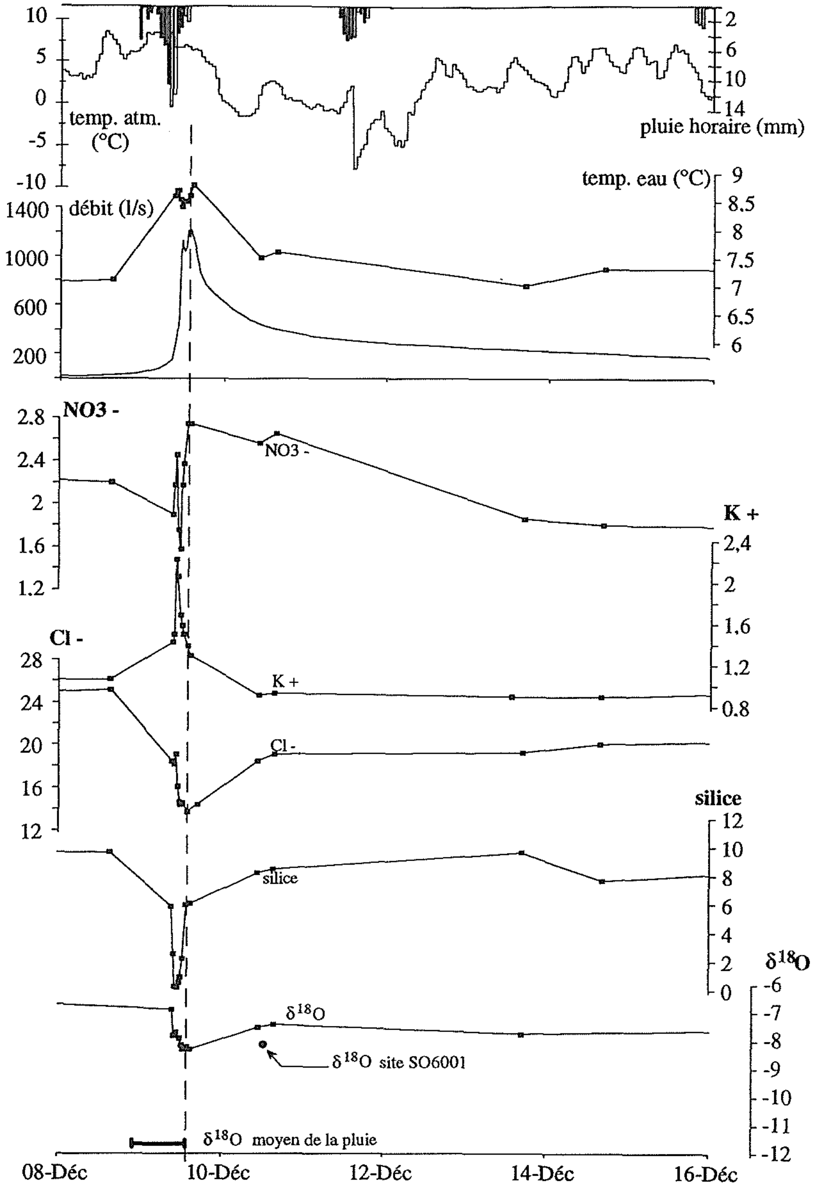

Fig. 3 Evolutions géochimiques dans le ruisseau des Maurets. Les concentrations sont exprimées en mg l^{-1} et le $\delta^{18}O$ en ‰.

– à la seconde pointe de débit, la silice retrouve une concentration non négligeable de 6 mg l^{-1} tandis que celle de K^+ chute brusquement. Cet apparent retour aux caractéristiques géochimiques initiales n'est validé ni par Cl^- qui connaît sa plus faible concentration, ni par NO_3^- qui montre une valeur maximale ni, enfin, par $\delta^{18}O$ dont on mesure une valeur éloignée de 1.4‰ par rapport à la concentration d'avant la crue. En outre, un prélèvement d'eau de subsurface effectué au niveau du site S06001 établit que les teneurs en Cl^- et en ^{18}O du mélange eau de pluie-eau du sol

Tableau 1 Comparaison des teneurs en Cl^- et en $\delta^{18}O$ dans les écoulements de subsurface et dans le ruisseau (seconde pointe de crue).

	$[Cl^-]$ (mg l^{-1})	$\delta^{18}O$ (‰)
Ruisseau (seconde pointe de débit)	13.7	−8.22
Site S06001	10.6	−8.14

avoisinent singulièrement celles mesurées dans le ruisseau à la seconde pointe de crue (Tableau 1). Tous ces éléments s'accordent, à cet instant de l'événement, pour attribuer à la composante souterraine une participation mineure tandis que la contribution de l'eau préexistante dans les horizons superficiels est essentielle.

- seulement en décrue, le retour progressif de la valeur initiale du $\delta^{18}O$ nous indique l'influence grandissante de l'eau souterraine sur le débit. Cependant, ces teneurs isotopiques restent pendant longtemps toujours en deçà de la valeur d'avant la crue, ce qui suggère une influence encore efficace de l'eau de pluie et de l'eau du sol (Cl^- a un comportement semblable). Ceci est d'ailleurs validé par l'évolution de NO_3^- dont les concentrations demeurent relativement élevées pendant plusieurs jours après la crue.

Ainsi, une séparation de l'hydrogramme en trois composantes peut être réalisée à partir des constats suivants:

- la première pointe de crue est uniquement composée d'eau de pluie (ruissellement superficiel). La décomposition commence à partir de la seconde pointe avec la participation de l'eau du sol puis de l'eau de la nappe.
- en admettant une concentration en silice semblable dans la nappe et l'eau du sol (l'assimilation de l'eau du sol au réservoir souterrain est justifiée par la spectaculaire reconcentration à la seconde pointe de crue, au moment où Cl^- et $\delta^{18}O$ sont encore très bas) et une teneur nulle dans la pluie, une séparation pluie-eau préexistante (sol+nappe) peut être menée avec cet élément. Etant donné le très probable enrichissement en silice de l'eau de ruissellement par rapport à l'eau météorique (Martin, 1986; Loye-Pilot & Jusserand, 1990; Marc, 1994), cet exercice conduit à calculer une valeur par défaut de la contribution de la pluie.
- comme nous l'avons déjà suggéré, il est possible de définir avec $\delta^{18}O$, à partir du relevé effectué au site S06001 (écoulement de subsurface), une composante "superficielle" (mélange eau de pluie-eau du sol) et une composante eau profonde (nappe). $\delta^{18}O$ est pour cela le meilleur traceur car le moins susceptible de varier dans l'espace et dans le temps, en particulier pour la composante "mélange" (les fortes conditions de saturation assurent le mélange et l'amortissement du signal isotopique dans les horizons superficiels).

Ces deux approches permettent d'obtenir indépendamment l'hydrogramme souterrain et l'hydrogramme du ruissellement superficiel, et de déduire ainsi celui de l'eau du sol (Fig. 4). De cette façon, en menant la séparation jusqu'au 16 décembre, on estime à 20%, la participation totale de l'eau souterraine, au moins à 20% celle de la pluie et au plus à 60% celle de l'eau préexistante dans le sol.

Le bassin versant du Rimbaud (Travi *et al.*, 1994) Les évolutions de la température de l'eau et des teneurs en Cl^- et en ^{18}O au cours de la crue sont représentées sur la

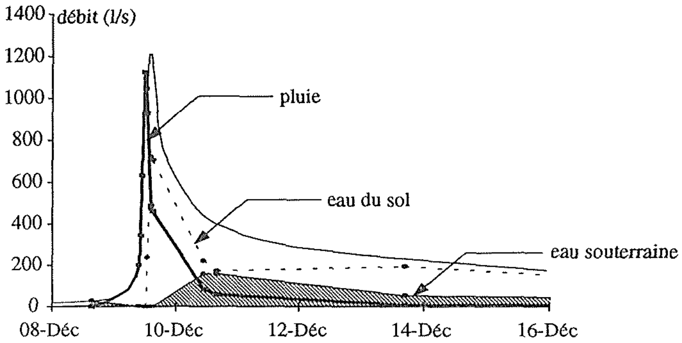

Fig. 4 Séparation en trois composantes de l'hydrogramme sur le bassin des Maurets.

Fig. 5. Les deux traceurs montrent un comportement très semblable, avec cependant une amplitude de dilution plus marquée pour Cl⁻, en relation avec un plus grand écart initial observé entre l'eau d'écoulement d'avant la crue et la pluie. Comparativement à la situation décrite sur le bassin des Maurets, la chute des concentrations est ici beaucoup plus intense. En effet, pour Cl⁻, on atteint un taux de dilution maximal (rapport entre la concentration de l'eau dans le ruisseau avant la crue et celle mesurée au plus fort de la dilution) de 4.6 tandis qu'il est inférieur à 2 dans le ruisseau des Maurets. D'autre part, on relève au moment de la seconde pointe de débit, un $\delta^{18}O$ voisin de la teneur moyenne

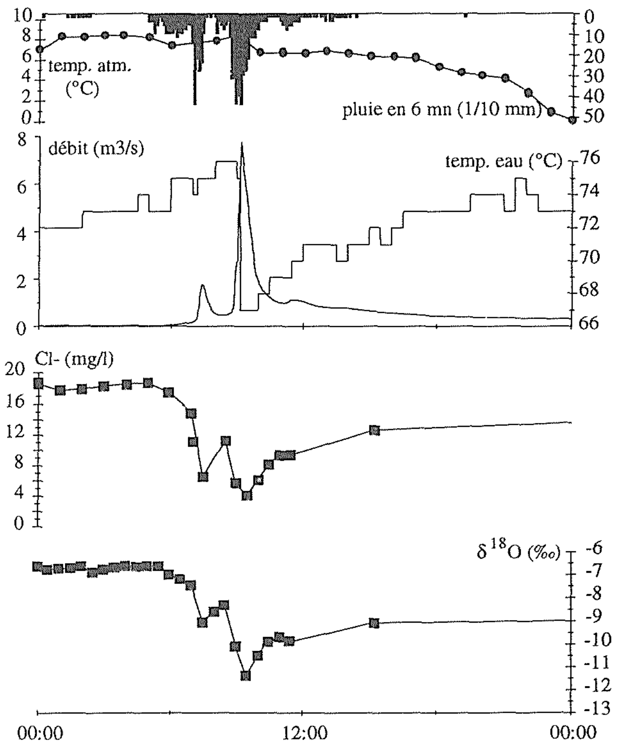

Fig. 5 Evolutions de Cl⁻ et de $\delta^{18}O$ dans le ruisseau du Rimbaud.

de l'épisode pluvieux (on en est très loin sur le bassin des Maurets). Enfin, on note au même moment dans l'eau du ruisseau, une chute de température de près de 1 °C (0.3 °C sur les Maurets). A l'évidence, ces comportements soulignent l'influence majeure du ruissellement superficiel. La forte dilution de Cl^- s'explique donc par l'absence d'altération du signal pluie par un éventuel lessivage des sols (sels + eau enrichie par évaporation) et par l'effet du pluvio-lessivage en raison de la disparition de la végétation suite à l'incendie de forêt d'août 1990. Ceci est confirmé par la teneur mesurée dans l'eau de ruissellement superficiel recueillie sur la parcelle de mesure de l'érosion (2 mg l^{-1}), qui se montre semblable à celle de la pluie (1.8 mg l^{-1}).

A partir de ces observations qui semblent n'accorder que peu de rôle à une eau préexistante dans les sols, la décomposition de l'événement peut être réalisée en considérant deux composantes: l'eau de pluie ($\delta^{18}O = -12.47‰$ et $[Cl^-] = 2$ mg l^{-1}) et l'eau souterraine ($\delta^{8}O = -6.66‰$ et $[Cl^-] = 18.6$ mg l^{-1}). Les calculs réalisés avec les deux traceurs sur toute la journée du 9, donnent des résultats très comparables: 43% d'eau souterraine avec Cl^- et 47% avec $\delta^{18}O$. L'obtention de ces valeurs voisines, en utilisant comme traceurs des éléments dont les effets de source et les réactions sont radicalement différents, prouve bien que deux réservoirs seulement sont concernés au cours de cette crue.

Un examen de détail révèle que la séparation menée avec Cl^- fournit une composante eau souterraine sensiblement plus faible au cours du premier pic de crue (Fig. 6). En accord avec les observations faites sur le bassin des Maurets, ce résultat montre qu'en négligeant ici la variabilité temporelle du signal isotopique entrée (c.a.d. en utilisant, pour tout l'événement, la concentration moyenne en ^{18}O de l'épisode pluvieux), on sous-estime le $\delta^{18}O$ de l'eau "nouvelle" en début de crue. En admettant un $\delta^{18}O$ plus positif pendant la première averse, les hydrogrammes de l'eau souterraine issus du calcul à partir de Cl^- et de $\delta^{18}O$ doivent se rapprocher significativement.

CONCLUSIONS ET DISCUSSION

Fonctionnements hydrologiques

Sur le bassin des Maurets, la réaction du ruisseau vis à vis de l'importante intensité de pluie, est relativement lente. Un effet d'amortissement est mis en évidence dans les horizons superficiels dont l'épaisseur peut être localement substantielle. En fonction des situations géomorphologiques, l'eau préexistante contenue dans ces formations peut être rapidement mise en mouvement et participer à l'écoulement. Ce phénomène, qui met en jeu un important volume d'eau, s'opère cependant relativement tardivement, au cours du second pic de crue. En première phase de crue, on note surtout un net ruissellement superficiel qui met en cause le réseau hydrographique, les pistes et les surfaces saturées contributives (surtout engorgement des profils de sols). Cet écoulement s'exprime de manière impulsionnelle et disparaît assez rapidement. La contribution de l'eau préexistante profonde (nappe) n'apparaît, quant à elle, qu'en phase de décrue et ne représente guère plus de 20% du volume total écoulé. Notons que, pendant très longtemps, le débit en décrue est surtout assuré par la vidange des horizons superficiels (écoulement retardé). Finalement, l'eau préexistante (eau du sol + eau souterraine) représente au total la plus grande contribution à l'écoulement (70 à 80%). Ce modèle de

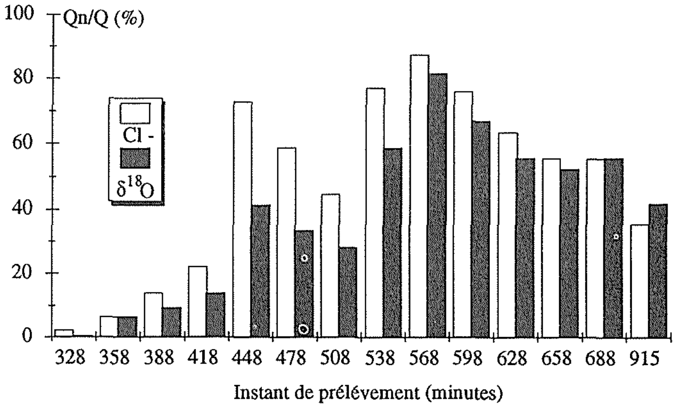

Fig. 6 Décompositions de l'hydrogramme avec Cl^- et $\delta^{18}O$ sur le bassin du Rimbaud.

fonctionnement, représenté par la Fig. 7, est à mettre en étroite relation avec les caractéristiques lithologiques du bassin. Constitué en majorité de phyllades et d'amphibolites, le bassin des Maurets est, en effet, non seulement très capacitif mais aussi hautement restitutif. Ainsi, malgré une grande potentialité de stockage, il montre une production non négligeable au sein des bassins du Réal Collobrier (Lavabre *et al.*, 1993). Bien entendu, la situation décrite est représentative des conditions spécifiques d'humidité du milieu préalables à la crue. En fonction du taux de saturation (et donc de la saison), ce schéma peut se trouver fortement modifié (Marc, 1994). Toutefois, à part quelques situations particulières (orage après l'été, par exemple, où le ruissellement

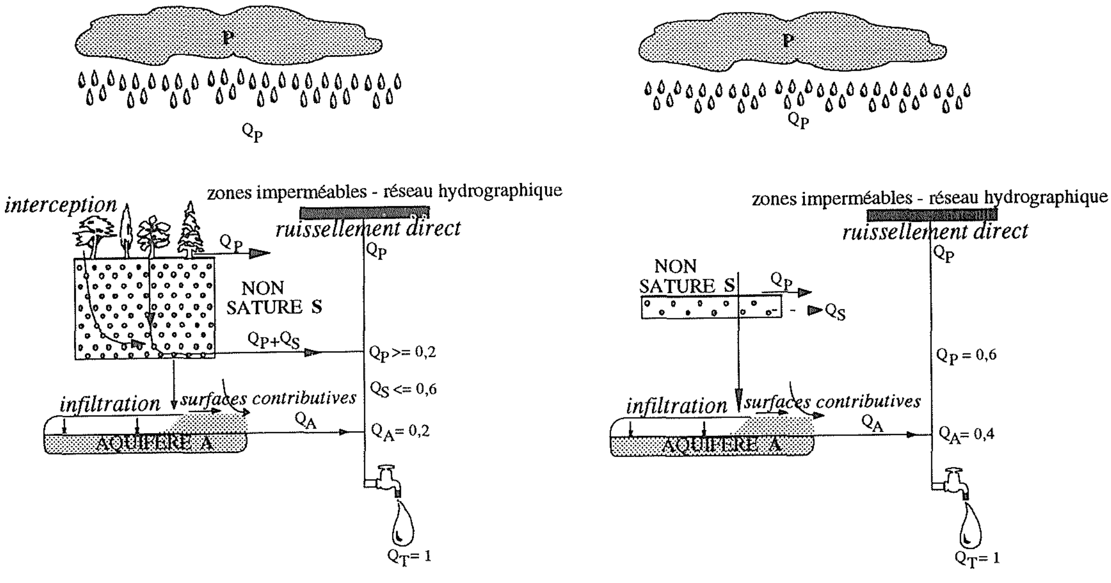

bassin versant des MAURETS

bassin versant de RIMBAUD

Fig. 7 Schéma conceptuel de fonctionnement hydrologique sur les bassins des Maurets et du Rimbaud pour la crue du 9 décembre 1990.

superficiel domine), l'importante contribution des eaux contenues dans les sols est toujours de rigueur.

Sur le bassin du Rimbaud, les conditions lithologiques (gneiss, roches massives) et pédologiques (sols sableux et caillouteux d'une épaisseur moyenne de 30-35 cm) garantissent une forte réactivité du ruisseau aux précipitations. La disparition de la couverture végétale à la suite de l'incendie d'août 1990, a amplifié ce phénomène en donnant au bassin un caractère impulsionnel au moment des crues (Lavabre *et al.*, 1993). Le traçage chimique et isotopique révèle cependant que la pluie à elle seule n'explique pas tout l'écoulement. En effet, la contribution de l'eau souterraine se montre non négligeable (environ 40%) et s'exprime tout au long de la crue. Dans des conditions de forte saturation, sa participation immédiate est donc vraisemblablement issue de l'affleurement rapide de la nappe et de l'extension des zones saturées contributives. Les caractéristiques lithologiques du bassin sont peu favorables à un stockage important dans les horizons superficiels et l'eau atteint très rapidement les niveaux saturés peu profonds au sein du gneiss. De cette façon, contrairement au bassin des Maurets, l'apparition de zones saturées par engorgement des sols est peu probable (Fig. 7). De même, la contribution d'une eau préexistante dans les horizons superficiels apparaît négligeable.

Réflexions méthodologiques

Comme d'autres auteurs l'ont déjà signalé (McDonnell *et al.*, 1990; Pionke *et al.*, 1993), nous observons que l'utilisation du traceur isotopique se révèle délicate si on méconnaît la variabilité temporelle du signal au cours de la pluie. Cette variabilité prend toute son importance pour les petits bassins très réactifs ou pour les plus grands bassins ayant atteint une saturation optimale. Dans une grande majorité de cas, il devient donc essentiel, pour comprendre l'évolution du $\delta^{18}O$ dans un ruisseau au cours d'une crue, de procéder à un échantillonnage fractionné de l'épisode pluvieux. Dans notre situation, la difficulté a été contournée par un examen détaillé de l'évolution des espèces chimiques qui donnent, selon le cas, des informations tant qualitatives que quantitatives.

Sur bassin forestier, les traceurs chimiques sont fortement influencés par un phénomène assez souvent négligé dans la littérature: le pluvio-lessivage. La comparaison du fonctionnement de Cl^-, par exemple, entre un bassin forestier intact et un bassin incendié a montré ici le rôle majeur de cette altération initiale.

REFERENCES

Domingo, F., Puigdefabregas, J., Moro, M. J. & Bellot, J. (1994) Role of vegetation cover in the biogeochemical balances of a small afforested catchment in southeastern Spain. *J. Hydrol.* **159**, 275-289.

Eshleman, K. N., Pollard, J. S. & Kuebler, O'Brien A. (1993) Determination of contributing areas for saturation overland flow from chemical hydrograph separation. *Wat. Resour. Res.* **29**(10), 3577-3587.

Ferguson, R. I., Trudgill, S. T. & Ball, J. (1994) Mixing and uptake of solutes in catchments: model development. *J. Hydrol.* **159**, 223-233.

Hinton, M. J., Schiff, S. L. & English, M. C. (1994) Examining the contributions of glacial till water to storm runoff using two- and three-component hydrograph separations. *Wat. Resour. Res.* **30**(4), 983-993.

Lavabre, J., Cernesson, F. & Torres, D. S. (1993) Changes in the hydrological response of a small mediterranean basin a year after a wildfire. *J. Hydrol.* **145**, 389-402.

Lavabre, J., Folton, N. & Cernesson, F. (1993) Projet DM2E, BVRE du Réal Collobrier, Modélisation des écoulements mensuels. *Actes Workshop DM2E* (Aix-en-Provence).

Loye-Pilot, M. D. & Jusserand, C. (1990) Décomposition chimique et isotopique d'un hydrogramme de crue d'un torrent méditerranéen. Réflexions méthodologiques. *Rev. Sci. de l'Eau* **3**, 211-231.

Marc, V. (1994) Etude de la relation pluie-débit sur bassin versant en climat méditerranéen par le traçage chimique et isotopique naturel de l'eau (Réal Collobrier, massif des Maures, Var). Thèse Univ., Montpellier II.

Martin, C. (1986) Contribution à l'étude de la dynamique des versants en roches métamorphiques. L'exemple du Massif des Maures. Thèse Etat, Paris I.

Martin, C., Quillard, J., Gimenez, H. & Chevalier, Y. (1993) Etude des pluviolessivats à la station du Boussicaut. *Actes Workshop DM2E* (Aix-en-Provence).

McDonnell, J. J., Bonell, M., Stewart, M. K. & Pearce, A. J. (1990) Deuterium variations in storm rainfall. Implications for stream hydrograph separation. *Wat. Resour. Res.* **26**(3), 455-458.

Pichon, A. & Travi, Y. (1993) Modifications chimiques et isotopiques du signal pluie lors de son passage au travers de la végétation en zone méditerranéenne (BVRE du Réal Collobrier, Var, France) – résultats préliminaires. *Actes Workshop DM2E* (Aix-en-Provence).

Pionke, H. B., Gburek, W. J. & Folmar, G. J. (1993) Quantifying stormflow components in a Pennsylvania watershed when ^{18}O input and storm conditions vary. *J. Hydrol.* **148**, 169-187.

Robson, A. J., Neal, C., Ryland, G. P. & Harrow, M. (1994) Spatial variations in throughfall chemistry at the small plot scale. *J. Hydrol.* **158**, 107-122.

Travi, Y., Lavabre, J., Blavoux, B. & Martin, C. (1994) Traçage chimique et isotopique (Cl^-, ^{18}O) d'une crue d'automne sur un petit bassin versant méditerranéen incendié. *Hydrol. Sci. J.* **39**(6).

Weesakul, U. (1992) Apports de la télédétection et de l'information géographique numérique à la compréhension du fonctionnement hydrologique des bassins versants méditerranéens. Thèse Univ., Montpellier II.

Tracer Technologies for Hydrological Systems (Proceedings of a Boulder Symposium, July 1995). IAHS Publ. no. 229, 1995.

Snowmelt runoff generation in a mountainous catchment

LADISLAV HOLKO
Institute of Hydrology, Slovak Academy of Sciences, Ondrasovecka 16,
031 05 Liptovsky Mikulas, Slovakia

Abstract Pre-event water contributed significantly to snowmelt runoff in the mountainous basin of Jalovecky potok creek in the Western Tatra Mountains in April 1992. A two-component separation model based on the environmental deuterium content of stream and snowmelt samples showed that on average 92% of runoff originated from pre-event water. The variation of deuterium content of stream water was nearly 4 times lower than that of snowmelt water. Daily variations of deuterium in snowmelt water are not pronounced, while day by day variations at the beginning of snowmelt and during its main phase are more significant. Snowmelt water samples indicate that light isotopes leave the snowpack first. Soil water samples could explain some uncertainties of the two-component model. Isotopic separation could not be used during the main phase of snowmelt due to the small differences between isotopic composition of snowmelt and stream water.

INTRODUCTION

Catchment runoff is the best measured water balance component. However, runoff generation is yet not fully understood. There is still scientific discussion on the role of overland, subsurface and groundwater flows in runoff generation and its mechanisms. Environmental isotopes are the tools that can help to answer some of the above mentioned problems. Water molecules are composed of oxygen and hydrogen isotopes. Ratios of heavier and lighter isotopes of oxygen and hydrogen are, in the hydrological cycle (evaporation, precipitation, runoff) controlled by evaporation and condensation processes only. During evaporation, lighter molecules are removed first and the remaining liquid becomes isotopically heavier. Condensation, on the other hand results in the preferential removal of heavier isotopes from the vapour. This natural labelling of water can be used to trace its origin and history.

Environmental isotopes have been using for runoff separation since the end of the 1960s. First applications used radioactive tritium as a tracer. Since the beginning of the 1970s stable isotopes of deuterium and later ^{18}O have also been used. Separation by means of stable environmental isotopes is based on the chemical mixing formulae:

$$Q_t = \Sigma Q_n \quad (1)$$

$$Q_t c_t = \Sigma Q_n c_n \quad (2)$$

where

Q_t, Q_n = total runoff and its components, respectively,

c = tracer concentration of particular flow.

Usually, a two-component model is used for which at least the isotopic composition of stream water and event water (snowmelt or rainfall) must be known. Pre-event water (usually referred to as groundwater) is supposed to have isotopic composition of streamflow before the event if there are no groundwater samples from wells available. The above equations then read:

$$Q_s = Q_p + Q_e \tag{3}$$

and

$$Q_s\, c_s = Q_p\, c_p + Q_e\, c_e \tag{4}$$

where Q_s, Q_p, and Q_e are flows of stream water, pre-event and event (snowmelt or rain) water and c_s, c_p and c_e are corresponding tracer concentrations.

Intensive sampling of precipitation, snow cover, runoff and soil water carried out in the Jalovecky potok creek catchment in hydrological years 1991-1993 should provide data on isotopic composition of natural waters in the highest part of Carpathians. Except precipitation and runoff also snow cover and to some extent soil water samples were collected for isotopic analyses. This paper deals with some results from the spring 1992 snowmelt period. It is focused on the problem of streamflow origin as recognized by means of environmental deuterium and on applicability of isotopic separation method for a runoff generation study in the given catchment.

CATCHMENT AND MEASUREMENTS

The Jalovecky potok creek catchment is a mountainous catchment situated in the Western Tatra Mountains. Institute of Hydrology SAS established the experimental network within the catchment which provides the data necessary to improve water balance calculations in mountains. First measurements in the catchment within the framework of this research were carried out in 1986.

The catchment area is 23 km^2 and the mean altitude 1500 m a.s.l. Geologically, it is formed mainly by Palaeozoic crystalline rocks and granodiorites. Only a narrow stripe of Mesozoic nappes with prevailing limestones and dolomites occur along the western boundary of the catchment. Vegetation is represented by forests (mainly spruce), dwarf pine and alpine and sub-alpine meadows that cover 44, 32 and 24% of catchment area, respectively. Mean annual precipitation is 1466 mm, runoff 874 mm and air temperature 3.5°C.

Water samples for runoff separation were collected from the stream and from the snow lysimeter. Stream samples were taken at the catchment outlet. The stream profile is equipped with a water level recorder so that continuous discharge data are available through the rating curve. The catchment outlet is at an altitude of 800 m a.s.l. A snow lysimeter – 2.25 m^2 thin plastic blanket laid on the ground surface before snowfall – at altitude 1100 m a.s.l. was used to collect samples from melting snow that represented event water. The construction of the snow lysimeter did not allow measurement of snowmelt discharge. Generally, 50 ml of water were taken as a sample. Isotopic analyses of samples were carried out in a laboratory of the International Atomic Energy Agency in Vienna. The results are expressed as δ-values in ‰.

RESULTS AND DISCUSSION

Snowmelt in spring 1992 started by a short melting episode in the end of March. The first large snowmelt between 5 and 10 April was followed by a smaller episode on 14 April. Due to following cold weather the snowmelt ceased. The main phase of snowmelt started on 25 April (Fig. 1).

Snowmelt water was sampled between 5 and 30 April. The samples were collected several times daily during the intense melting, otherwise once daily. Results are shown in Fig. 1 and Fig. 2. Deuterium concentrations varied from −100.1‰ to −65.1‰. Daily variations were not very large. However, a gradual increase of concentrations of heavy isotopes in the melting snow is clearly pronounced. Light isotopes left the snowpack first.

Stream water was sampled during the whole winter season. Between 5 and 30 April the samples were taken together with snowmelt samples (Figs 1 and 2). Unlike snowmelt, the range of deuterium concentrations in stream water during the snowmelt is not very large. The deuterium content between 5 and 30 April varied from −68.9‰ to −78.6‰. Daily variations were small.

Runoff separation during the snowmelt episode on 5-10 April was calculated by the two-component model. The application is based on the difference between isotopically heavier groundwater and lighter winter precipitation accumulated in snow cover that melts in the spring. Deuterium was used as the tracer. The groundwater was supposed to have a constant concentration of deuterium -72.9‰. As the samples were taken manually, we were interested in the possibility of filling in some data according to known pattern of isotopic composition of stream- and snowmelt water (daily and day by day variations). Values of deuterium for snowmelt as well as stream water at midnight on 5 April were calculated as average values of mean concentrations of successive days.

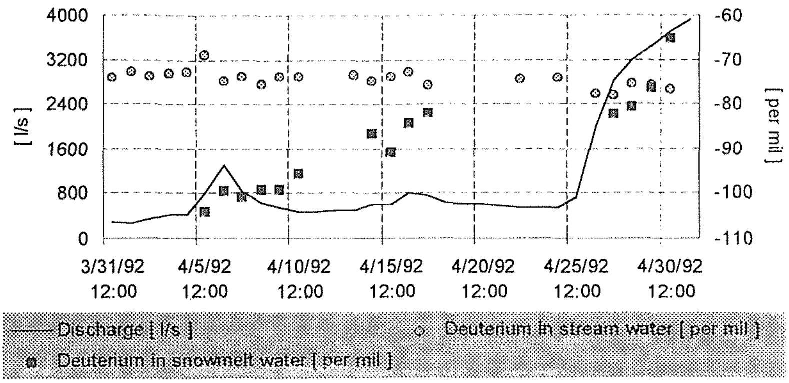

Fig. 1 Daily discharge and deuterium concentrations of stream and snowmelt water in April 1992.

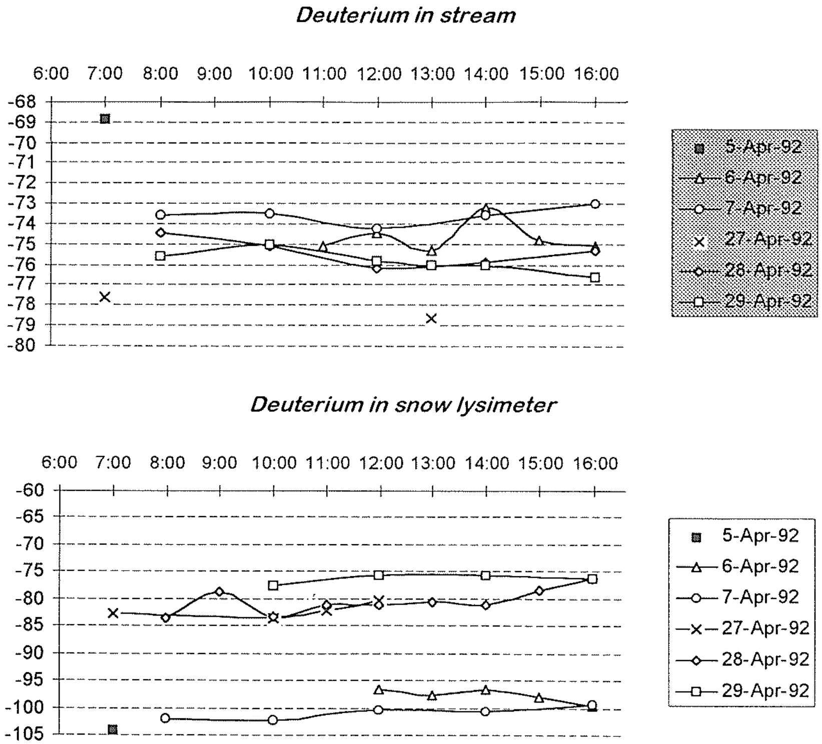

Fig. 2 Variations of deuterium (in per mille) in stream and snowmelt water during the day.

According to the separation 90-100% of the total runoff (92% on average) during the event was contributed by the pre-event water (Fig. 3).

Originally, isotopically separated runoff components were thought to be groundwater and snowmelt (rainfall) contributions. Sklash & Farvolden (1979) summarized the assumption behind application of isotopic separation as follows:

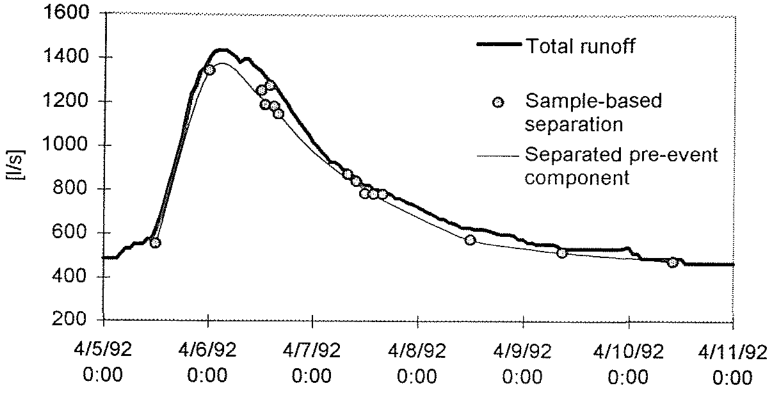

Fig. 3 Separated pre-event component during snowmelt event on 5-10 April 1992.

- Isotopic compositions of event and pre-event components significantly differ.
- Event component has stable isotopic composition.
- Isotopic composition of groundwater is equal to that of vadose water or the contribution of vadose water is negligible.
- Surface storages contribute minimally to runoff events.

The main result of our separation is that runoff was dominated by pre-event water. The choice of a representative value of tracer concentration of groundwater was found to be the most sensitive task in our calculation. The calculated portion of pre-event water seems to be rather high. A possible explanation is that soil water contributions were higher than the two-component modes assumes. The two-component model masks the importance of soil water by lumping it with groundwater which leads to erroneous results (DeWalle *et al.*, 1988). Although soil water importance as a possible storm flow contribution is uncertain (e.g. Herrmann *et al.*, 1987), some isotopic separations showed that it can form some small part of runoff (DeWalle *et al.*, 1988). Soil water samples could improve separations in our case, too.

Due to the above mentioned problems separated runoff components are denoted as pre-event and event rather than groundwater and snowmelt contributions. Naturally, there are problems of estimating catchment-representative values of deuterium concentrations in infiltrating snowmelt water, too. Catchment surveys of isotopic composition of snow cover have shown that it is not altitude dependent (Holko, 1993). Considering time-dependent melting in the lower and higher parts of the catchment it is possible to assume that snowmelt samples taken from the snow lysimeter at an altitude 1100 m a.s.l. are representative for the separated runoff event. Thus, we can conclude that at least during the initial phase of snowmelt that the runoff is dominated by pre-event water. Isotopic composition of snowmelt and stream water was very similar during the main phase of snowmelt. Therefore, runoff separation could not provide reliable results for that part of the snowmelt.

Acknowledgement This work has been partially supported by the International Atomic Energy Agency in Vienna. I would like to express my gratitude to Mr W. Stichler for his support and comments on data results.

REFERENCES

DeWalle, R. D., Swistock, R. B. & Sharpe, E. W. (1988) Three-component tracer model for stormflow on a small Appalachian forested catchment. *J. Hydrol.* **104**.

Herrmann, A., Koll, J., Schöniger, M. & Stichler, W. (1987) A runoff formation concept to water pathways in forested basins. In: *Forest Hydrology and Watershed Management* (ed. by R. H. Swanson, P. Y. Bernier & P. D. Woodard) (Proc. Vancouver Symp., August 1987), 519-529. IAHS Publ. no. 167.

Holko, L. (1993) Isotopic composition of precipitation and snow cover in the Western Tatra Mountains. In: *Advances in Water Sciences* (Proc. Int. Symp., High Tatras, Slovakia).

McDonnell, J. J., Stewart, M. K. & Owens, I. F. (1991) Effect of catchment-scale subsurface mixing on stream isotopic response. *Wat. Resour. Res.* **27**(12).

Rodhe, A. (1987) The origin of streamwater traced by oxygen-18. Doctoral Thesis at Uppsala University, Report Series A, no. 41, Sweden.

Sklash, M. G. & Farvolden, R. N. (1979) The role of groundwater in storm runoff. *J. Hydrol.* **43**.

Tracer Technologies for Hydrological Systems (Proceedings of a Boulder Symposium, July 1995). IAHS Publ. no. 229, 1995.

A mathematical approach based on tritium tagging technique to evaluate recharge to groundwater due to monsoon rains

BHISHM KUMAR & RM. P. NACHIAPPAN
National Institute of Hydrology, Roorkee-247667, Uttar Pradesh, India

Abstract Recharge values to groundwater have been evaluated in the Bundelkhand region of Uttar Pradesh state, India, using a tritium tagging technique at 25 locations. The experimental data have been analysed to develop a mathematical formulation with respect to rainfall which can be used to estimate the recharge to groundwater due to monsoon rains in future. This technique has also been tried for various other regions of the country where recharge values to groundwater have been determined using the tritium tagging technique by other investigators who have also developed empirical relationships. The results indicate that the empirical relationship established by various investigators for different regions in India, using one or more parameters which affect the rainfall recharge process, do not hold good neither for the study area used by the authors nor for the region for which these relationships have been developed. Mathematical formulations have been suggested which are based on experimental data. In the present paper, it has been shown that one region may have a number of mathematical formulations depending upon the prevailing hydrogeological and other conditions in the area.

INTRODUCTION

In order to evaluate recharge to groundwater, a water table fluctuation approach is in vogue in most countries. However, water table fluctuations may occur due to many processes like recharge due to rainfall, irrigation and percolation from surface water bodies, use of groundwater for irrigation, drinking, industrial and similar purposes, flow of groundwater to rivers or *vice versa*, leakage from shallow aquifers to deep aquifers etc. Therefore, the water table fluctuation approach may lead to the wrong predictions, if the data about the effects of individual parameters are not accurately known. In such conditions, the tritium tagging technique, which provides information on recharge to groundwater without being influenced by any of the above processes, can be used.

Although a large area can be covered by using the tritium tagging technique, it is very difficult to carry out the field experiments repeatedly for the evaluation of recharge to groundwater using this technique. Therefore, it is necessary to develop some mathematical formulation to calculate the recharge due to monsoon rains, if only information on rainfall is available. But it is also not advisable to develop an empirical relationship using only one or more of those hydrological parameters which act as constants but affect the rainfall-recharge process. The authors have given emphasis to study the recharge to groundwater due to monsoon rains since the major recharge to groundwater takes place during this season; however, the method suggested here can also be applied for estimating recharge to groundwater during other seasons.

Groundwater recharge by rainfall is a very complex process influenced by numerous surface and subsurface parameters including rainfall intensity, its frequency and several other local factors (e.g. vegetation cover, soil properties, etc.). Therefore, it is advisable that once the recharge to groundwater due to rain and/or irrigation is determined using the tritium tagging technique, a suitable mathematical approach can be developed which will account for all the known and unknown factors affecting the rainfall-recharge procedure. If the correct information of all the processes and parameters which affect the rainfall-recharge process are possible to obtain, a suitable mathematical model can be developed.

In the present paper, a study of recharge to groundwater, carried out in a large problematic area using the tritium tagging technique, is reported along with the mathematical formulations developed based on the field experimental data. This approach has also been applied to areas where studies have been carried out by other investigators earlier and the difference between the methods adopted for the development of empirical relationships has been highlighted.

STUDY AREA

The Bundelkhand region in India comprises 12 districts out of which five fall in Uttar Pradesh and seven in Madhya Pradesh. The study area comprises four districts, namely Jalaun, Banda, Hamirpur and Jhansi, covering an area of approximately 24 079 km^2. The Bundelkhand region of India falls in a subtropical region characterized by a hot and prolonged summer followed by a rainy season and a cold winter. The distribution of rainfall is not only erratic in the region but the same situation persists even in a small area, causing occasional drought conditions. Jalaun, Banda and parts of Hamirpur (60%) and Jhansi (10%) are underlain by indo-gangetic marginal alluvium of quaternary age and comprise mainly sand of various grades, clay and clay mixed with kankar, while the major parts of Jhansi and about 40% area of Hamirpur fall under rocky formation, and therefore the surface soil is more compact in comparison to that in other two districts.

The Bundelkhand region in India faces acute water deficiency due to high losses of rain and surface waters. Although the rainfall in this region is less in comparison to the surrounding region, it is much higher in comparison to the rainfall in semi-arid regions. The groundwater reserves found are very limited and the groundwater level is also deep at a number of places. Hence it is treated as an undeclared semi-arid region in India. Keeping in view the prevailing conditions in the Bundelkhand region, it is necessary to estimate the correct value of recharge to groundwater due to monsoon rains, the main source.

TRITIUM TAGGING TECHNIQUE AND METHODOLOGY

Tritium is a radioactive isotope of hydrogen having a half-life 12.26 years. Being a part of the water molecule, tritium is commonly used as an artificial tracer for hydrological studies. Although the analysis of tritium activity requires some costly laboratory facilities, keeping in view the low health hazard possibilities and the accuracy in water tracing studies, its use is increasing in developing countries.

The tritium tagging technique was developed by Zimmermann *et al.* (1967a,b) and Munnich (1968a,b) with the assumption that the movement of soil moisture in an unsaturated zone is similar to piston type flow i.e. if any amount of water is added to the ground surface due to precipitation or irrigation, it will percolate by pushing an equal amount of water beneath it further down and so on such that an equal amount of the moisture of the last layer in the unsaturated zone is added to the groundwater. However, it can be well understood that in the case of unsaturated flow where air and water are found, which have entirely different properties, the movement of soil moisture cannot be a piston type flow. Therefore, a number of questions have been raised by various researchers (Datta *et al.*, 1990; Mookerjee, 1990; Singh & Kumar, 1993) on the assumption of piston flow movement and some evidences have been reported where the soil moisture flow does not follow piston type movement. At the same time, it has also been mentioned that the results of recharge to groundwater determined using tritium tagging technique are comparable to those determined using other methods. Therefore, there is no doubt about the sufficient approach of the results obtained by using this technique.

In this technique, tritium is injected at a depth well below the root and sun heating zone (70 to 100 cm) at selected sites in the study area. The tritium injection sites are left open for agricultural and other activities including natural variations. However, soil samples are collected from different depths at the time of tritium injection for obtaining information on initial soil moisture conditions. The injected tritium is removed by collecting soil samples from the tritium injection points at an interval of 10 cm depth after a chosen time interval. These soil samples are analysed to study the soil moisture and dry density. The soil samples are also subjected to distillation in order to get the tritiated water samples from the corresponding depths. The tritium activity is determined in the distilled water samples in order to know the movement of the tritium peak. It has been noticed that the tritium peak obtained after the chosen period broadens due to diffusion, streamline dispersion and input water irregularities. Therefore, the centre of gravity of the broad tritium peak is considered in order to calculate the recharge to groundwater (Zimmermann *et al.*, 1967b). The recharge to groundwater is calculated by multiplying the tritium peak shift with the average volumetric moisture content obtained in the tritium peak shift region.

RECHARGE STUDY IN BUNDELKHAND REGION OF UTTAR PRADESH STATE

As mentioned earlier, the Bundelkhand region faces acute water scarcity and uncertainty of groundwater availability. Therefore, it is important to have the information of recharge to groundwater due to monsoon rains and irrigation etc. Tritium was injected at 25 sites before the start of monsoon rains (Fig. 1). The soil sampling was carried out at the injected sites in the month of November and recharge was calculated. Since sampling was carried out in November, the water input for irrigation was also taken into account while determining the recharge percentage.

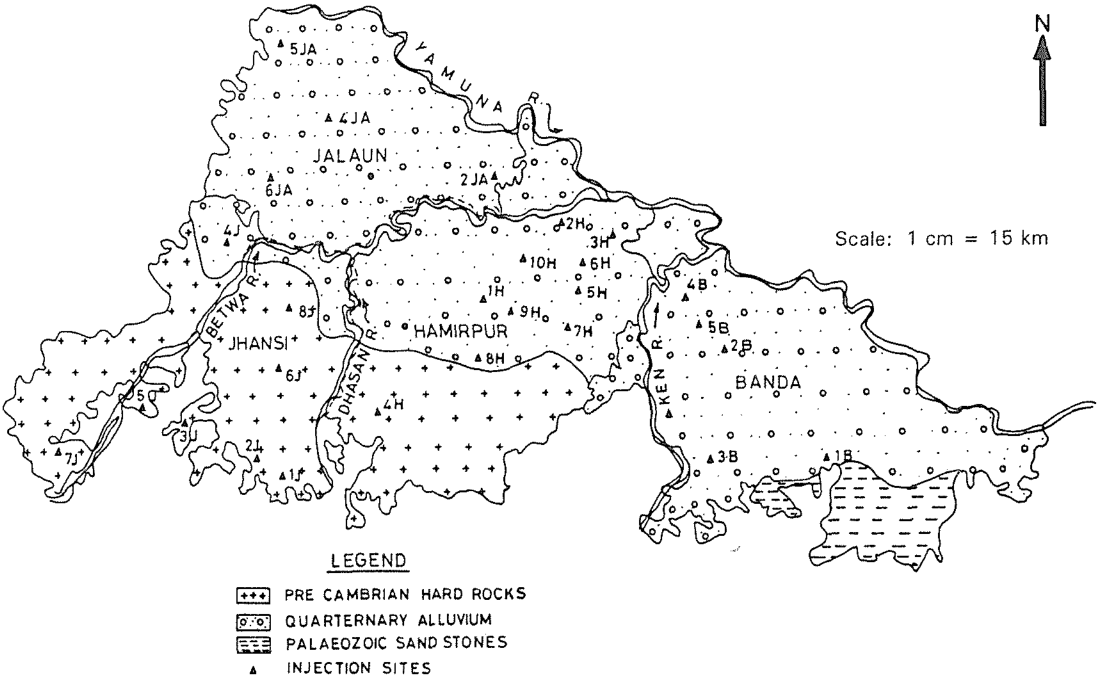

Fig. 1 Study area falling in the Bundelkhand region showing sites of tracer injection.

It is clear from the results obtained that there is a wide variation in the values of recharge to groundwater (Table 1). This variation may be due to different type of soil, topography, hydrogeology, groundwater level conditions, cropping pattern, rainfall pattern, evapotranspiration and several other local factors which are very difficult to account for.

MATHEMATICAL APPROACH

The recharge values were analysed with respect to clay percentage, clay/sand ratio, water table fluctuation and rainfall data. It has been observed that the recharge values follow a unique logarithmic relationship with rainfall, for similar site conditions, while different relationships are observed for the other sites. The plots of recharge values obtained at 25 sites in four districts are shown in Fig. 2. The following two mathematical formulations fairly satisfy the variation of recharge values.

$$\text{Group A} \quad Rg = 29.316 \ln(P) - 111.259 \quad (r = 0.83) \tag{1}$$

$$\text{Group B} \quad Rg = 12.861 \ln(P) - 48.757 \quad (r = 0.85) \tag{2}$$

where Rg is recharge to groundwater in cm and P is rainfall/precipitation in cm.

It is interesting to note that when the two different trends of variation were correlated with hydrogeological conditions, it was found that recharge values for the

Table 1 Rainfall + Irrigation and estimated recharge at different stations in the Bundelkhand region, U.P., India for the period from June 1980 to November 1980.

Code	Station	District	Rainfall + irrigation (cm)	Estimated recharge (cm)
1B	Bania Ka Purwa	Banda	72.16	13.12
2B	Murwal	Banda	64.38	11.25
3B	Padmai	Banda	79.76	14.64
4B	Tara	Banda	81.99	12.81
5B	Mrighani	Banda	91.99	19.87
1J	Khillara	Jhansi	81.20	8.05
2J	Siyoni Khurd	Jhansi	104.06	8.29
3J	Khirak	Jhansi	79.32	23.48
4J	Khilli	Jhansi	88.05	16.15
5J	Baruwa Sagar	Jhansi	95.30	10.97
6J	Panduwah	Jhansi	86.85	10.69
7J	Manipur Moitra	Jhansi	99.40	6.35
8J	Mandori	Jhansi	92.50	11.78
2JA	Kadaura	Jalaun	164.70	17.86
4JA	Jalaun	Jalaun	106.20	13.00
5JA	Rampura	Jalaun	134.30	34.00
6JA	Konch	Jalaun	103.70	10.19
1H	Muskara	Hamirpur	81.21	21.95
2H	Lalpura	Hamirpur	95.18	22.04
3H	Kuchchecha	Hamirpur	95.18	22.78
4H	Rewai	Hamirpur	111.77	11.60
5H	Engohta	Hamirpur	71.90	6.09
6H	Gatak Nahar	Hamirpur	81.20	7.31
7H	Khanna	Hamirpur	81.21	15.50
8H	Bharwara	Hamirpur	76.21	18.98

sites which fall in the marginal alluvium region follow equation (1) and those which fall in the hard rock region follow equation (2).

Besides the above, recharge values were also calculated using the well known Chaturvedi formula (Chaturvedi, 1973) and Amritsar formula (Sehgal, 1973) which are popular in India. The plots of these values are also shown in Fig. 2 which clearly indicate that the Amritsar formula gives in general consistently higher estimates while the Chaturvedi formula seems to be partly applicable.

In addition to the experimental values obtained for the Bundelkhand region, this mathematical approach has also been applied to the Sabarmati basin and Mahi Command

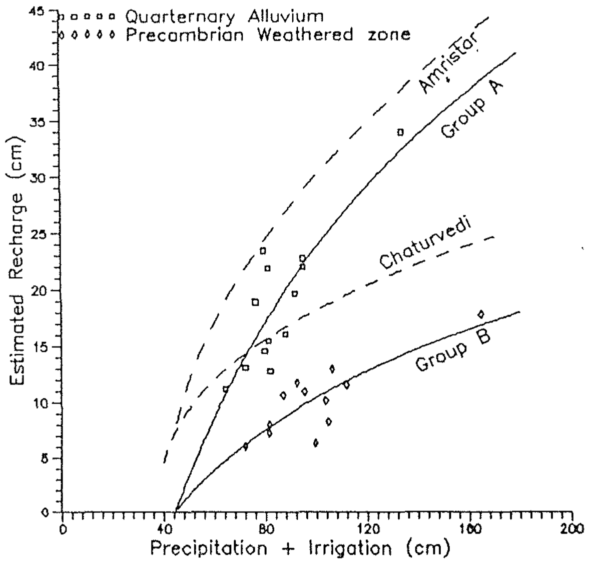

Fig. 2 Variation of recharge to groundwater with rainfall in the Bundelkhand region.

Area in Gujarat State for which Bhandari *et al.* (1986) have studied recharge to groundwater using the tritium tagging technique. These investigators have developed an empirical relationship using precipitation and in some cases type of soil approaches. The results indicate that the empirical relationship does not cover the variation in results truly. The map of the Sabarmati basin along with locations of study points and categorization of area with respect to the trends of variation in recharge values according to the authors approach is shown in Fig. 3. The plots of recharge values with respect to rainfall are shown in Fig. 4(a) and (b) taking into account two and three trends of variation (if higher accuracy is required) along with the plots based on the empirical relationship developed by Bhandari *et al.* (1986). Due to fewer experimental points, the curve representing the fourth trend of variation in recharge values has not been shown in Fig. 4(b). If two trends are considered the correlation coefficient of the groups are 0.59 and 0.61. But if three trends are considered the equations are as follows:

$$\text{Group A} \quad Rg = 20.469 \ln(P) - 60.568 \quad (r = 0.80) \tag{3}$$

$$\text{Group B} \quad Rg = 14.345 \ln(P) - 42.376 \quad (r = 0.94) \tag{4}$$

$$\text{Group C} \quad Rg = 15.681 \ln(P) - 58.174 \quad (r = 0.92) \tag{5}$$

Similarly, the map of the Mahi Command Area with above referred information is shown in Fig. 5 and the plots of recharge values with respect to rainfall indicating the curves based on the mathematical approach suggested by the authors (the empirical relationship has not been indicated by the earlier investigators for this region) are shown in Fig. 6. The correlation coefficient, if the entire data set is considered as a single population is 0.42, but if two trends are considered then, the correlation coefficients of group A and B are 0.72 and 0.58. The above two examples of the Sabarmati basin and

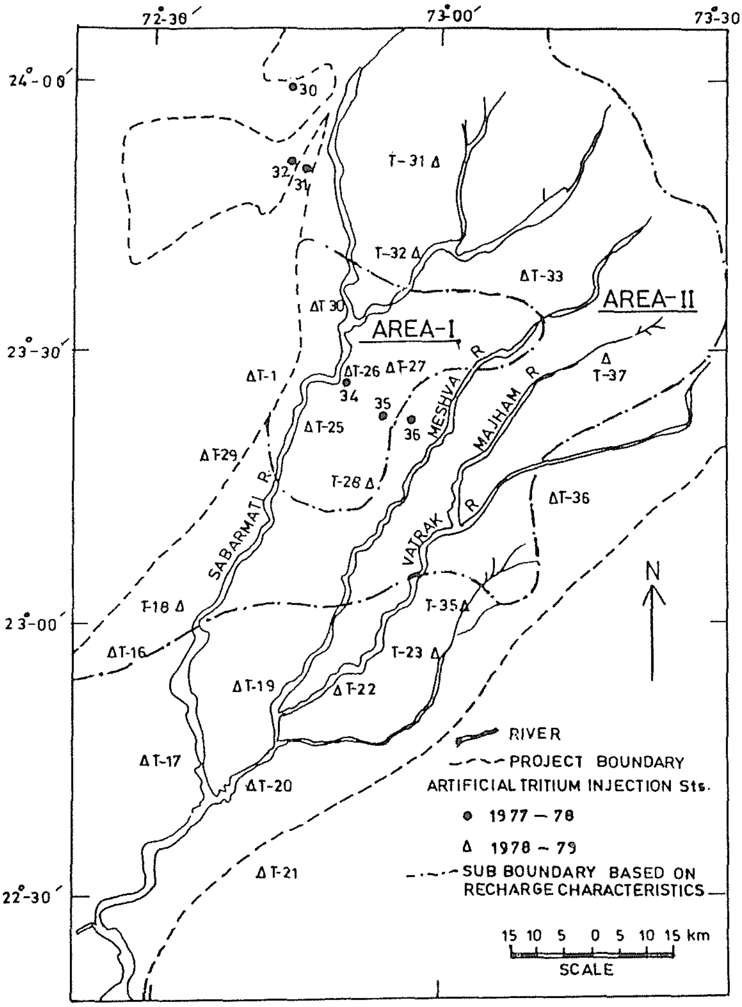

Fig. 3 Map of the Sabarmati basin showing subdivisions with different recharge characteristics (modified after Bhandari *et al.*, 1986).

the Mahi Command Area are indicative of the fact that the net result is better if the area under question is subdivided on the basis of observed variations in the precipitation-recharge plots and equations are developed than to treat them as one single unit and try to relate the recharge with other factors with poor statistical parameters.

ESTIMATION OF BASEFLOW

The tritium tagging technique can also be used for the study of baseflow. Therefore, a study was carried out in the Jalaun district during the monsoon season. The determination of baseflow using the present case is based on the comparison of recharge values determined with the help of the tritium tagging technique to those calculated using the water table fluctuation approach. Therefore, the basic assumption associated with

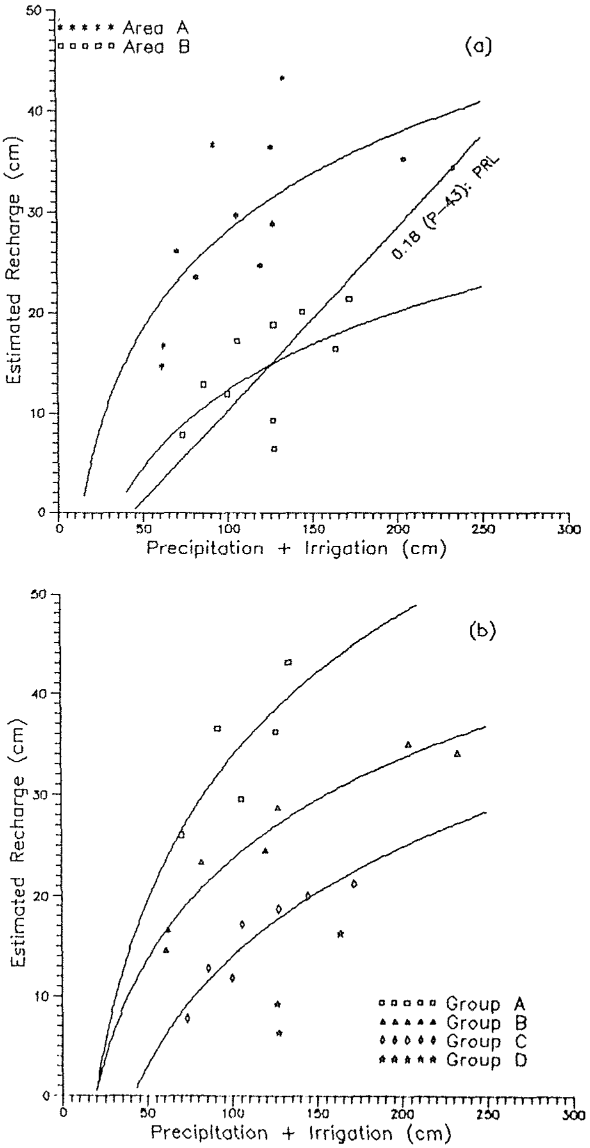

Fig. 4 Variation of recharge to groundwater with rainfall based on the results obtained by the tritium tagging technique in the Sabarmati basin (studied by Bhandari *et al.* 1986): (a) Data analysed considering two different trends; (b) Data analysed considering three different trends.

this approach is that except for rainfall, no other source of groundwater recharge is active nor is groundwater being exploited for irrigation etc. during the study period in the area under study. A study was carried out in the Jalaun district where the groundwater is already scarce. Therefore except for drinking and irrigation (minor scale) purposes, it is not used. During the rainy season, the groundwater is not used for irrigation except in drought conditions. Therefore, the difference of recharge calculated using the tritium tagging technique to that calculated using the water table fluctuation

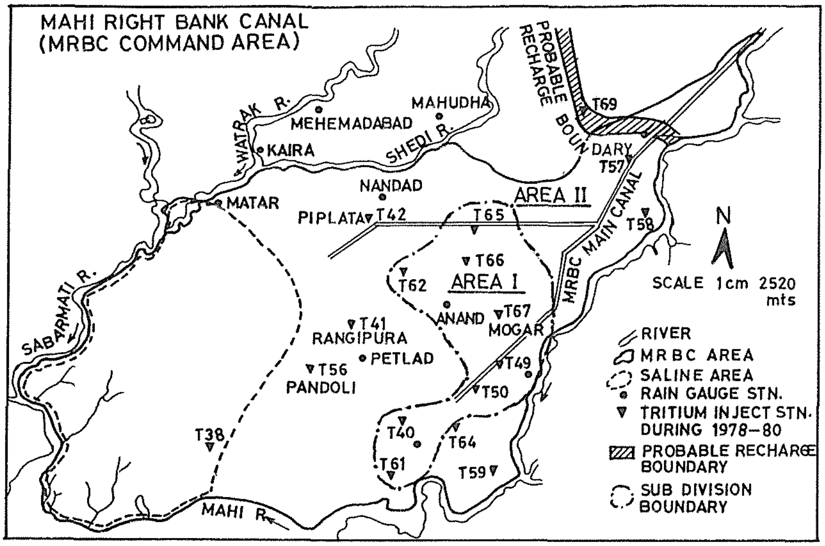

Fig. 5 MRBC Command Area showing sub-divisions I and II with different recharge characteristics (modified after Bhandari *et al.*, 1986).

approach will provide the information of baseflow of groundwater to river or *vice versa.*

The Jalaun district is bordered by the rivers Yamuna and Betwa from two directions (Fig. 7). The water level in both these rivers remains generally lower than the groundwater level in the area of Jalaun. Therefore, to estimate the baseflow of groundwater to both rivers, tritium was injected at four selected sites before the start of

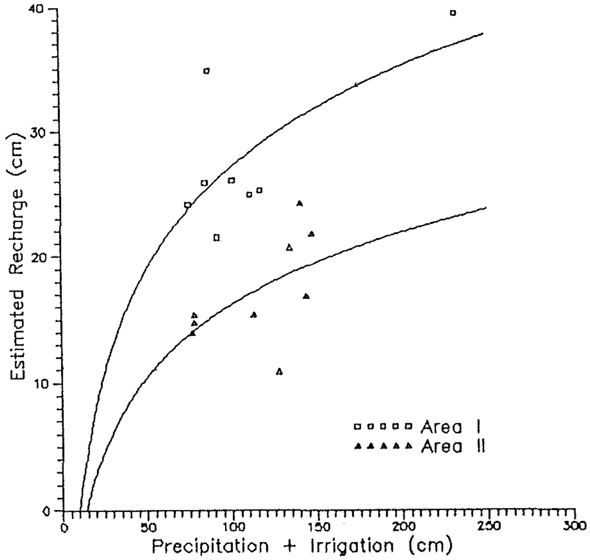

Fig. 6 Variation of recharge to groundwater with rainfall based on the results obtained by the tritium tagging technique in Mahi Command Area (studied by Bhandari *et al.*, 1986).

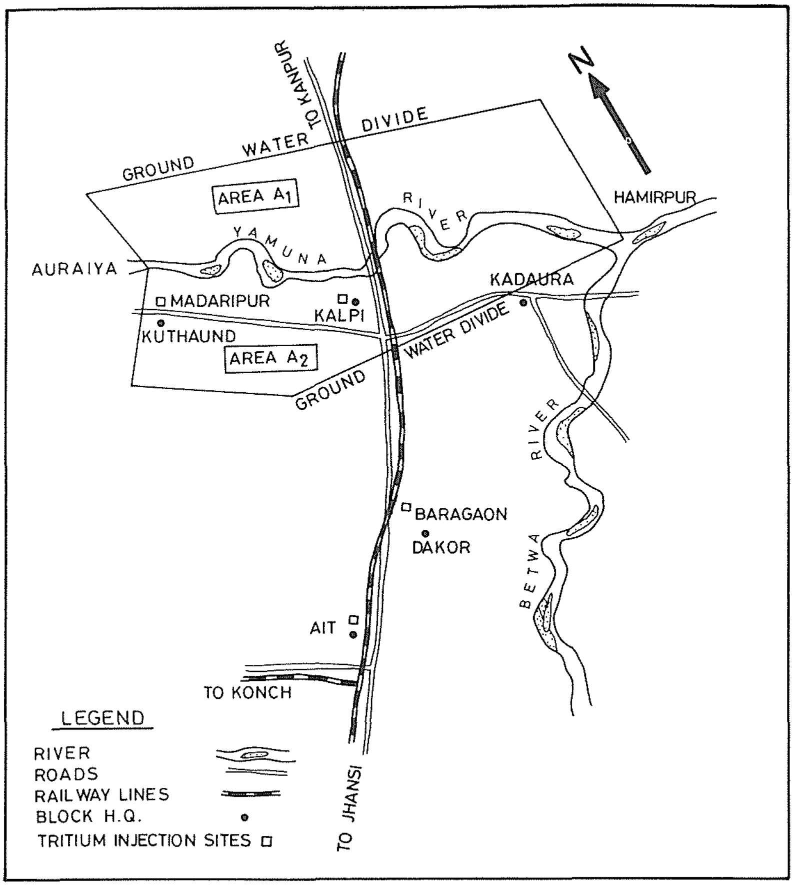

Fig. 7 Map showing tritium injection sites at different places in the Jalaun district for baseflow studies.

the monsoon and soil sampling was carried out in the month of September (Fig. 7). The recharge to groundwater was calculated using the tritium tagging technique as discussed above and by water table fluctuation approach. These results are given in Table 2.

The total groundwater flow towards the river or *vice versa* can be estimated by knowing the difference in discharge of the river at its upstream and downstream ends in the study area. The groundwater flowing to the River Yamuna has been calculated by dividing the difference in discharge at points A and B with the area of the Jalaun district contributing to the groundwater flow on the basis of groundwater divide. The calculation of rate of baseflow using the discharge measurement technique is shown in Table 2 along with the results of baseflow studies. It is interesting to note that the rate of baseflow calculated using the river discharge method comes to be 0.26 cm day^{-1} while by tritium tagging technique it is 0.2363 cm day^{-1}, results which are comparable.

DISCUSSION

From the results presented, the following points emerge:

Table 2 Comparison of baseflow results obtained by tritium peak shift and river discharge measurement methods.

Area between the ground water divide on the north and River Yamuna (A_1)	2174 km^2
Area between the ground water divide on the south and River Yamuna (A_2)	1113 km^2
Total area contributing groundwater flow to the River Yamuna between Auraiya and Hamirpur	3287 km^2
Ave. volume of flow into the river between Auraiya and Hamirpur as per observed values of river discharges from 19.06.79 to 12.09.79 (86 days)	$85.7 * 10^5$ m^3 day^{-1}
Ave. volume of flow from area A_2 during 86 days	$29.01 * 10^5$ m^3 day^{-1}
Ave. volume of flow per square km. of the area A_2	$2.6 * 10^3$ m^3 day^{-1}
Ave. rate of flow calculated by discharge measurement method between Auraiya and Hamirpur sites	0.26 cm day^{-1}
Ave. recharge to groundwater at four sites indicated in Fig. 7 using tritium tagging technique	18.995 cm
Ave. recharge to groundwater calculated at four sites indicated in Fig. 7 using water table approach	−1.33 cm
Difference in recharge determined by above referred two techniques in 86 days	20.325 cm
Ave. rate of flow calculated by the tritium peak shift method at Kalpi and Madaripur sites	0.2363 cm day^{-1}

(a) It is clearly seen from the plots of recharge to groundwater with respect to rainfall for the Bundelkhand region of Uttar Pradesh State and the Sabarmati basin and Mahi Command Area in Gujarat State, India, that a single empirical relation may not hold good for the whole region. Therefore, in order to explain the wide variations in the experimental results, it is advisable to consider the area under study in small sub-regions on the basis of observed trends in plots. Subsequently it may be verified in the field for the influencing parameters viz. hydrogeology, physiography and other local factors.

(b) Most of the field agencies in developing countries have the tendency to use the water table fluctuation approach to estimate the recharge to groundwater due to precipitation/irrigation. The results in the Bundelkhand region indicate that at some places while there has been some recharge to groundwater (determined using the tritium tagging technique) the water table had in fact moved down. The conventional technique would have failed to depict the true picture.

(c) The authors are of the opinion that if reliable information on recharge to groundwater is required for any area, neither the water table fluctuation approach nor an empirical relationship that has been developed for another area should be used. Instead the tritium tagging technique which is simple and fairly accurate should be used to develop a separate empirical relationship for the area under question, for further use.

(d) The tritium tagging technique can also be used to estimate the baseflow to/from rivers, provided there is no other source of recharge to groundwater except precipitation and no major abstraction from groundwater during the study period in the area under study.

REFERENCES

Bhandari, N., Gupta, S. K., Sharma, P., Premsagar, Ayachit, V. & Desai, B. I. (1986) Hydrogeological investigations in Sabarmati and Mahi basins and Coastal Saurashtra using radioisotope and chemical tracers. *Tech. Report, HILTECH, Roorkee, India.*

Chaturvedi, R. S. (1973) A note on the investigation of groundwater resources in western districts of Uttar Pradesh. *Annual Report, UPIRI, Roorkee*, 86-122.

Datta, P. S., Mookerjee, P., Chandrasekaran, H. & Mukherjee, T. K. (1990) Variability in groundwater recharge through the unsaturated zone. *Bull. Radiation Protection* **13**(1), 127-130.

Mookerjee, P. (1990) New concept of profile moisture and depth of injection in tritium tagging technique for evaluation of groundwater recharge as a component of the water balance equation. *Bull. Radiation Protection* **13**(1), 147-150.

Munnich, K. O. (1968a) Moisture movement measured by isotope tagging. In: *Guide Book on Nuclear Techniques in Hydrology*, 112-117. IAEA, Vienna.

Munnich, K. O. (1968b) Use of nuclear techniques for the determination of groundwater recharge rates. In: *Guide Book on Nuclear Techniques in Hydrology*, 191-197. IAEA, Vienna.

Sehgal, S. P. (1973) Groundwater resources of Punjab state. *III Annual Research Session of CBIP, New Delhi.*

Singh, B. P. & Kumar, B. (1993) Is it correct to assume that soil moisture movement in unsaturated strata is a piston flow. *Abs. Vol., Intl. Conf. on Hydrology and Water Resources* (December, New Delhi, India).

Zimmermann, U., Ehhalt, D. & Munnich, K. O. (1967a) Soil water movement and evapotranspiration; changes in the isotopic composition of the water. In: *Isotopes in Hydrology*, 567-586. IAEA, Vienna.

Zimmermann, U., Munnich, K. O. & Roether, W. (1967b) Downward movement of soil moisture traced by means of hydrogen isotopes. *Am. Geophys. Union, Geophys. Monogr.* **11**, 28-36.